Oceanic Pillow Lavas and Hyaloclastites as Habitats for Microbial Life Through Time – A Review

Harald Furnes, Nicola McLoughlin, Karlis Muehlenbachs, Neil Banerjee, Hubert Staudigel, Yildirim Dilek, Maarten de Wit, Martin Van Kranendonk, and Peter Schiffman

Abstract This chapter summarizes research undertaken over the past 15 years upon the microbial alteration of originally glassy basaltic rocks from submarine environments. We report textural, chemical and isotopic results from the youngest to the oldest *in-situ* oceanic crust and compare these to data obtained from ophiolite and greenstone belts dating back to c. 3.8 Ga. Petrographic descriptions of the granular and tubular microbial alteration textures found in (meta)-volcanic glasses from pillow lavas and volcanic breccias are provided and contrasted with textures produced by abiotic alteration (palagonitization). The geological setting in particular the degree of deformation and metamorphism experienced by each study site is documented in outcrop photographs, geological maps and stratigraphic columns (where possible). In addition, X-ray mapping evidence and carbon isotopic data that are consistent with a biogenic origin for these alteration textures is explained and a model for their formation is presented. Lastly, the petrographic observations and direct radiometric dating techniques that have been used to establish the antiquity and syngenicity of these microbial alteration textures are reviewed.

The combined dataset presented herein suggests that the microbial alteration of volcanic glass extends back to some of the earliest preserved seafloor crustal fragments. We use observations collected from well preserved, *in-situ* oceanic crust as a guide to interpreting comparable mineralized micro-textures from the ancient seafloor. It emerges that textural evidence is best preserved in undeformed to little-deformed, low grade, meta-volcanic rocks, and that chemical tracers, in particular the $\delta^{13}C_{carb}$ signatures, are more robust and can survive relatively strong deformation and metamorphic conditions. Drawing together all of this data we propose a tentative model for microbial life in the Archean sub-seafloor. Overall, it is argued

H. Furnes
Department of Earth Science & Centre for Geobiology, University of Bergen, Allegt. 41, 5007 Bergen, Norway
e-mail: Harald.Furnes@geo.uib.no

Y. Dilek et al. (eds.), *Links Between Geological Processes, Microbial Activities & Evolution of Life*,

that bioalteration textures in (meta)-volcanic glasses provide a valuable tracer of the deep oceanic biosphere, which constitutes one of the largest and least explored portions of the modern, and especially the ancient, biosphere.

1 Introduction

Microbial activity has until recently only been sought largely in (meta)-sedimentary rocks and environments. It is now, however, realized that microbial life can also colonise volcanic rocks within the Earth's crust to considerable depths, where carbon and energy sources are available and where physical conditions do not inhibit life (e.g., Lovley and Chapelle 1995; Pedersen 1997; Pedersen et al. 1997; Amend and Teske 2005; Schippers et al. 2005). During the last decade, it has also been demonstrated that the upper volcanic part of the *in situ* oceanic crust is a habitat for microbial life (e.g., Thorseth et al. 1992; Thorseth et al. 1995a; Furnes et al. 1996; Fisk et al. 1998; Torsvik et al. 1998; Furnes and Staudigel 1999; Furnes et al. 1999, 2001a, b; Thorseth et al. 2001, 2003; Banerjee and Muehlenbachs 2003; Fisk et al. 2003; Staudigel and Furnes 2004; Staudigel et al. 2004). The *in-situ* oceanic crust however, only extends back to approximately 170 Ma, with the oldest oceanic crust being found in the western Pacific Ocean. Evidence of microbial activity in older oceanic volcanic rocks must be sought in fragments of ancient oceanic crust preserved in ophiolites and greenstone belts. Reliable evidence for microbial life has been found in several ophiolites ranging in age from Cretaceous to Paleoproterozoic (Furnes et al. 2001c, 2002a, 2005), and putative evidence of microbial life has been described from Mesoarchean pillow lavas of the Barberton greenstone belt, South Africa (Furnes et al. 2004; Banerjee et al. 2006) and the Pilbara Craton, Western Australia (Staudigel et al. 2006; Banerjee et al. 2007).

In this chapter, we summarize the various accounts of microbial alteration that span the youngest, *in-situ* oceanic crust to the oldest greenstone belts and present new data pertaining to these findings. In particular, we provide in one manuscript a compilation of lithological logs from the *in-situ* oceanic crust where microbial alteration has been found, along with geological maps, stratigraphic sections and outcrop photographs of all of the ophiolites and greenstone belt examples studied to enable direct comparisons to be made. Previous reviews have largely treated evidence of microbial alteration from the *in situ* oceanic crust (e.g., Fisk et al. 1998; Furnes et al. 2001b) and ophiolites (e.g. Furnes and Muehlenbachs 2003) separately; or largely focussed on a single line of evidence such as textural information (e.g., Furnes et al. 2007a). This manuscript extends the study of Staudigel et al. (2006) to document in detail, the main lines of evidence that have been presented to support microbial alteration in volcanic glass from 11 drill cores from the *in-situ* oceanic crust; 5 ophiolite examples and 4 greenstone belts (Fig. 4). In addition to the review of all relevant aspects covered below, we present new textural and carbon isotope data from several of the investigated ophiolites and greenstone belts that is consistent with bioalteration.

2 Biogenicity and Antiquity – Criteria Used for Establishing Bioalteration

Alteration of basaltic glass in modern pillow lavas and hyaloclastites results from two fundamentally different processes – abiotic and biotic alteration. Abiotic alteration results in the formation of the long-recognized, but enigmatic, material termed *palagonite*. The more recently-recognized biotic alteration involves etching of the glass by rock dwelling (endolithic) microbes creating textures that can be regarded as ichnofossils. These two alteration processes may be contemporaneously active within the temperature limit of life. In a number of recent papers the abiotic and biotic alteration processes have been discussed at length. Below we will only briefly comment on abiotic alteration and focus instead upon the biotic processes of alteration. We present biogenicity and antiquity criteria developed to assess these structures, as well as a refined version of recent models proposed to explain the bioalteration of basaltic glass (Staudigel et al. 2006; Furnes et al. 2007a; McLoughlin et al. 2008). In addition, we briefly review what is currently known about the microorganisms that are thought to be responsible for the bioerosion of volcanic glass.

2.1 Abiotic Alteration

The aqueous alteration of basaltic glass produces a pale yellow to dark brown material referred to as palagonite. Palagonitization has traditionally been regarded as a purely physico-chemical phenomenon and is a complex and continuous aging process involving incongruent and congruent dissolution accompanied by precipitation, hydration and pronounced chemical exchange that occurs at low to high-temperatures (e.g., Thorseth et al. 1991; Stroncik and Schmincke 2001; Walton and Schiffman 2003; Walton et al. 2005). The resulting palagonite occurs around the rims of glass shards and as banded material on either side of fractures with a relatively smooth interface between the fresh and altered glass. Palagonite can be divided into two types: (1) early stage amorphous gel-palagonite that matures to form, (2) fibro-palagonite which consists of clays, zeolites and iron-oxy-hydroxides (Peacock 1926).

2.2 Biotic Alteration

Over recent years mounting evidence has been collected to support the biological mediation of processes involved in the alteration of volcanic glass. One of the earliest reports of the biological etching of glass is the description of surface pitting on church window-pane glass in the vicinity of growing lichens (Mellor 1922; see also Krumbein et al. 1991 for review). Bioerosion of natural glasses was reported somewhat later with the finding of surface grooves on glass shards from Miocene

tephra that were likened to those produced by fungi which bore into carbonate grains (Ross and Fisher 1986). This scenario was confirmed with the observation of bacteria within surface pitting textures on sub-glacial volcanic breccias from Iceland, which lead Thorseth et al. (1992) to propose that the microbes locally modify the pH and thereby accelerate glass dissolution. A range of biochemical mechanisms are employed by microorganisms to dissolve volcanic glass and are thought to include secretion of organic acids, production of siderophores and complexing agents that help to complex metal ions, particularly Al whilst modifying the pH to promote silica glass dissolution (Paul and Zaman 1978). The initial stages of glass pitting have been experimentally investigated by Thorseth et al. (1995b), and Staudigel et al. (1995,1998), who confirmed that volcanic and synthetic glasses inoculated with microbes develop etch pits and surface alteration rinds under laboratory conditions.

Numerous studies have followed to document the widespread occurrence of microbial bioerosion textures in volcanic glass from Ocean Drilling Program (ODP) and Deep Sea Drilling Project (DSDP) drill cores from *in-situ* oceanic crust (e.g., Thorseth et al. 1995a; Furnes et al. 1996; Fisk et al. 1998; Furnes et al. 2001a, b; Thorseth et al. 2001, 2003; Banerjee and Muehlenbachs 2003). Distinct textural, elemental and isotopic signatures are produced by these microbial alteration processes and are reviewed below. As a preface to the individual studies it is first informative to draw together and explain the various lines of evidence and the key observations used to distinguish such bioalteration textures from the products of abiotic palagonitization (see also McLoughlin et al. 2007).

2.2.1 Textures

The bioalteration of volcanic glass produces two principal types of textures that have been termed *granular* and *tubular* textures (Furnes and Staudigel 1999). These are markedly different from the regularly banded alteration rinds that result from abiotic palagonitization (Fig. 1A), and we regard these textures as our prime evidence for the bioalteration of basaltic glass. A model for the textural development of such bioerosion traces is given in Fig. 1. The top line shows abiogenic alteration which results in the production of banded palagonite around glass fragments and along the margins of fractures, with a relatively smooth interface between the fresh and altered glass. This should be contrasted with the granular and tubular ichnofossils shown in the lower lines of the figure which are formed by microorganisms carried by circulating fluids into fractures in the rock. These microbial consortia progressively etch the fresh glass, generating more abundant tubes and granular aggregates around fractures and creating an increasingly ramified alteration front between the fresh and altered glass. In Fig. 1, this is schematically shown from left to right across the diagram and illustrated by the back-scatter electron (BSE) images of real examples. The granular alteration textures consist of micron-sized spherical cavities filled with amorphous to very fine-grained phyllosilicate phases. At the initial stage of bioalteration the granular textures appear as isolated spherical bodies along fractures in the glass (Fig. 1B, stage t_1). With progression of bioalteration these become more

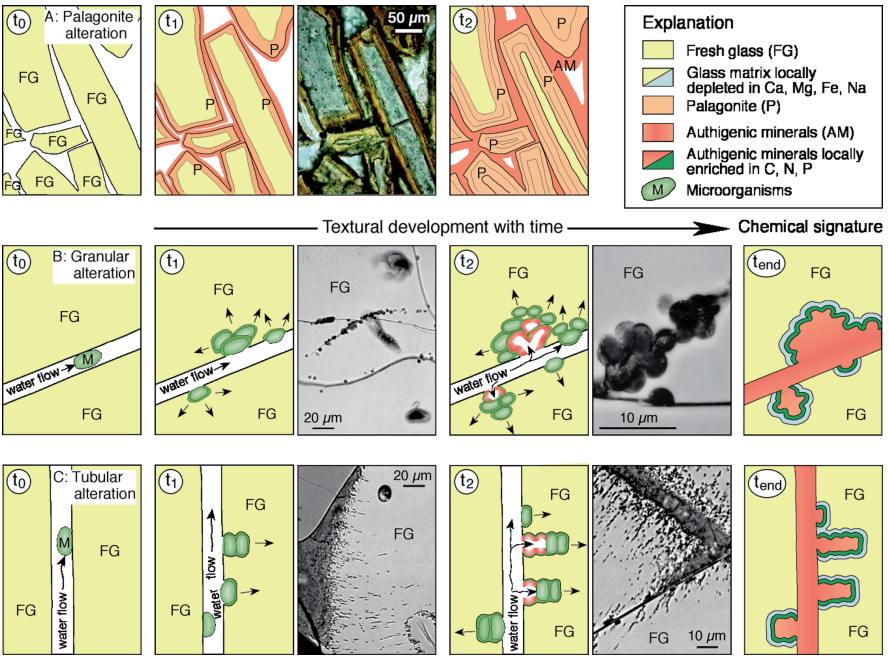

Fig. 1 Schematic diagram showing the generation of alteration textures in fresh volcanic glass (FG) from initial time (t_0) to the final time (t_{end}), accompanied by back scattered electron and thin section images of real examples. The *top line* (**A**) shows abiotic palagonite alteration which produces banded palagonite rims and authigenic minerals around glass fragments. The *middle line* (**B**) shows the growth of granular type textures from isolated spheres in the early stages (t_1) to dense granular aggregates (t_2). The *lower line* (**C**) shows the growth of tubular type from incipient short tubes at stage (t_1) to longer tubes at (t_2). The *right* hand column in (**B**) and (**C**) shows the resulting compositional signatures that are found when these bioalteration textures are infilled by authigenic mineral phases

numerous and coalesce into aggregates that form irregular bands which protrude into the fresh glass along fractures (Fig. 1B, stage t_2). The tubular alteration textures (Fig. 1C) are also concentrated along surfaces in volcanic glass where water once permeated, and become longer and form denser aggregates with progressive alteration.

During the formation of both morphologies of microbially-driven glass dissolution, the total surface area of fresh glass available progressively increases. Staudigel et al. (2004) calculated that the surface area of fresh glass would increase by factors of 2.4 and 200 during the formation of tubular and granular morphotypes, respectively. In contrast, abiotic alteration causes the surface area of fresh glass to progressively decrease, acting as a negative feedback that inhibits further alteration. As long as seawater is accessible to the fresh glass, alteration, whether biotic or abiotic, will continue until all of the fresh glass is altered. With time, the bioalteration textures are filled with authigenic phases and alteration will proceed at a much slower rate until, seawater no longer has access to the fresh glass and alteration will

stop. The final column in Fig. 1 shows the chemical signatures that are preserved, including enrichment in C, N and P along the margins of the bioerosion traces, and depletion in Mg, Fe, Ca, and Na in the surrounding modified glass (discussed further in Section 5, below). We stress that this is a schematic diagram and that the distribution of bioalteration textures will differ in fractures of varying geometries under different fluid flow regimes in and around vesicles and as authigenic minerals precipitate and thereby modify the diffusion processes. Further real examples of bioalteration textures from *in-situ* oceanic crust are described in Section 4.1 and Figs. 23 and 24; from ophiolites in Section 4.2 and Fig. 25; and from greenstone belts in Section 4.3 and Fig. 26.

2.2.2 Syngenicity and Antiquity

To establish the syngenicity of bioalteration textures and exclude an origin from modern endolithic organisms relies in the first instance upon relative age relationships observed by optical microscopy. In volcanic glasses and hyaloclastites (i.e., brecciated volcanic glass), it is therefore necessary to check the distribution of bioalteration textures in pillow margins or glass fragments with respect to fractures that may have acted as conduits for younger fluids and, possibly, also for microbes. In ancient metamorphic samples, the originally hollow bioalteration textures are now filled by secondary minerals (e.g., quartz, chlorite, titanite) and have been overgrown by metamorphic minerals (e.g., Figs. 26 and 27). In such cases, the metamorphic age of the overgrowing mineral gives a minimum age constraint for the bioalteration of the rock, as for example in the case of the $\sim$3.5 Ga bio-etching of the pillow lavas of the Barberton greenstone belt, South Africa (Furnes et al. 2004; Banerjee et al. 2006). This may not always be a trivial task and in some cases it is not possible to confidently establish the timing of bioalteration. However, direct radiometric U-Pb dating of titanite that is commonly found to fill the bioalteration textures, is sometimes possible and has been done for tubular alteration textures in hyaloclastites of the 3350 Ma Euro Basalt of the Kelly Group (Pilbara Craton, Western Australia), yielding a minimum age estimate for bioalteration of $2921 +/- 110$ Ma (Banerjee et al. 2007); this study is discussed in more detail in Section 7.4, below.

2.2.3 Geochemistry

The localised concentration of biologically significant elements in and around volcanic bioalteration textures offers support for the biogenicity of these textures. X-ray element mapping in the vicinity of bioalteration textures (e.g., Furnes et al. 2001b; Banerjee and Muehlenbachs 2003; also Section 5 below and Figs. 28–30), has shown that the tubular and granular textures are commonly lined with carbon. Importantly, these elevated levels of carbon are not associated with enrichments of elements such as calcium, iron, or magnesium that commonly form carbonates. Instead, the source of the carbon is likely residual organic matter (Torsvik et al. 1998). Element maps of bioalteration textures also commonly show enrichments and/or uneven distributions of K, Fe, P, N, and S. For example, Alt and Mata (2000) used

TEM to study nano- to micro- sized alteration textures in 6 Ma-old basaltic glasses and proposed an incongruent dissolution process with significant losses of Mg, Fe, Ca and Na, accompanied by slight loss of Al and Mn and a substantial increase in K due to the circulation of >100 fracture volumes of seawater. Intriguingly, their data lead them to highlight the possible contribution of nano-sized organisms in the bioalteration processes. In another study, Storrie-Lombardi and Fisk (2004) investigated the local chemical composition of biotically and abiotically altered 0.5–170 Ma-old volcanic glasses by electron microprobe and showed through principal component analysis that the alteration products of biotic and abiotic alteration are distinct. In brief, the clays produced by biotic alteration had higher Fe and K contents, whereas abiotic alteration produced clays with higher Mg values. Further geochemical work, applying methods like those just described may help to distinguish between biotic and abiotic alteration structures.

Fresh volcanic glass is scarce throughout the rock record (e.g., Shervais and Hanan 1989), and the oldest reported occurrence is of Mesoproterozoic (ca. 1.1 Ga) age (Palmer et al. 1988). Textural evidence for bioalteration in ophiolites and greenstone belts is therefore more unlikely and of diminishing quality with increasing geological age and thus geochemical fingerprints in the form of elevated levels of biologically important elements provide useful substantiating evidence. These geochemical signatures from *in-situ* oceanic crust, ophiolites and greenstone belts are described and discussed in further detail in Section 5 below.

2.2.4 Stable Carbon Isotope Signatures

Systematic shifts in the carbon isotope values measured from disseminated carbonate in the glassy rims and crystalline cores of pillow basalts have been taken to support the operation of bioalteration processes (e.g., Furnes et al. 2001a). These carbon isotope patterns can also give clues as to the putative microbial metabolisms that may be involved. Typical pillow basalts contain less than 1 wt.% of disseminated carbonate and the $\delta^{13}C_{carb}$ values obtained from fresh unaltered basalts yield values similar to mantle CO_2 between $-5‰$ to $-7‰$ (Alt et al. 1996; Hoefs 1997). These contrast with $\delta^{13}C_{carb}$ values of marine carbonate of $0‰$ and provide the reference frame for the interpretation of $\delta^{13}C_{carb}$ values obtained from volcanic glass (see Fig. 2). The microbial oxidation of organic matter produces ^{12}C-enriched CO_2, which may subsequently be precipitated in carbonate depleted in $^{13}C(-\delta^{13}C)$, as shown by the left hand arrow on Fig. 2. Positive $\delta^{13}C_{carbonate}$ values on the other hand, can result from the lithotrophic utilization of CO_2 by methanogenic Archaea. These microorganisms produce methane from H_2 and CO_2 preferentially producing ^{12}C-enriched methane and leaving the remaining CO_2 enriched in ^{13}C, which will be recorded in any precipitated carbonate as shown by the right hand arrow on Fig. 2. The existence of the latter archaeal processes is supported by the discovery of diagenetic dolomite with $\delta^{13}C$ as high as $+14‰$ in sediments from DSDP Hole 479 (Gulf of California), suggesting a biogenic CO_2 reservoir related to active methanogenesis (Kelts and McKenzie 1982). Compiled $\delta^{13}C_{carbonate}$ data from the *in-situ* ocean crust, ophiolites and greenstone belts of different metamorphic grades is presented

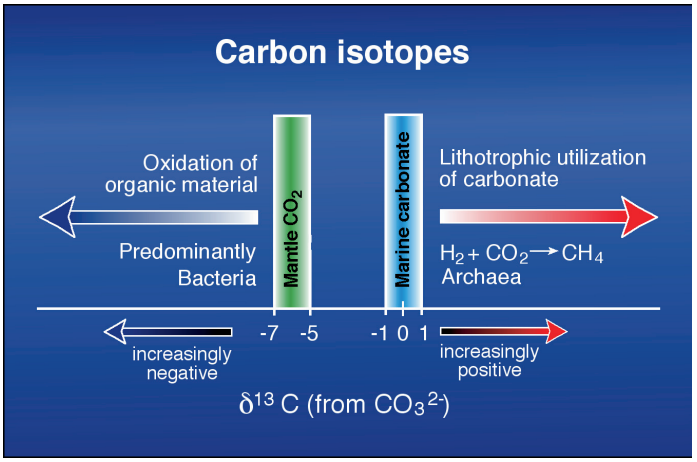

Fig. 2 Diagram summarizing the interpretation of $\delta^{13}C$ values measured on disseminated carbonates from pillow lavas. For reference the $\delta^{13}C$ values of mantle CO_2 and marine carbonates are plotted. The oxidation of organic matter in pillow rims by bacteria is argued to shift the $\delta^{13}C_{carb}$ to progressively more negative values, as low as −25‰ (see for example Fig. 31B). Whereas the lithotrophic utilization of carbonate in pillow rims by archaea shifts the $\delta^{13}C_{carb}$ to more positive values as high as +3.9‰ (see for example Figs. 30 and 31). In contrast, carbonate measured from pillow cores yields a mantle value and carbonate from amygdales gives a marine value. Actual $\delta^{13}C_{carbonate}$ data from pillow lavas are plotted in Figs. 31, 32 and 33

and discussed in detail below (see Section 6 and Figs. 30–32). In summary, it is found that values obtained from pillow interiors are bracketed between primary mantle CO_2 values and those expected from marine carbonates whereas those measured from pillow rims and hyaloclastites display a significantly greater range in $\delta^{13}C_{carbonate}$ values that is consistent with microbial activity. In addition, it has been suggested that variations in the structure and lithology of the oceanic crust may influence the colonizing microbes and resultant carbon isotope signatures (Furnes et al. 2006 and Section 7.3, below).

2.2.5 DNA-Analyses and Microfossil Remains

Nucleic acids derived from bacterial and archaeal DNA are commonly localized within recent bioalteration textures in pillow lavas of young, *in-situ* oceanic crust (Thorseth et al. 1995a, 2001; Giovannoni et al. 1996; Torsvik et al. 1998). The application of DAPI (4, 6 diamino-phenyl-indole) dye which binds to nucleic-acids, along with fluorescent oligonucleotide probes that target bacterial and archaeal RNA has revealed that biological material is concentrated at the ramified interface between fresh and altered glass (e.g., Giovannoni et al. 1996; Torsvik et al. 1998, Fig. 2; Banerjee and Muehlenbachs 2003, Fig. 14; Walton and Schiffman 2003, Fig. 8). For example, staining of volcanic glass samples from the Costa Rica Rift (Fig. 3) show that the most concentrated biological material occurs at the interface of fresh and altered glass, especially in the tips of tubular structures and that the

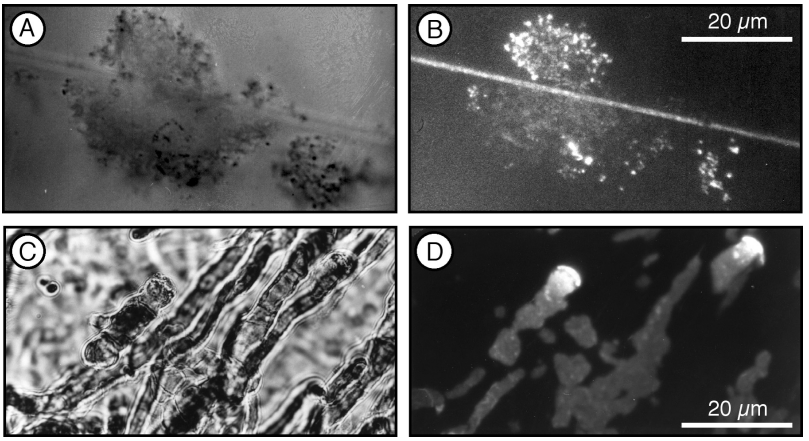

Fig. 3 (**A**) Transmitted light image of the granular bioalteration type; (**B**) epiflourescence image of the same sample showing that the biological material is concentrated along the edges of the granular alteration and within the fracture; (**C**) transmitted light image of the tubular bioalteration type; (**D**) epiflourescence image of the same sample showing that the biological material is concentrated at the ends of the tubes. Both samples (**A** and **C**) are from hole 148-896A-11R-1, 73-73 cm from the Costa Rica Rift (Furnes et al. 1996). The epiflourescent images were obtained using a Nikon Microphot microscope with excitation at 365 nm and emission at 420 nm on samples stained with 10 g/mL DAPI

biogenic material decreases in concentration towards the centre of fractures (Furnes et al. 1996; Giovannoni et al. 1996). We find it appropriate to mention that the application of DAPI may result in ambiguities since some clay minerals may autofluoresce. To ascertain the extent of autofluoresence, Giovannoni et al. (1996) used three different DNA-binding dyes (Hoechst 33342, PO-PRO-3, and Syto 11), which all supported the conclusions of Thorseth et al. (1995a) and Furnes et al. (1996) that microorganisms were present at the glass-alteration interface. Genetic material is not stable over geological lengths of time and so this type of data is not found in ophiolites and greenstone belts. The finding of DNA from *in-situ* oceanic crust that is 122 million-years-old has lead to the suggestion that viable microorganisms may still be active within these bioalteration textures long after eruption of the lavas (Banerjee and Muehlenbachs 2003).

Partially fossilized, mineral encrusted microbial cells have also been observed by scanning electron microscopy (SEM) on the surface of altered glasses from *in-situ* oceanic crust, with morphologies that included filamentous, coccoid, oval, rod and stalked forms (e.g., Thorseth et al. 2001). Moreover, these forms commonly occur in, or near, etch marks in the glass that exhibit forms and sizes resembling the attached microbes, suggesting that it was the microbes that were responsible for the formation of the etch marks (e.g., Thorseth et al. 2003). Within microtubules in volcanic glass fragments from the Ontong Java Plateau, delicate hollow and filled filaments attached to the tube walls have been observed (e.g., Banerjee and Muehlenbachs 2003, Figs. 5–9), along with spherical bodies and thin films

interpreted to represent desiccated biofilms (e.g., Banerjee and Muehlenbachs 2003, Figs. 5–9).

2.2.6 Microbiological Constraints

A consortium of microorganisms that includes heterotrophs and chemolithoautotrophs is thought to be involved in the bioalteration of volcanic glass. Heterotrophs use organic carbon delivered by circulating seawater as a carbon source and chemolithoautotrophs use oxidized compounds principally O_2 and NO_3^- derived from circulating seawater as electron acceptors within the modern sub-seafloor along with Fe(II) and Mn(II) in volcanic glass as electron donors (Edwards et al. 2005). The energetically viable reactions that are possible in these environments and their energy yields are given in Table 1 of Edwards et al. (2005). Under anaerobic conditions hydrogen consuming reactions can support appreciable biomass production and this H_2 may have been supplied by abiotic sources especially on the early earth. In addition, the microbial consortia may derive key nutrients especially phosphorus from the glass, which is found only in low concentration in typically nutrient poor, sub-seafloor conditions.

The suggestion that Mn oxidation is a potentially important chemolithoautotrophic metabolism involved in the bioerosion process is supported by the isolation of diverse manganese oxidizing bacteria from basaltic seamounts where they enhance the rate of Mn oxidation (e.g., Templeton et al. 2005). The possibility that these microbial consortia may also employ iron oxidation is consistent with the resemblance of bacterial moulds found on volcanic glass fragments to the branched and twisted filaments of the Fe-oxidizing bacteria *Gallionella* (e.g., Thorseth et al. 2001, 2003). Moreover it has recently been discovered that a group of bacteria distantly related to the heterotrophic organisms *Marinobacter sp*. and *Hyphomonas sp*. are also capable of chemolithoautrophic growth and employ Fe-oxidation at around pH 7 on substrates including basaltic glass (Edwards et al. 2003). Isolation of a new anaerobic, thermophilic facultative chemolithoautotrophic bacterium from a terrestrial hot spring that is capable of Fe (III) reduction using molecular H as the only energy source and CO_2 as a carbon source (Zavarzina et al. 2007), is also relevant to mention in this connection (see Section 7.3).

Culture independent molecular profiling studies have found that basaltic glass is colonized by microorganisms that are distinct from those found in both deep seawater and seafloor sediments. For example, indigenous microbial sequences obtained from basaltic glass samples dredged from the Arctic seafloor ranging in age from 1 Ma to 20 Ma were found to be affiliated with eight main phylogenetic groups of bacteria and a single marine Crenarchaeota group (Lysnes et al. 2004). Although it is not possible to confidently infer the metabolisms of uncultured microorganisms from molecular phylogenetic relationships, this study did find sequences that were related to known Fe and S metabolizing bacteria and methanogenic archea. Furthermore, it is reported that autotrophic microbes tend to dominate the early colonizing communities and that heterotrophic microbes are more abundant in older,

more altered samples (Thorseth et al. 2001; Santelli et al. 2006). In other words, it appears that prokaryotic microbial consortia, which include microorganisms that employ Fe and Mn oxidation, are plausible candidates for the bioerosion of basaltic glass and that these are associated with a heterotrophic community. There are even reports of eukaryotes from within the oceanic crust, with the finding of microbial remains argued to be marine, cryptoendolithic fungi in carbonate filled amygdales from Eocene Pacific seafloor basalts (Schumann et al. 2004).

Efforts to generate bioalteration textures in laboratory experiments using natural inoculums and various glass substrates have generated useful insights, although each with their own limitations. This work was motivated in part by etch pits found in Icelandic hyaloclastites that show "growth rings", which were taken to suggest that they might develop into tubular shaped alteration structures (Thorseth et al. 1992), although no such extended tubular morphologies have yet to be produced in the laboratory. These early studies involved basaltic glass inoculated with microbes taken from the submarine Surtsey volcano that were cultivated in 1% glucose solution at room temperatures for one year and produced etch pits and alteration rinds (Thorseth et al. 1995b). Monitoring of these experiments over time suggested that the microbes corrode the volcanic glass first via congruent dissolution, followed by incongruent dissolution and it was hypothesized that these involved the secretion of organic acids and metal complexing agents by the microbes (Thorseth et al. 1995b). The limitation of this work was the use of a nutrient rich media that is not comparable to sub-seafloor conditions. Another experimental approach was utilized by Staudigel et al. (1998) who constructed flow through experiments with basaltic glass that was continuously flushed with a natural seawater microbial population and monitored both chemically and isotopically for periods of up to 583 days. These biologically mediated experiments produced twice the mass of authigenic phases compared to the abiotic controls and caused particularly marked Sr exchange. Again, however, these experiments are not directly analogous to sub-seafloor conditions because surface seawater inoculums were used.

Thus, in summary it appears that heterotrophic bacteria, along with chemolithoautotrophs which utilize Fe and Mn oxidation, are responsible for the bioalteration of volcanic glass. However, the full diversity of microorganisms involved is yet to be fully documented, and the conditions under which tubular alteration structures are formed are yet to be replicated in the laboratory.

3 Material Investigated

We have investigated pillow lava and hyaloclastite samples from a large number of DSDP/ODP sites from the *in-situ* (modern) oceanic crust spanning the youngest to the oldest oceanic basins (0–170 Ma). The search for bioalteration has been extended into fragments of ancient oceanic crust preserved in ophiolites of different ages (Section 3.2) and Proterozoic to Archean greenstone belts (Section 3.3). All of

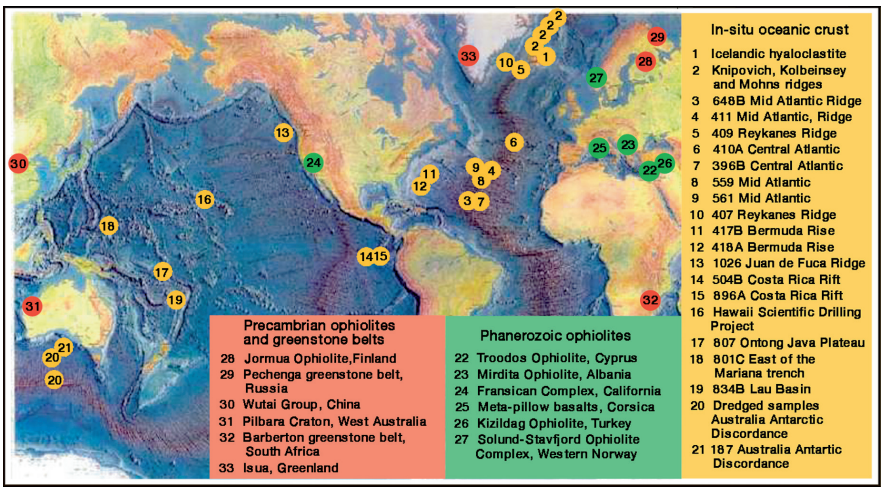

Fig. 4 Map showing the distribution of bioalteration textures documented to date in volcanic glass: examples from *in situ* oceanic basins are shown by *yellow circles*; from fragments of oceanic crust preserved in Phanerozoic ophiolites by *green circles*; and from Precambrian ophiolites and greenstone belts by *red circles*. References for each locality: (1) Thorseth et al. 1991; (2) Thorseth et al. 2001; (3) and (4) Furnes et al. 2001b, Lysnes et al. 2004; (5) Furnes et al. 2001b and Staudigel et al. 2004; (6) H. Furnes et al. 2001b; (7) Furnes et al. 2001b; (8) and (9) Fisk et al. 1998; (10) Staudigel and Furnes 2004; (11) Furnes et al. 2001b; (12) Staudigel and Furnes 2004; (13) Fisk et al. 2000; (14) Furnes et al. 1999; (15) Torsvik et al. 1998; (16) Walton and Schiffman 2003; (17) Banerjee and Muehlenbachs 2003; (18) Fisk et al. 1999; (19) Furnes et al. 2001a,b; (20) and (21) Thorseth et al. 2003; (22) Furnes et al. 2001b; (23) Furnes and Muehlenbachs 2003; (24) herein and K Muehlenbachs, unpub; (25) and (26) herein; (27) Furnes et al. 2002a; (28) Furnes et al. 2005; (29) herein; (30) herein; (31) Banerjee et al. 2007; (32) Furnes et al. 2004; Banerjee et al. 2006; (33) herein

the material discussed in this review are located on the world map shown in (Fig. 4) and plotted on the geological timescale shown in Fig. 36.

3.1 Modern Oceanic Crust (Atlantic, Costa Rica, Lau Basin)

The material from the modern oceanic crust has been collected from DSDP/ODP cores from the Atlantic Ocean, Lau Basin, Costa Rica Rift and the Ontong Java Plateau. The basaltic glass from the Atlantic (Fig. 5) forms the bulk of the investigated samples and was collected from eight drill sites (Holes 407, 409, 410A, 411, 417D, 418A, 396B and 634B). Holes 417D and 418A were drilled during DSDP Legs 51, 52 and 53, and have been described by Robinson et al. (1979). Holes 407, 409, 410A and 411, are situated in the north-central Atlantic Ocean and at the Reykjanes Ridge (Fig. 4), and were drilled during DSDP Leg 49 described by Luydendyk et al. (1978). Holes 396B and 648B are located in the central Atlantic Ocean and were drilled during DSDP Leg 46 and ODP Legs 106/109, described

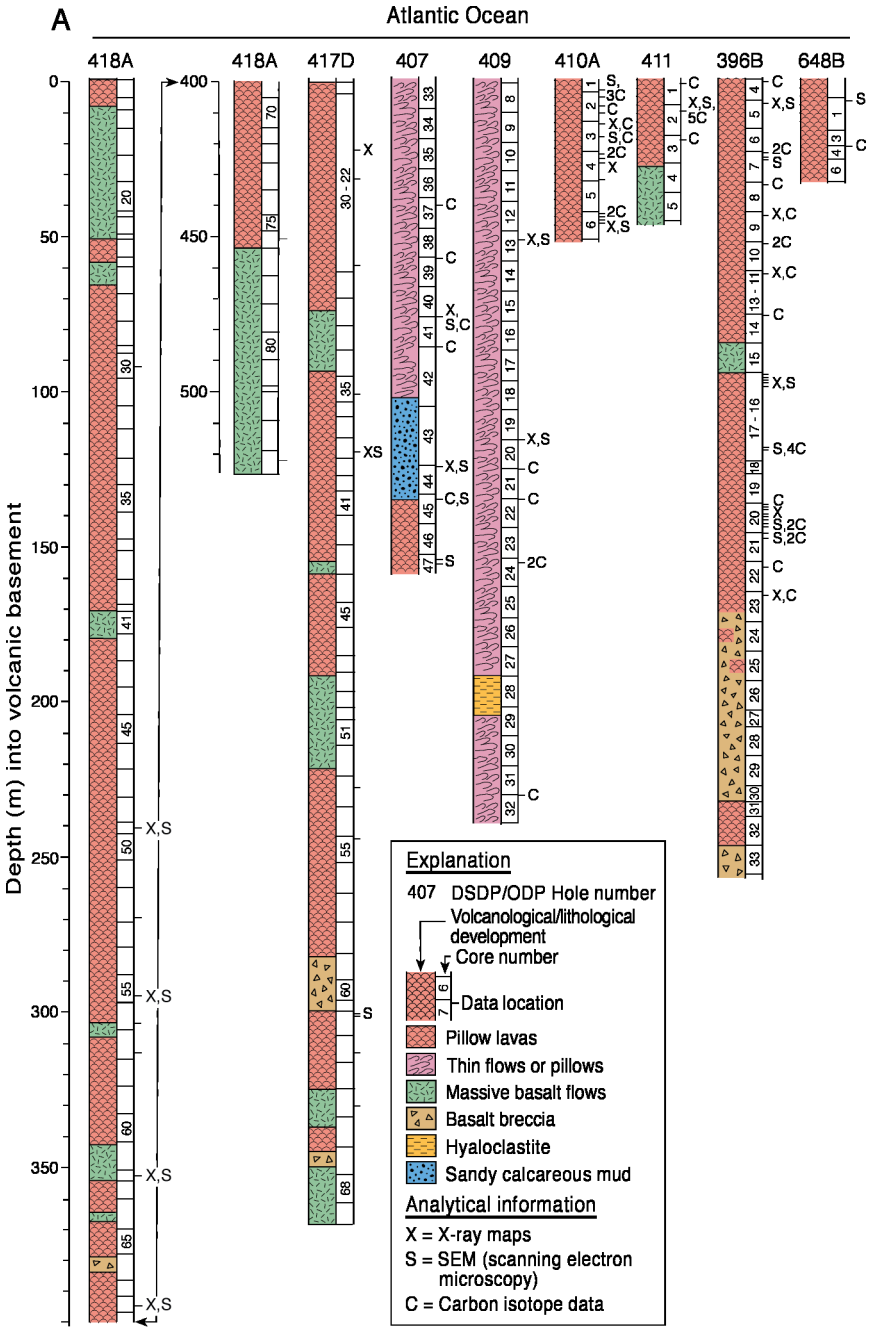

Fig. 5 *Continued*

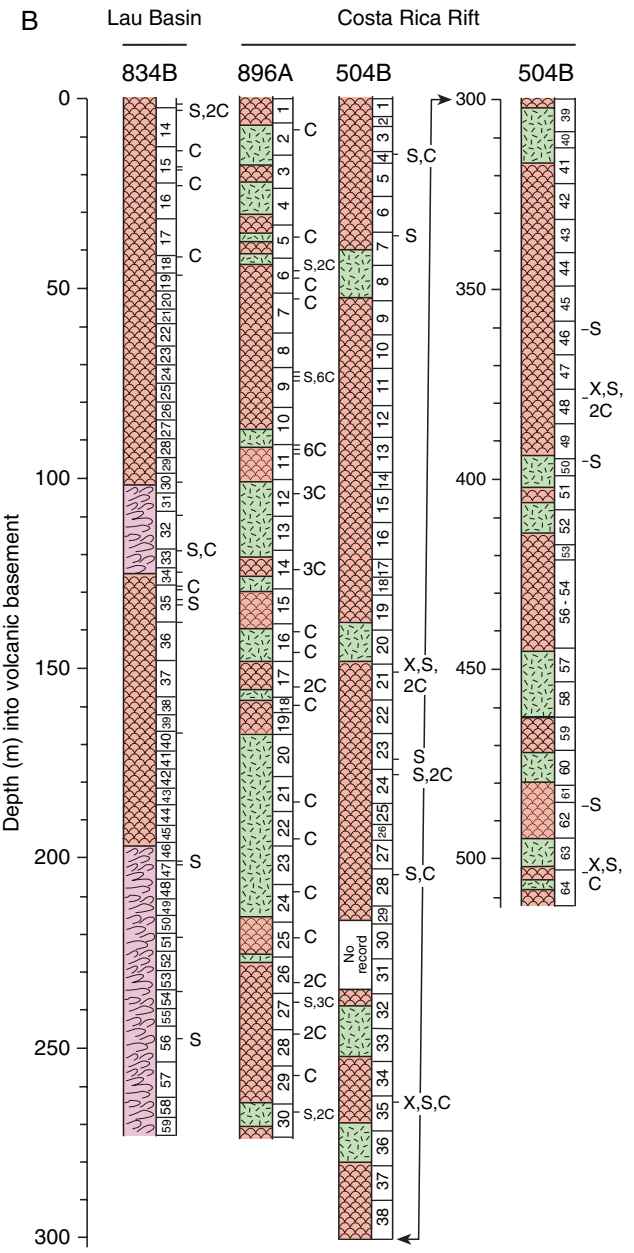

Fig. 5 Compilation of DSDP and ODP holes from the Atlantic Ocean (holes 418A, 417D, 407, 409, 410A, 411, 396B and 648B), the Lau Basin (hole 834A) and Costa Rica Rift (holes 896A and 504B) showing the lithological variations with depth into the volcanic basement. Heights at which bioalteration textures have been studied using scanning electron microscopy (SEM), X-ray mapping (X) and carbon isotopes (C) are shown along with the numbers of samples collected

in Dmitriev et al. (1978) and Detrick et al. (1988) respectively. Pillow lava is the dominant lithology of the ocean crust drilled at these sites, and varies in age from Quaternary to Early Cretaceous. The depth of penetration into the volcanic basement at these drill sites ranges from 33.3 m to 555 m, and the core recovery ranges from 15% in the youngest (648B) to 72% in the oldest (417D) crust (see Furnes et al. 2001a).

The samples investigated from the Lau Basin are from ODP Hole 834B (Fig. 5) described by Parson et al. (1992). The age of the ocean crust is Late Miocene, the depth of penetration into the volcanic basement is 272 m, and the core recovery is 28%. The basalts are composed entirely of pillow lavas and/or thin sheet flows.

The samples from the Costa Rica Rift are from DSDP/ODP Holes 504B and 896A (Fig. 5) described by Alt et al. (1993). Hole 504B is located about 200 km south of the Costa Rica Rift spreading centre and penetrates 550 m of volcanic basement that consists of approximately 75% pillow lavas and 25% massive lavas. Hole 896A (cored during Leg 148) is a re-occupation of Hole 678 (cored during Leg 111), where the palaeontological age of the basal sediment is 5.8–6.4 Ma which is consistent with the ages of the basal sediments of Hole 504B (5.9 Ma) (Alt et al. 1993). The penetration into the basement here was 273.9 m and the volcanic sequence was composed of approximately 60% pillow lava and 40% massive flows (Alt et al. 1993). The core recovery rate was 22% and 27% for Holes 504B and 896A, respectively.

3.2 Ophiolites

The ophiolites from which we present data range in age from Cretaceous to middle Proterozoic. The degree of lithological preservation in these investigated ophiolites varies from a complete Penrose-type ophiolite stratigraphy to dismembered parts of such sequences. We present the detailed volcanic stratigraphy for five of the most complete ophiolites examined in this study (Fig. 6). The degree of deformation varies from undeformed to highly deformed and the metamorphic grade from zeolite to blueschist facies metamorphism. The pillow lavas from the Cretaceous Troodos (Fig. 7A) and Kizildag (Fig. 7B) ophiolites, the Jurassic Mirdita (Fig. 7C) ophiolite, and a Jurassic Californian Coast Range ophiolite fragment (Fig. 7D) are all undeformed, whereas those from the Upper Ordovician Solund-Stavfjord ophiolite (Fig. 8A,B) and the middle Proterozoic Jormua ophiolite (Fig. 8C) vary from little- to highly-deformed. A blueschist pillow breccia from Corsica is shown in Fig. 9A alongside blueschist grade pillow lavas from the Franciscan complex of California in Fig. 9B,C.

3.2.1 Troodos

The Cretaceous Troodos ophiolite of Cyprus (Fig. 10) contains all the components of a Penrose-type complete ophiolite (harzburgite, overlain by layered cumulates, high-level gabbros and trondhjemites, a sheeted dike complex and mafic extrusive rocks) and represents one of the most thoroughly investigated terrestrial fragments

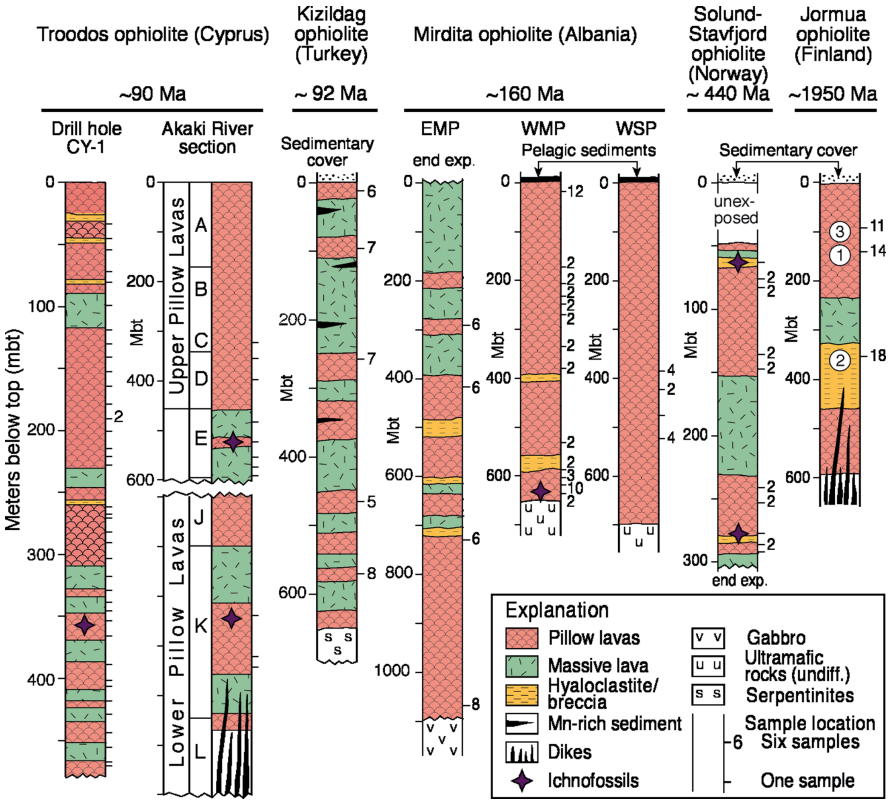

Fig. 6 Compilation of stratigraphic sections measured through the ~90 Ma Troodos ophiolite of Cyprus from drill hole CY-1 and the Akaki River (see also Fig. 10); the ~92 Ma Kizildağ ophiolite of Turkey (see also Fig. 11); the ~160 Ma Mirdita ophiolite of Albania at three sites EMP (eastern main profile), WMP (western main profile) and WSP (western sub-profile) (see also Fig. 12); the ~440 Ma Solund-Stavfjord ophiolite (SSOC) of Norway (see also Fig. 15); and the ~1950 Ma Jormua ophiolite of Finland (see also Fig. 16). The heights at which bioalteration textures or so called ichnofossils have been found are shown by a red star along with the number and positions of samples collected

of ancient oceanic crust (e.g., Panayiotou 1980; Malpas et al. 1990). More than half of the volcanic rocks are pillow lavas, and the remainder are breccias associated with pillow lavas and sheet flows (Schmincke and Bednarz 1990). Samples were taken from various well-exposed parts of the volcanic sequence, also from the drill core CY-1, and from the Akaki River section (boxed area of Fig. 10; for further details see Fig. 1 in Furnes et al. 2001c).

3.2.2 Kizildag

The Cretaceous (~92 Ma) Kizildag ophiolite complex (KOC) in southern Turkey (Fig. 11) occurs in the same Neo-Tethyan ophiolite belt as the Troodos ophiolite,

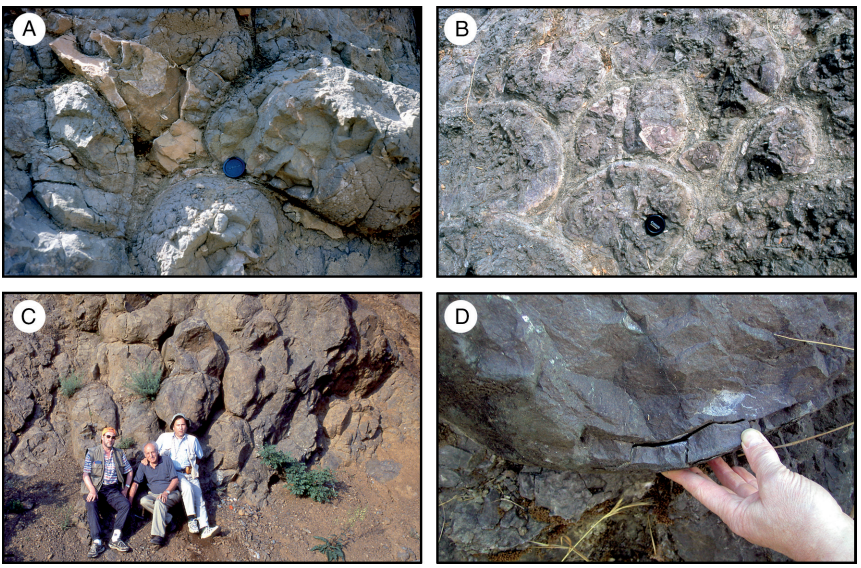

Fig. 7 Outcrop photographs of pillow lavas from: (**A**) the Troodos ophiolite of Cyprus; (**B**) the Kizildag ophiolite of Turkey showing pale *grey*, glassy pillow rims; (**C**) rounded pillows of the Mirdita ophiolite of Albania; and (**D**) the Nicasio Reservoir in California showing the collection of a pillow rim sample. For scale the camera lens cap is 5 cm across

and also displays a complete Penrose pseudostratigraphy. The Kizildag ophiolite rests tectonically on the northwest edge of the Arabian platform and is overlain by Campanian-Maastrichtian clastic sediments. The crustal units of the ophiolite are exposed in a NE-trending, topographically and structurally well-defined graben system, which has been argued to represent a fossilized oceanic spreading axis (Dilek et al. 1998). Based on its internal structure and crustal architecture, the KOC has been interpreted as a slow to intermediate rate spreading axis (Dilek et al. 1998). The extrusive rocks of the KOC form a 300 to 700-m-thick sequences of massive and pillowed lavas intercalated with hyaloclastites, metaliferous umber, and pelagic limestone layers. In addition, there are boninitic lavas which are ~4 Ma younger than the main extrusive sequence. The location of the measured section illustrated in Fig. 6 which was sampled for bioalteration textures is shown on the map in Fig. 11.

3.2.3 Mirdita

The Jurassic (160 Ma) Mirdita ophiolite complex (MOC) in Albania occupies a NNE-SSW-trending corridor within the Dinaride-Hellenide mountain belt of the Alpine-Himalayan orogenic system (Fig. 12). The MOC has been subdivided into western (WMOC) and eastern (EMOC) type complexes based on the rock types and their geochemical characteristics (e.g., Shallo 1995; Dilek et al. 2007). The

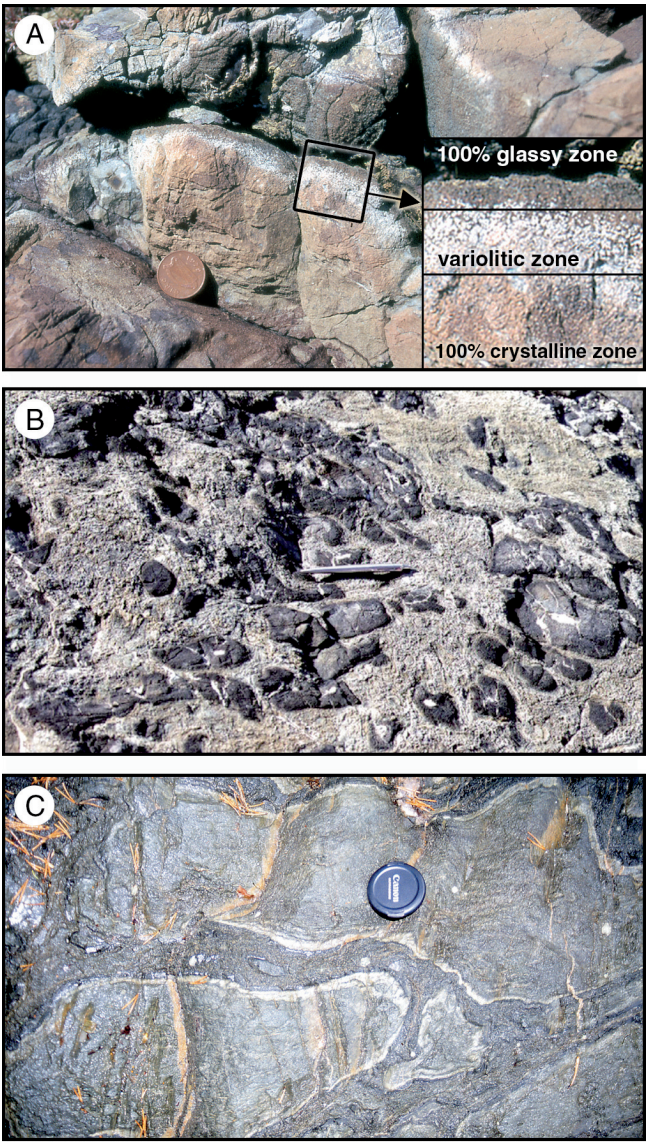

Fig. 8 Outcrop photographs of: (**A**) pillow lavas from the SSOC ophiolite of Norway with an enlarged view of the variolitic zone that occurs around a centimeter inwards of the glassy pillow rim; (**B**) a hyaloclastite breccia also from the SSOC; (**C**) flattened pillow lavas from the upper greenschist grade Jormua ophiolite of Finland. For scale the camera lens cap is 5 cm across

ca. 6-km-thick WMOC contains ~700 m of volcanic rocks composed mainly of MORB-type pillow basalts (Shallo 1995; Bebien et al. 1998), which rest directly on gabbros or mantle lherzolites and/or harzburgites. A well-developed sheeted dike complex is absent within the WMOC, though locally dike swarms and numerous

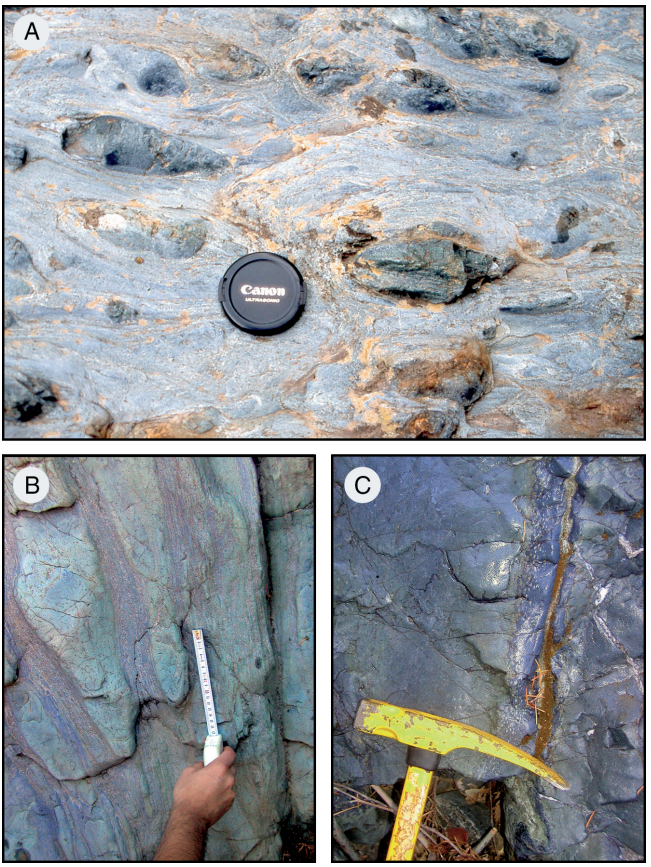

Fig. 9 Outcrop photographs of pillow breccias and pillow lavas from: (**A**) the blueschist grade metabasites of Corsica; (**B**) flattened, blueschist grade pillows from Ward Creek (California) with "streaky" pillow rims; (**C**) glassy pillow rim also from Ward Creek with the variolitic zone (white spots in distinctive blue zone) still visible

single dikes crosscut the peridotites and the lavas. The ca. 10-km-thick EMOC contains a ∼1.1 km thick heterogeneous extrusive sequence consisting of pillowed basalts and basaltic andesite, with massive flows of andesite, dacite, and rhyolite; also sheeted dike swarms composed of the above-mentioned lava compositions and boninites. The EMOC is intruded by numerous small to large diorite bodies. There is no apparent tectonic break between the western- and eastern-type sequences of the MOC and recent studies by Nicolas et al. (1999) have ascribed the contrast between the WMOC and EMOC to successive episodes of magmatic and amagmatic spreading in a slow-spreading environment. Samples were collected from pillow lava rinds from both the WMOC and the EMOC. The profiles from which samples have been collected are shown in Fig. 12.

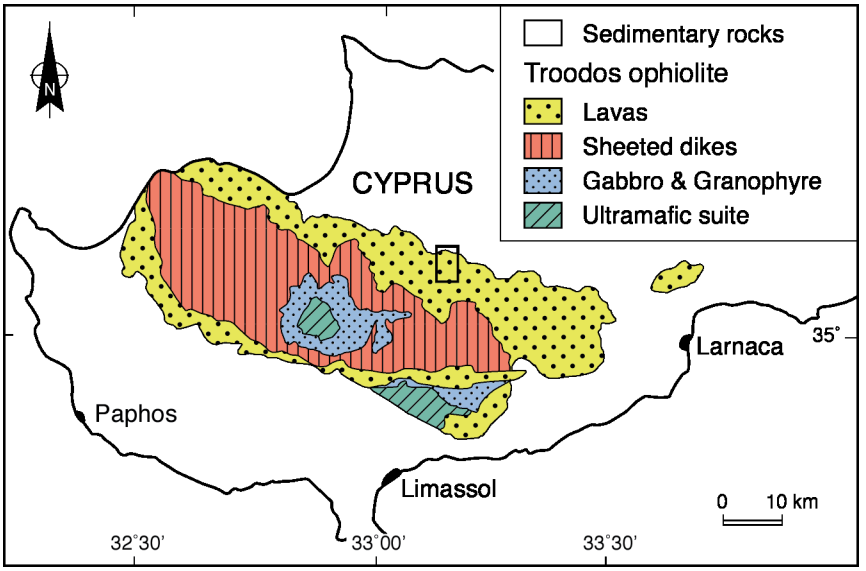

Fig. 10 Schematic geological map of the ~90 Ma Troodos ophiolite in Cyprus. The location of the Akaki River section and drill core CY-1 (shown in Fig. 6) is shown by the boxed area within the lava section. Map is modified from Furnes et al. (2001c)

3.2.4 California: Nicasio Reservoir and Ward Creek

In California, fragments of Jurassic-aged oceanic crust are exposed both in coherent sequences within the California Coast Range Ophiolite (CCRO), as well as in tectonic blocks within the Franciscan Complex. Submarine lavas in the CCRO were recrystallized under zeolite, prehnite-pumpellyite, and greenschist facies conditions during ocean-floor metamorphism (Schiffman et al. 1984, 1991; Evarts and Schiffman 1983). Submarine lavas within the Franciscan Complex were metamorphosed in a subduction zone setting and exhibit zeolite, blueschist- and eclogite-facies metamorphism (Wakabayashi 1999; Swanson and Schiffman 1979). Samples were collected from two pillow lava locations the Nicasio Reservoir and the Ward Creek of low- and high-grade metamorphism, respectively, both are within the Central Belt of the Franciscan Complex (Fig. 13).

The Nicasio Reservoir pillow lava pile is over 1 km thick and associated with a structural horizon that is intermediate within the Franciscan Complex (Wakabayashi 1992). The pillows are undeformed and their mineral composition includes albitized plagioclase phenocrysts, in a matrix of chlorite, pumpellyite, and laumonite. The metamorphic grade is thus of zeolite to prehnite pumpellyite facies (Swanson and Schiffman 1979). This pillow lava pile is considered to represent part of a seamount that became incorporated into the Franciscan subduction complex in late Mesozoic/early Cenozoic time (Cloos 1990).

The Ward Creek pillow lavas form part of a complex association of tectonic blocks of metabasaltic rocks, serpentinites, metagreywackes and glaucophane-bearing rocks

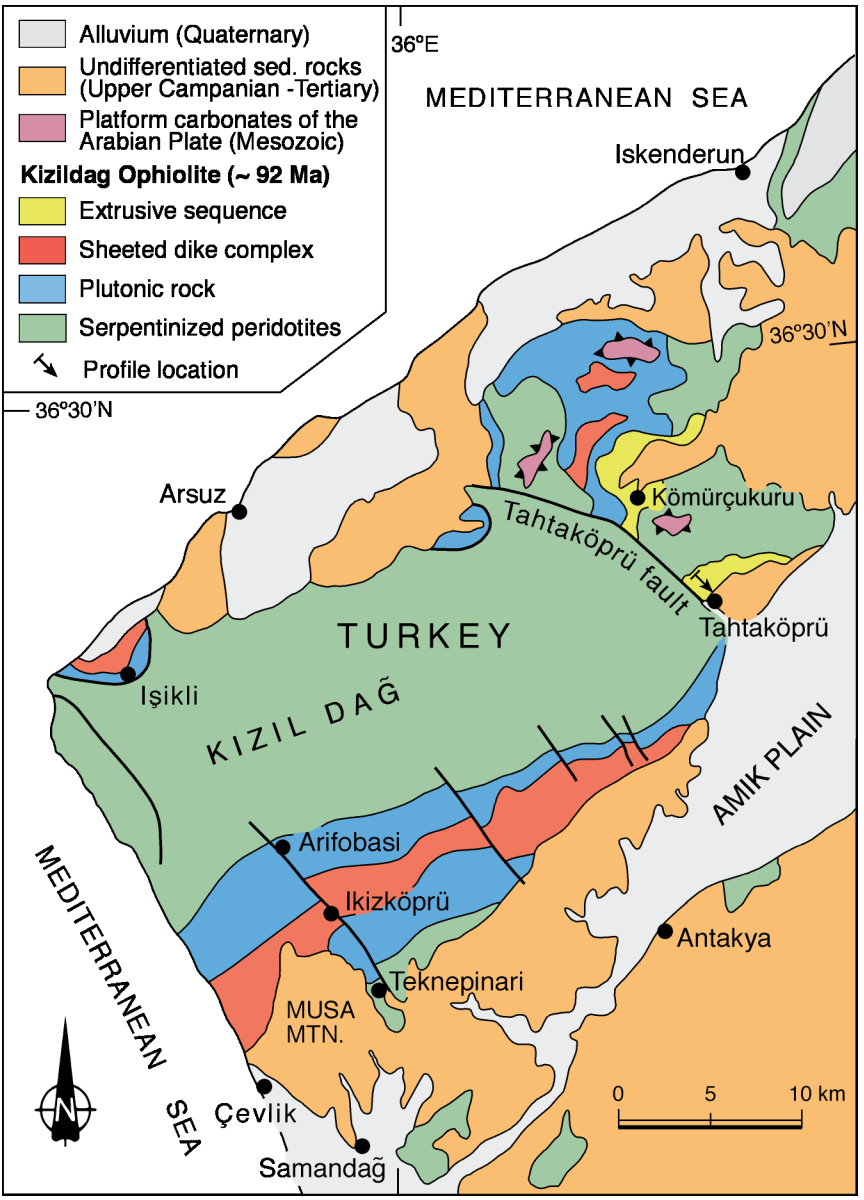

Fig. 11 Schematic geological map of the ~92 Ma Kizildağ ophiolite in Turkey showing the location of the measured section given in Fig. 6. Map is modified from Dilek and Thy (1998)

that were described by Coleman and Lee (1963). These high-pressure low temperature metamorphic rocks preserve various metamorphic grades such as lawsonite-, pumpellyite-, and epidote-zones (Maruyama and Liou 1988). In the lawsonite and pumpellyite zones pillow structures and primary igneous textures are well-preserved,

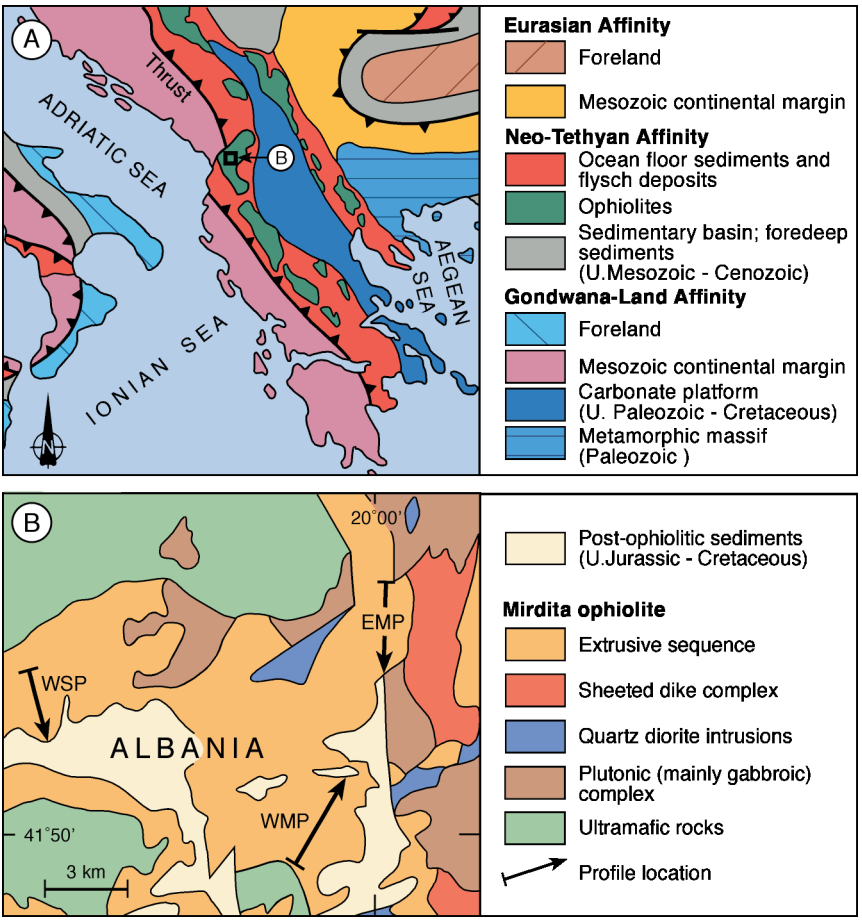

Fig. 12 (**A**) regional geological map of Albania and adjacent countries; (**B**) enlarged geological map of part of the ~160 Ma Mirdita ophiolite in Albania showing the location of the measured sections WSP (western sub-profile), WMP (western main profile) and EMP (eastern main profile) shown in Fig. 6. Map is modified from Dilek et al. (2007)

whereas in the epidote-zone the metabasalts which contain glaucophane and red garnet (~ 290°C, 6.5–9 Kb) are more strongly deformed, their primary igneous textures are largely obliterated, although pillow structures can still be discerned (Fig. 9B,C).

3.2.5 Corsica

Ophiolitic rocks and associated sedimentary rocks (Fig. 14) that represent the remnants of the former Mesozoic Ligurian Tethys Ocean are found in the north/northeastern part of Corsica (Lemoine et al. 1987). These ophiolitic units occur in nappe sheets emplaced during the Alpine orogeny (Ohnenstetter et al. 1976) and

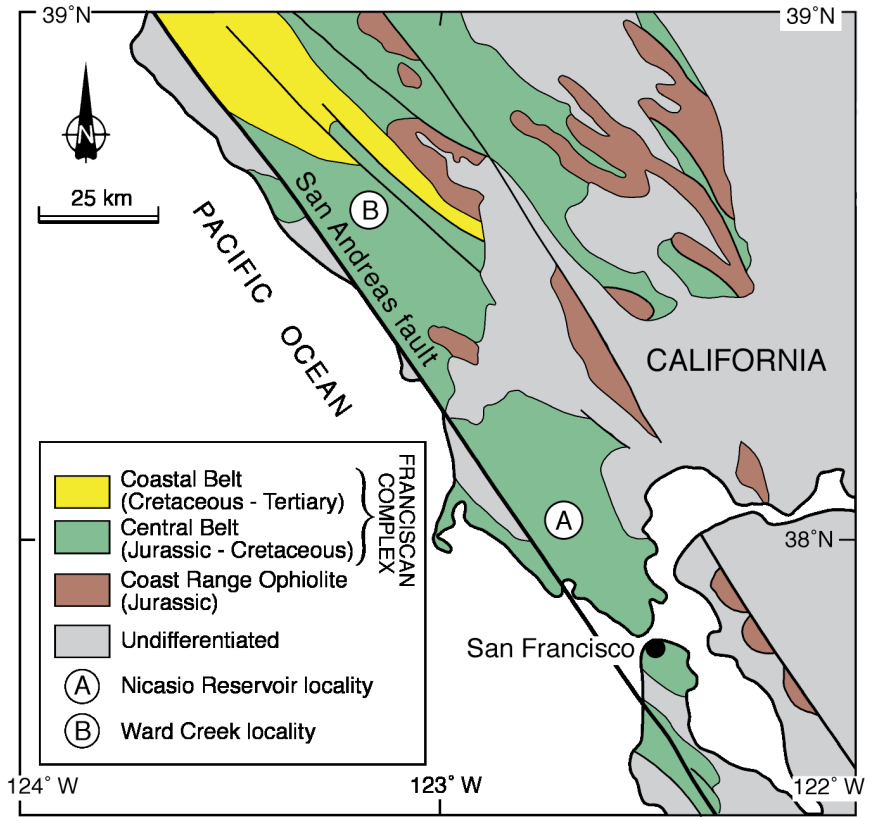

Fig. 13 Schematic geological map of north western California showing the Franciscan Complex sampled at the zeolite grade Nicasio Reservoir (**A**) and the blueschist grade Ward Creek (**B**) localities. Map is modified from Coleman (2000) and Ingersoll (2000)

experienced high pressure low temperature blueschist metamorphism with relics of eclogites (Ohnenstetter et al. 1976; Dal Piaz and Zirpoli, 1979; Fournier et al. 1991). The blueschist-facies pillow lavas and pillow breccias (Fig. 9A) have been subject to pressure of at least 11 kbar (Fournier et al. 1991). Sampling locations are shown in Fig. 14.

3.2.6 Solund-Stavfjord

The Late Ordovician (443 +/ − 3 Ma) Solund-Stavfjord ophiolite complex (SSOC) in the western Norwegian Caledonides (Fig. 15) displays a well-preserved, ca. 800-m-thick volcanic sequence of basaltic pillow lavas and pillow breccias (Fig. 8A,B), sheet flows and volcanic breccias, a ca. 1000-m- thick sheeted dike complex and minor amounts of high-level gabbro (Furnes et al. 2001d, and references therein). These volcanic rocks experienced pervasive lower greenschist facies

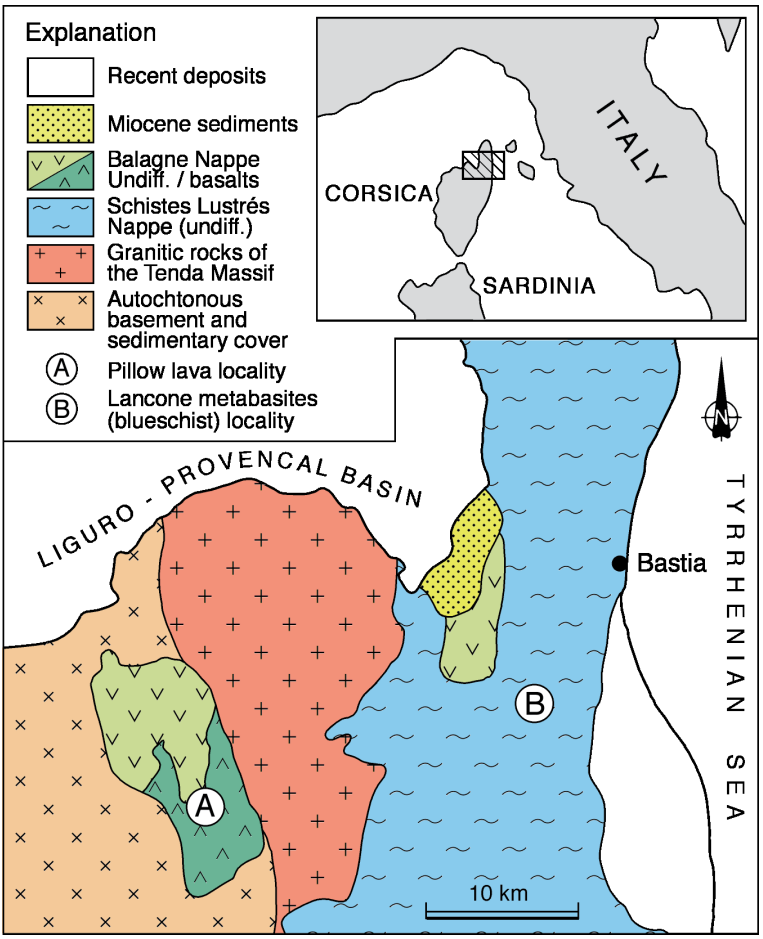

Fig. 14 Schematic geological map of the Mediterranean Island of Corsica showing the Jurassic pillow basalt locality (**A**) and the blueschist metabasite locality (**B**) also illustrated in Fig. 9A. Map is modified from Daniel et al. (1996)

metamorphism (chlorite, actinolite and epidote form the principal minerals). The extent to which the volcanic rocks were deformed varies significantly depending on their position in major folds (Furnes et al. 2001d).

3.2.7 Jormua

The Jormua ophiolite complex (JOC) is located in central northern Finland (Fig. 16) and contains all of the principal components of a Penrose-type ophiolite, i.e. pillow lavas and volcanic breccias, a sheeted dike complex, plutonic rocks, and mantle peridotites (Kontinen 1987). The age of the complex has been determined as 1.95 Ga (Peltonen et al. 1996). The volcanic sequence consists of pillow lavas, pillow

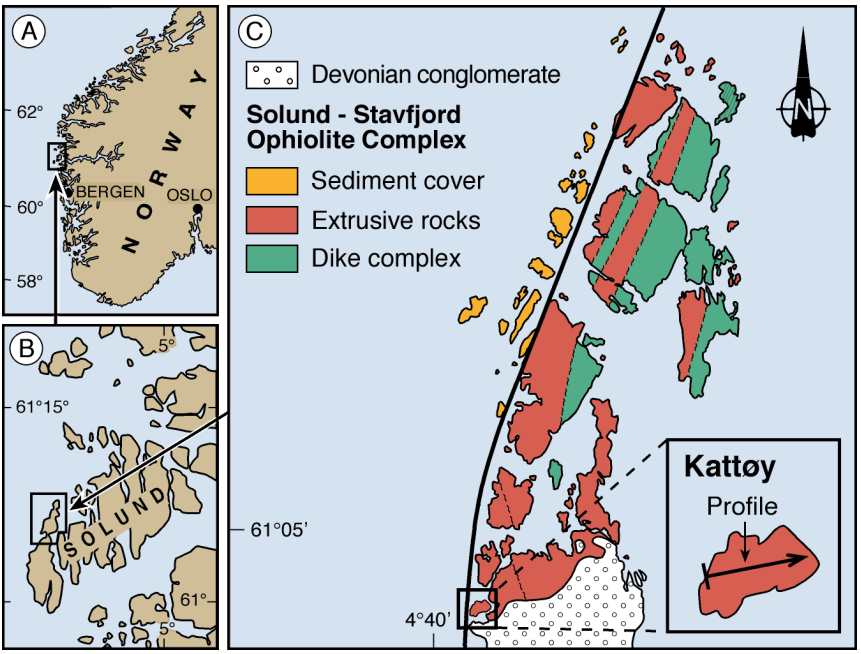

Fig. 15 Regional map of the ~440 Ma Solund-Stavfjord Ophiolite Complex (SSOC) of Norway (**A** and **B**), with an enlarged map (**C**) showing a schematic geological map and the location of the measured profile given in Fig. 6 from the extrusive rocks of Kattøy which contain bioalteration textures. Map is modified from Furnes et al. (2002a)

breccias and hyaloclastites (Fig. 8C) and its thickness appears to be at least 500 m. The volcanic rocks and the sheeted dikes experienced lower amphibolite-facies metamorphism, as evidenced by the mineral assembly composed of pale-green amphibolite, oligoclase-andesine plagioclase, epidote and chlorite (Kontinen 1987). The volcanic rocks also display a pronounced foliation.

3.3 Greenstone Belts

Greenstone belts are deformed sequences of Archean and Proterozoic rocks comprising meta-volcanic rocks and intercalated metasedimentary rocks that are preserved between granitoid complexes. Greenstone belts that were sampled for bioalteration studies include the Barberton greenstone belt of South Africa, the Pilbara Supergroup of Western Australia and the Pechenga greenstone belt of Russia (Fig. 17), ranging in age from Middle Proterozoic to MesoArchean. In addition restricted sampling has been undertaken in the PaleoArchean Isua supracrustal belt of Greenland, and in the NeoArchean Wutai, China (N. McLoughlin et al., unpub. data), and Abitibi greenstone belt, Canada (N. Banerjee et al. unpub. data). The

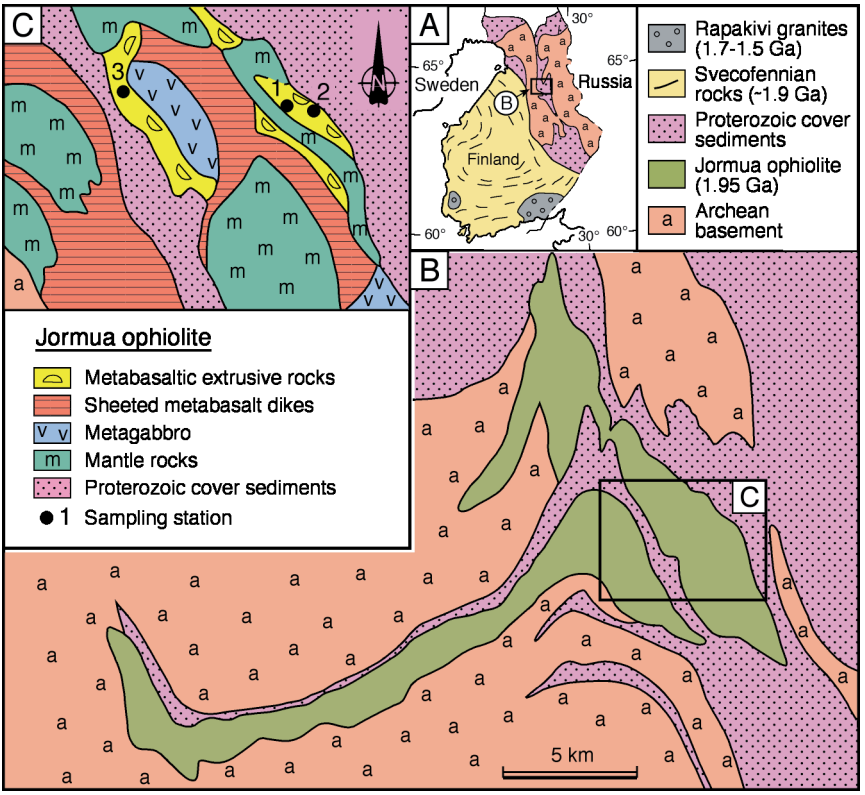

Fig. 16 (**A**) regional geological map of northern Finland and Russia showing the location of the ~1.95 Ga Jormua ophiolite; (**B**) enlarged geological map, and (**C**) showing the location of sampling stations 1–3 in the metabasaltic extrusive rocks shown in the composite section in Fig. 6. Map is modified from Furnes et al. (2005)

preservation of pillow lavas is remarkably good at all of these sites (see Fig. 18) and an overview of their stratigraphy is given below.

3.3.1 Isua Supracrustal Belt, West Greenland

The Paleoarchaean Isua supracrustal belt (ISB) is situated in southwest Greenland and contains metabasalts (amphibolite), metagabbros and ultramafic rocks that are associated with metapelites, cherts, banded iron formation (BIF) and felsic rocks (e.g., Nutman 1986; Rosing et al. 1996). The rocks are in general strongly deformed and metamorphosed to amphibolite facies. Primary features are scarce and their protoliths are a matter of debate, but undisputable (ocelli bearing) pillow lavas have been found within the metabasalts (Komiya et al. 1999; Myers 2001). A whole rock Sm-Nd isochron (amphibolite-grade meta-basaltic pillows and metagabbro) defines an age of 3777 +/− 44 Ma (Boyet et al. 2003). Komiya et al. (1999)

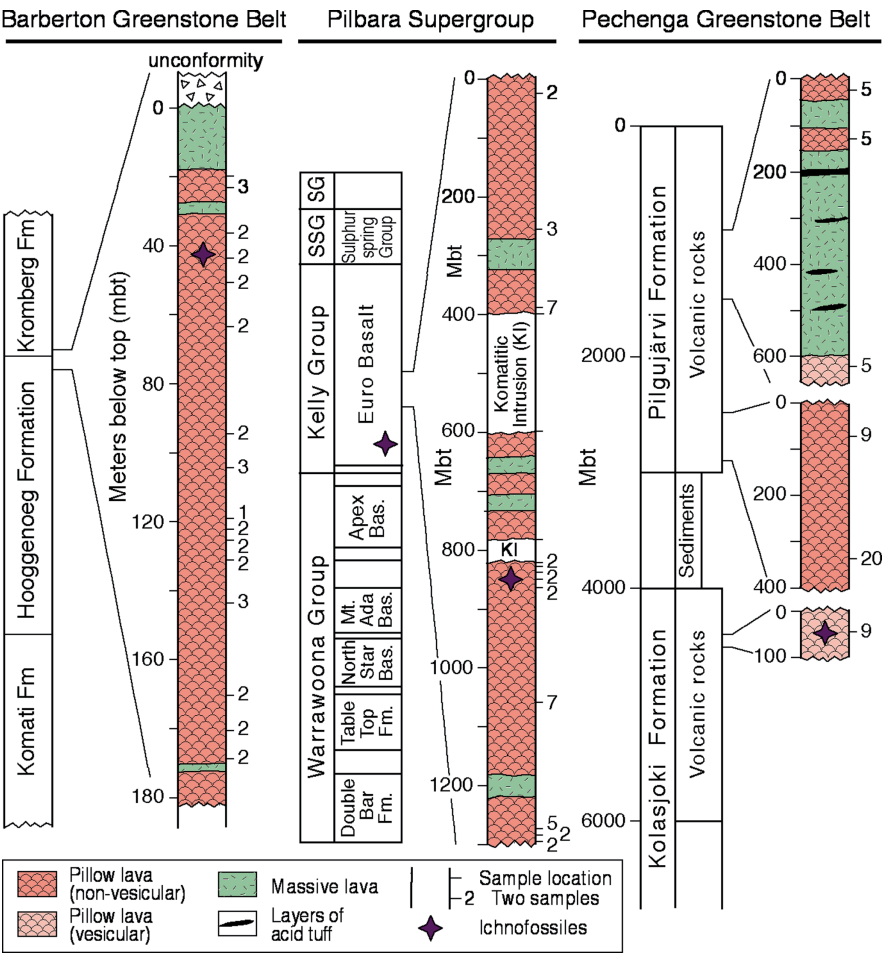

Fig. 17 Compilation of stratigraphic sections measured from the ~3.5 Ga upper Hooggenoeg and lower Kromberg Formations of the Barberton greenstone belt of South Africa (see also Fig. 19) (modified from de Wit et al. 1987); the ~3.4 Ga Euro Basalt of the Kelly Group of the Pilbara Supergroup of Western Australia (see also Fig. 20) (modified from Van Kranendonk 2006. Note that the unlabelled boxes represent acid volcanics and cherts); and volcanic rocks from the ~2.0 Ga Pilgujärvi and Kolasjoki Formations of the Pechenga greenstone belt Russia (see also Fig. 21) (modified from Melezhik et al. 2007). The bioalteration localities from the *upper part* of the Hooggenoeg Formation and the *lower part* of the Euro Basalt (indicated within the box) are from Furnes et al. (2004) and Banerjee et al. (2007), respectively. The bioalteration localities from the middle part of the Euro Basalt and from the upper part of the Kolasjoki Formation are unpublished

suggested that this oceanic-like crust may have been emplaced within an accretionary wedge around 3.7 Ga and Furnes et al. (2007b) reported the occurrence of a sheeted dike complex suggesting the presence of a c. 3.8 Ga ophiolite in the Isua supracrustal belt.

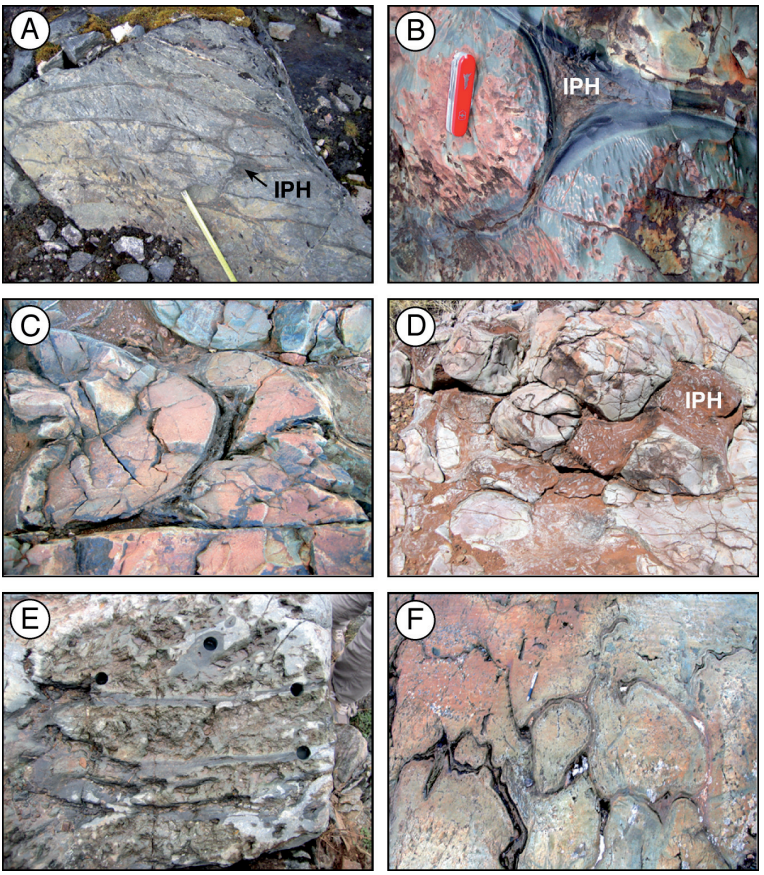

Fig. 18 Outcrop photographs of: (**A**) deformed pillow lavas exhibiting chilled margins (dark selvages) and pockets of inter-pillow hyaloclastite (IPH) from the ~3.8 Ga Isua supracrustal belt, West Greenland; (**B**) pillow lavas from the ~3.5 Hooggenoeg Formation of the Barberton greenstone belt in South Africa with dark glassy rims and a pocket of interpillow hyaloclastite (see also Fig. 19); (**C**) pillow lavas from the ~3.4 Ga Euro Basalt of the Pilbara Craton, Western Australia (see also Fig. 20); (**D**) carbonate altered pillow lavas from the ~3.4 Ga Euro Basalt of the Pilbara Craton, Western Australia displaying large pockets of inter-pillow hyaloclastite; (**E**) flattened pillow lavas from the ~2.5 Ga Wutai Group of the North China Craton, showing well preserved pillow rims that have been sampled by micro-drilling; (**F**) pillow lavas from the ~2.0 Ga Pechenga greenstone belt of the Kola Peninsula, Russia

3.3.2 Barberton Greenstone Belt, South Africa

The Mesoarchean Barberton greenstone belt, South Africa (Fig. 19) contains some of the world's oldest and best-preserved pillow lavas (de Wit et al. 1987; Brandl and de Wit 1997). The magmatic sequence comprises 5–6 km of predominantly basaltic and komatiitic extrusive (pillow lavas, minor hyaloclastite breccias and sheet flows) of the Theespruit, Komati, Hooggenoeg, and Kromberg Formations of the ca. 3.52–3.35 Ga Onverwacht Group, and subordinate intrusive rocks. This igneous

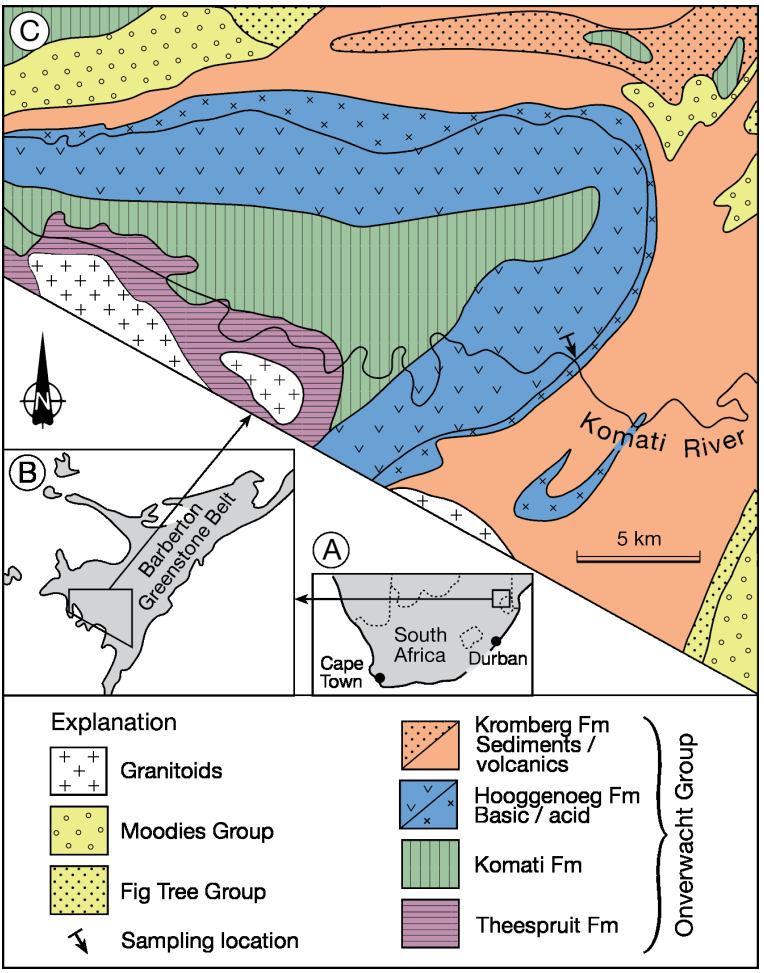

Fig. 19 (**A**) Regional map showing the location of the Barberton greenstone belt in South Africa, enlarged in (**B**) with a simplified geological map of the Onverwatch antiform shown in (**C**) giving the location of the measured section through the Hooggenoeg Fm and sample sites shown in Fig. 17. Map is modified from de Wit et al. (1987)

sequence is intercalated with chert layers and is overlain by cherts, banded iron formations (BIF) and shales. The Onverwacht Group has been interpreted by some workers to represent a fragment of Archean oceanic crust, termed the Jamestown Ophiolite Complex (de Wit et al. 1987; de Wit 2004), that developed in a successor subduction environment at between approximately 3480–3220 Ma (Armstrong et al. 1990; de Ronde and de Wit 1994). Moving upwards from the middle to the upper part of the Onverwacht Group the metamorphic grade decreases from greenschist to prehnite-pumpellyite facies. Stratigraphically downward into the Theespruit Formation, there is a rapid increase in the metamorphic grade to lower amphibolite facies (de Ronde and de Wit 1994).

3.3.3 Pilbara Craton, Western Australia

The Pilbara Craton, Western Australia (Fig. 20) contains some of the best preserved geological record of the early Earth (Van Kranendonk and Pirajno 2004; Van Kranendonk et al. 2002, 2004, 2007). The ancient nucleus of the craton is preserved in the East Pilbara Terrane, which contains a 20-km-thick succession of low-grade metamorphic, dominantly volcanic supracrustal rocks of the Pilbara Supergroup that were deposited in four autochthonous groups from 3.52–3.165 Ga (Van Kranendonk 2006; Van Kranendonk et al. 2007). These include, from base to top, the 3.52–3.43 Ga Warrawoona Group, the 3.42–3.31 Ga Kelly Group, the 3.27–3.23 Ga Sulphur Springs Group, and the 3.23–3.165 Ga Soanesville Group. Pillows and interpillow hyaloclastites were collected from the Dresser Formation

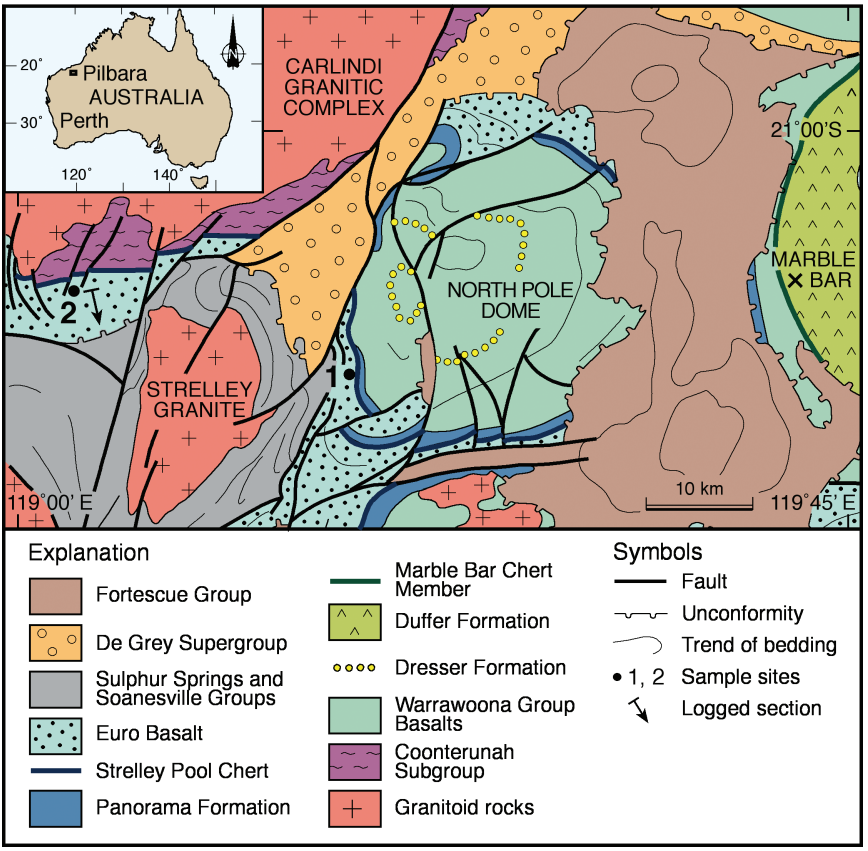

Fig. 20 Simplified geological map of the Pilbara region of Western Australia showing the location of sample sites 1 and 2 where bioalteration has been identified within the Euro Basalt of the Kelly Group and the location of the section measured at site 2 that is illustrated in Fig. 17. Map is modified from Van Kranendonk (2006)

and Apex Basalt of the Warrawoona Group and the Euro Basalt of the Kelly Group. To date, bioalteration textures have only been found in the Euro Basalt (Fig. 20).

3.3.4 Wutai Group, North China Craton

In the Eastern Block of the North China Craton, oceanic pillow lavas form part of the Wutai Group (Fig. 21) which consists of late Archean to Paleoproterozoic granitoid rocks and metamorphosed volcanic and sedimentary rocks (Zhou et al. 1998; Zhao et al. 2001). Traditionally, the Wutai Group has been considered a typical greenstone belt (Zhai et al. 1985; Kröner et al. 2001) and zircon ages for the complex range in age from 2.52 Ga to 2.57 Ga (Kröner et al. 2001). Deformed, yet well-preserved pillow lavas occur in the Baizhiyan Formation of the Middle Wutai Group. They are

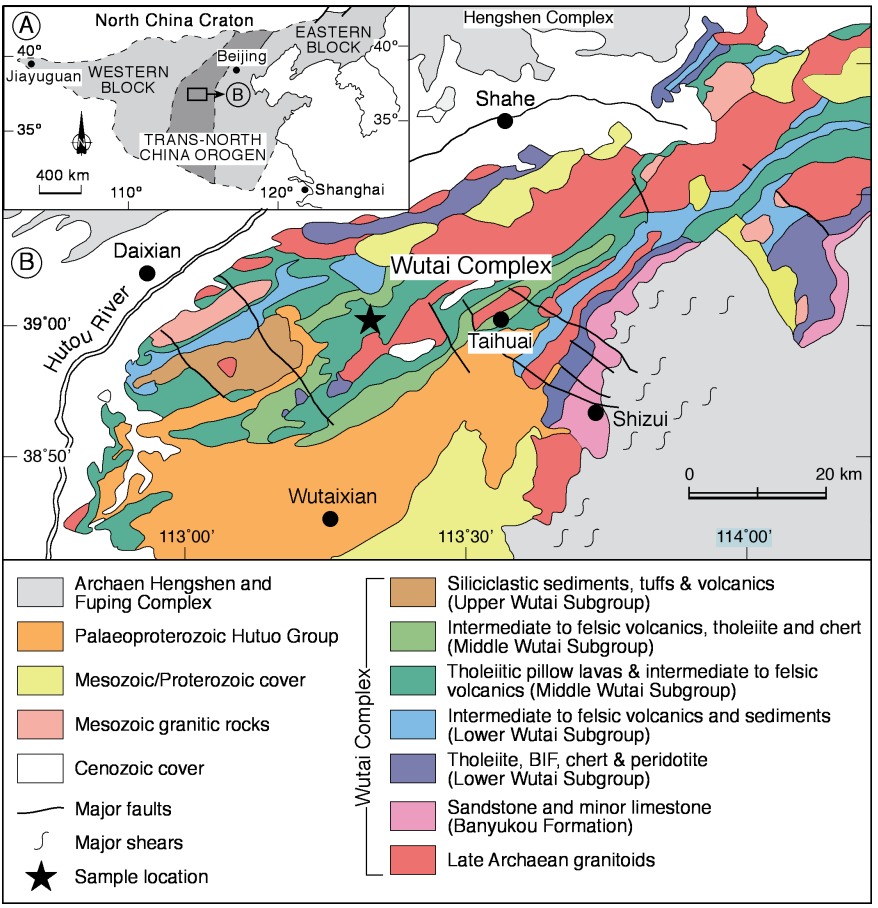

Fig. 21 Geological map of the North China Craton, and the Wutai Complex within the Trans-North China Orogen. Pillow lavas sampling (shown by star) was undertaken within the greenschist facies tholeiites of the Middle Wutai Subgroup. Map is modified from Zhao et al. (2001)

delineated by 1–2 cm wide epidote-rich rims that surround a core of fine-grained material composed chiefly of chlorite, carbonate, albite and epidote. A variety of mafic and felsic lavas and tuffs are associated with the pillow lavas, ranging in composition from MORB-like basalts to calc-alkaline andesites and rhyolites (Kröner et al. 2001).

3.3.5 Pechenga Greenstone Belt, Kola Peninsula, Russia

The Paleoproterozoic Pechenga greenstone belt (Fig. 22) is in the Russian part of the Fennoscandian Shield situated in the Kola Peninsula (Melezhik and Sturt 1994). The > 10-km-thick Northern Pechenga Group is composed of four sedimentary-volcanic cycles whose evolution spans more than 400 Ma of Earth history with a total thickness of more than 10 km. Although the rocks have experienced polyphase metamorphism ranging from prehnite-pumpellyite to upper amphibolite grades, their sedimentary and volcanic features are locally well preserved.

The most voluminous of the volcanic units is the 3-km-thick uppermost Pilgujärvi Volcanic Formation. The bulk of the Pilgujärvi volcanic rocks are submarine

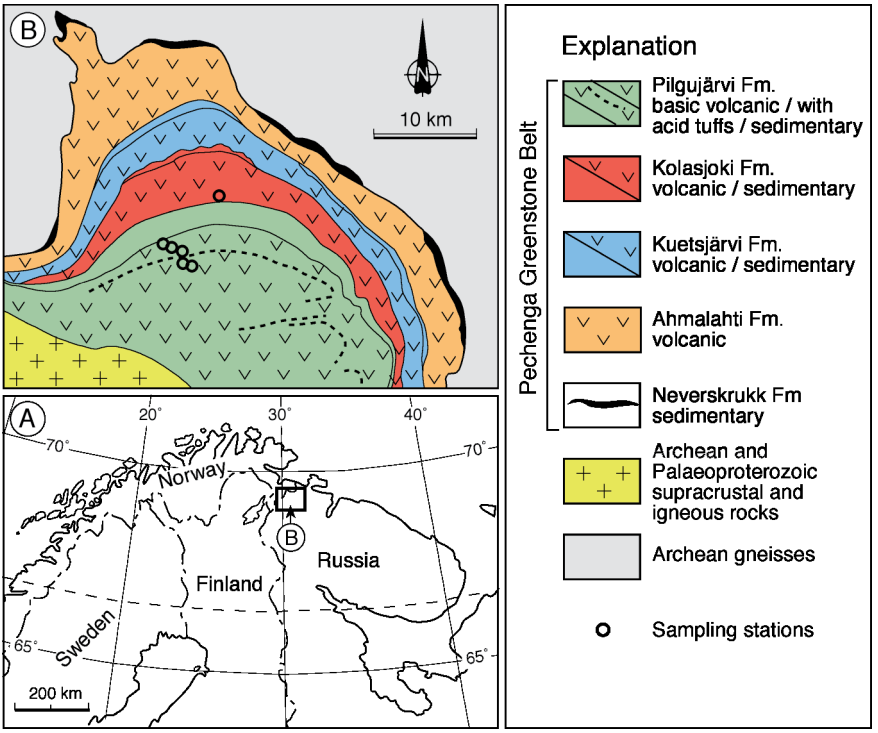

Fig. 22 (**A**) regional location map of the Pechenga greenstone belt of the Kola Peninsula, Russia; (**B**) simplified geological map showing sampling sites for bioalteration studies in volcanic horizons of the Pilgujärvi and Kolasjoki Formations. Map is modified from Melezhik and Sturt (1994)

tholeiitic basalts occurring as massive and pillowed lavas and hyaloclastites. An acid tuffaceous unit with a thickness of a few tens of meters occurs in the middle part of the formation (Fig. 22). U-Pb, Sm-Nd and Rb-Sr systems have yielded ages of ca. 1980 Ma for ferropicritic and tholeiitic metavolcanites and genetically related intrusive rocks from the Pilgujärvi Volcanic Formation (Hanski et al. 1990; Balashov 1996; Smolkin et al. 2003). A similar U-Pb zircon age (1970 ± 5 Ma; Hanski et al. 1990) has also been obtained for a thin felsic unit.

4 Bioalteration Textures in Pillow Lava and Hyaloclastite

Textures that we ascribe to microbial dissolution of originally glassy pillow lava rims and hyaloclastites have been found in sequences ranging in age from recent to 3.5 Ga. In this section, we document some of the most characteristic bio-generated textures from *in-situ* oceanic crust, ophiolites and greenstone belts.

4.1 Modern Oceanic Crust

Granular bioalteration (Fig. 23) does not generally display symmetrical arrangement on the opposite sides of fractures along which it develops with a variable thickness and distribution. Thus, we can distinguish the bands and aggregates of granular alteration from the more symmetric alteration produced by abiotic palagonitization (e.g., Fig. 1 lines A and B). Locally, banded abiotic palagonite can be found in the centre of a fracture with granular or tubular textures occupying the outermost interface with the fresh glass (e.g., Fig. 23D). Less commonly, granular and tubular textures can be seen on the opposite sides of the same fracture (e.g., Fig. 23F). The diameter of the granules, regardless of age, location, as well as depth into the crust, varies from 0.1 μm to 1.4 μm, with the most common size around 0.4 μm (Furnes et al. 2007a).

The tubular bioalteration textures are most typically unbranched, straight and/or curved (Fig. 23A,B,C,F and Fig. 24) although rare, branched examples also occur (e.g., Fig. 23H,I). With progressive bioalteration they develop from small, isolated individuals into dense bundles of long, numerous tubes originating from fractures in the glass (Fig. 23C). Individual tubes may show segmentation and localized swellings (e.g., Fig. 24E,F). In some cases the tubes propagate perpendicular to the alteration front (e.g., Fig. 23F), although random orientations are also common (Fig. 24C). Rare tube alignment, independent from the orientation of the fracture in which the tubes are rooted is attributed to tube-propagation controlled by strain-orientation in the glass (Furnes et al. 2001b). In samples that contain vesicles and or varioles the tubes can be seen to have grown radially outwards into the fresh glass (e.g., Fig. 23B). Tubular structures have also been observed to exploit concentric stress fractures that have developed around phenocrysts (e.g., Furnes et al. 2007a). The tubular bioalteration textures are substantially larger than the granular textures, and there is only a minor overlap in their size distributions (Furnes et al. 2007a).

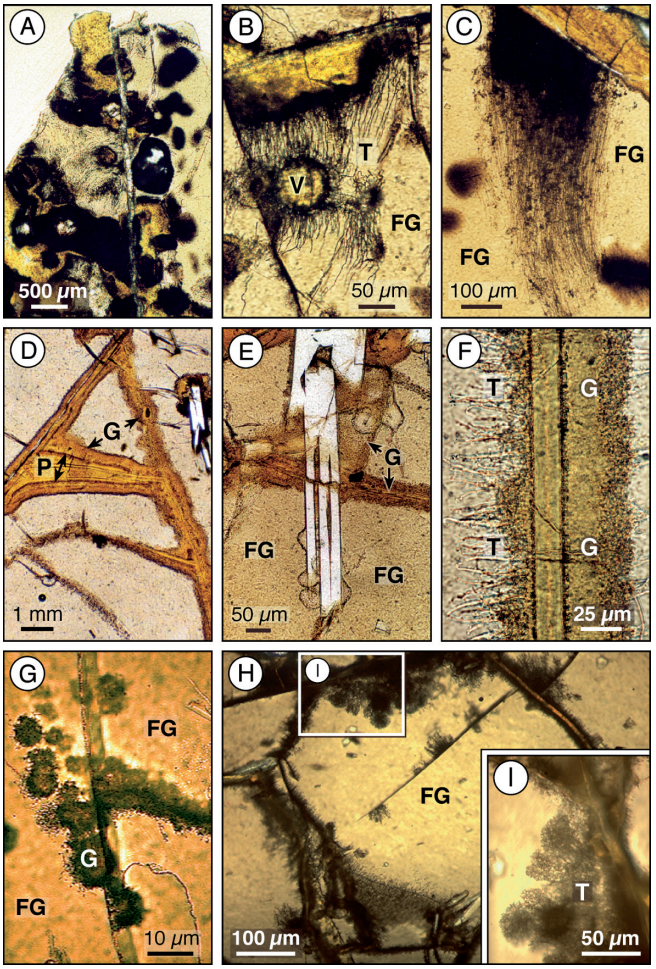

Fig. 23 Transmitted light photomicrographs of microbial alteration textures in volcanic glass from in situ oceanic crust. (**A**) Portion of pillow basalt thin section showing pale-cream glass, *yellow* palagonite alteration, tubular alteration textures enlarged in (**B**) and *dark brown* circular, varioles or quench textures. (B) Enlarged view showing tubular alteration (T) in fresh volcanic glass (FG) radiating from fractures and around a vesicle (V). (**C**) A dense cluster of tubes growing from a palagonite filled fracture in the top of the image. (**D**) Banded palagonite alteration (P) at the centre of fractures in volcanic glass with granular alteration (G) on the outer margins. (**E**) Granular alteration along a fracture in volcanic glass which is interrupted by a large plagioclase phenocryst. (**F**) Fracture in volcanic glass with tubular alteration on the left hand side and granular alteration on the right hand side of the same fracture. (**G**) Granular alteration along intersecting fractures in volcanic glass accompanied by circular clusters of granular alteration in the nearby glass. (**H**) Branched tubes radiating from a network of fractures in a volcanic glass. (**I**) enlarged view showing the dendritic branching. Samples: (**A** and **B**) Hole 396B thin Section 43; (**C**) Hole 418A thin Section 2; (**D**) Hole 418A thin Section 12; (**E**) Hole 418A thin Section 12; (**F**) Hole 896A thin Section 23; (**G**) Hole 396B thin Section 28; (**H** and **I**) Hole 396B thin Section 38; (**I**)

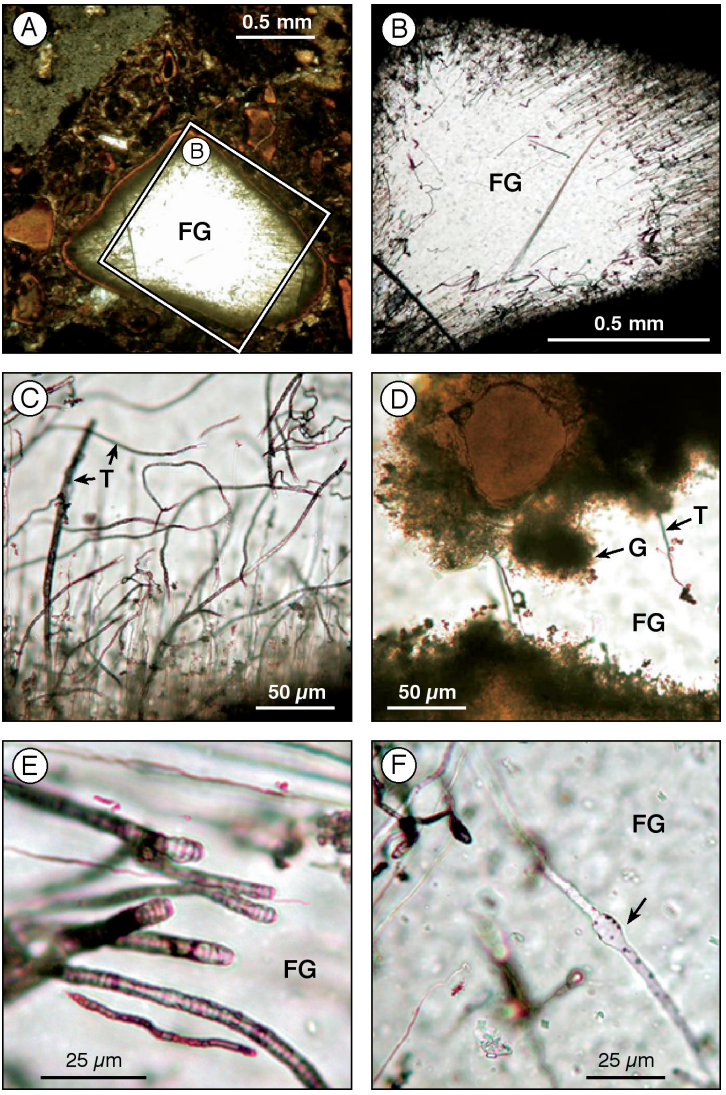

Fig. 24 Transmitted light photomicrographs of microbial alteration textures in volcanic glass fragments in a vitric tuff from the Ontong Java Plateau: (**A**) A glass grain with tubular bioalteration textures radiating inwards from the margin, rimmed by red-brown clay and in a volcaniclastic matrix comprising altered glass and lithic fragments cemented by clay and zeolites. (**B**) Enlarged view showing the tubular alteration textures radiating inwards. (**C**) Assemblage of unbranched tubular (T) structures extending from a granular alteration boundary. (**D**) Granular (G) and tubular alteration textures extending from the clay alteration boundary into fresh glass. (**E**) Tubular structures with dark walls and segmented appearance. (**F**) Hollow tubular structure with swelling (arrowed)

Their diameters range from ~0.5 μm to 6 μm with an average diameter of 1.4 μm (Furnes et al. 2007a). The lengths of the tubes are highly variable, from a few microns up to several hundred microns (Furnes et al. 2007a).

4.2 Ophiolites

Bioalteration textures in pillow lavas and or hyaloclasties from the Troodos, Mirdita and Solund-Stavfjord ophiolite complexes are shown in Fig. 25. In the Troodos ophiolite abundant fresh glass is still present and both granular and tubular textures (Fig. 25A–C) are found at all stratigraphic levels within the lava sequence. These textures occur at the boundary between fresh and altered glass (Fig. 25B). The most common type is the isolated and/or persistent zones consisting of coalesced spherical bodies about 1–3 μm in diameter. Although the alteration is most commonly asymmetrically arranged around cracks, it can also, sometimes be symmetric. In close association with the patches of coalesced spherical bodies are abundant, unbranched mainly straight but also curved tubes that may attain lengths of up to 100 μm (Fig. 25A–C). Spectacular examples of spiral shaped tubes are found, both single helical tubes and forms with a simple central tubular shaft around which is coiled an outer spiralled tube, analogous to a "pogo stick"(Fig. 25C). Another tubular form may reach lengths of up to 500 μm, diameters up to 20 μm and show well-defined segmentation with 5–10 μm spacing and sometimes a terminal swelling. These are generally seen to be closely associated with vesicles, with one end terminating at a vesicle wall (Fig. 25A). These bioalteration textures may be hollow, especially many of the tubular examples or filled with very fine-grained phyllosilicate phase.

The Mirdita ophiolite contains both granular and tubular bioalteration textures preserved in volcanic glass and also zeolites (Fig. 25D–F). Granular alteration textures occur as asymmetric bands along palagonite filled fractures (Fig. 25D) and as cluster in the adjacent glass (Fig. 25F). Simple unbranched tubes, locally with complex twisted shapes are also found (Fig. 25E) both in the fresh glass and in zeolites. These structures are mineralized by titanite.

The Solund-Stavfjord ophiolite contains lower greenschist grade meta-volcanic glass now composed predominantly of chlorite (Fig. 25G,H). This contains band of titanite with tubular projections that are interpreted as mineralized zones of tubular bioalteration.

4.3 Greenstone Belts

In the originally glassy, chilled rim of pillow lavas and associated interpillow hyaloclatites from Barberton, Pilbara, Pechenga and Wutai greenstone belts (Fig. 17) we have found titanite filled tubes, interpreted as mineralized microbial alteration textures (Fig. 26A–D) restricted to localized horizons in the thick volcanic sequences

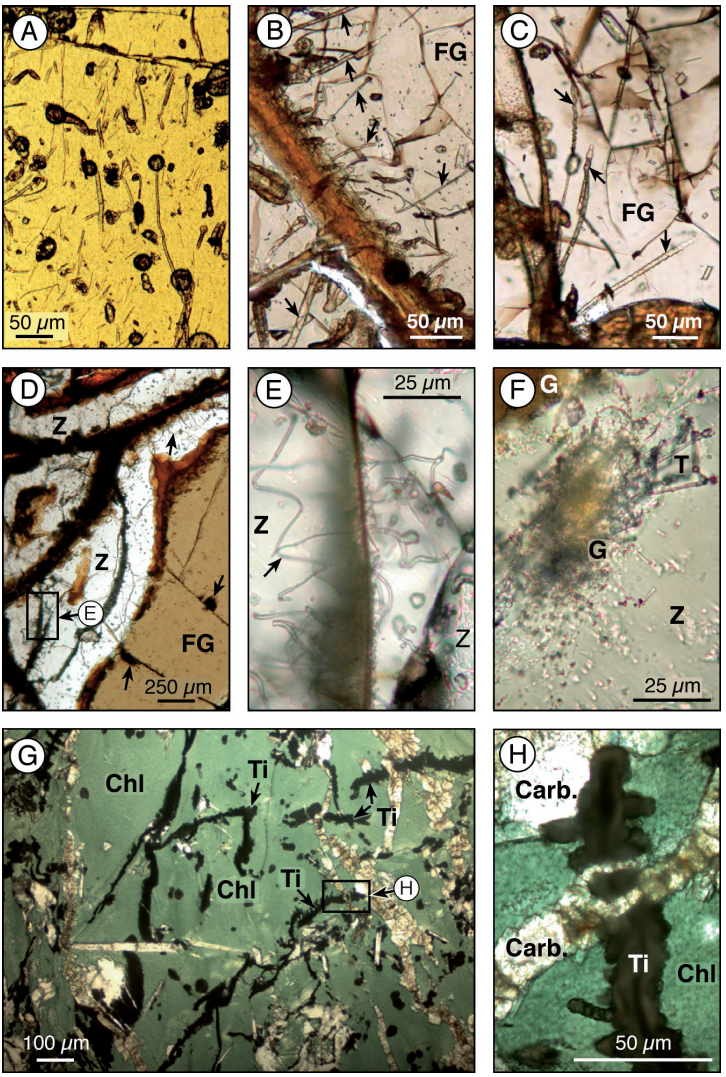

Fig. 25 Transmitted light photomicrographs of microbial alteration textures in (meta) volcanic glass from selected ophiolites. (**A**) Image of volcanic glass from the Troodos ophiolite contains hollow tubular alteration textures aligned largely north-south in this image and large, dark circular vesicles. (**B**) Palagonite filled fractures around the rims of a volcanic glass fragments containing tubular alteration textures arrowed, also from the Troodos ophiolite. (**C**) Alteration textures in volcanic glass from the Troodos ophiolite show a central tube with an outer spiral (arrowed). (**D**) Volcanic glass (FG) from the Mirdita ophiolite with zeolite (Z) and brown palagonite filled fractures. (**E**) Enlarged view showing tubular bioalteration textures preserved in zeolites. (**F**) Cluster of granular (**G**) alteration textures and a few tubes (T) also from the Mirdita ophiolite. (G) Image of meta-volcanic glass from the Solund-Stavfjord ophiolite, matrix is now largely composed of chlorite and contains bands of titanite with tubular projections. (**H**) Enlarged and rotated view of a titanite band with tubular projections on the margins

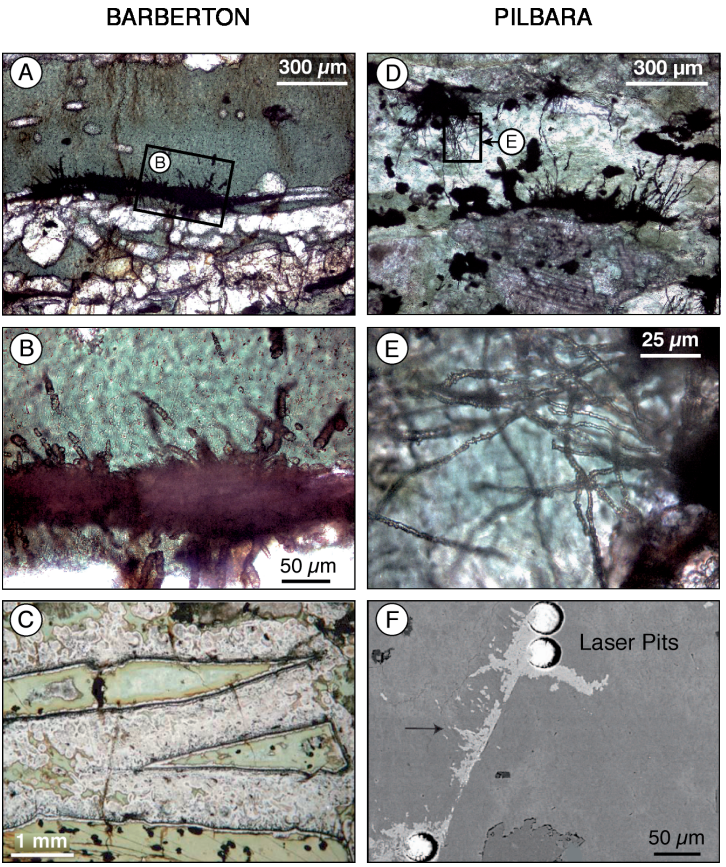

Fig. 26 Tubular bioaltextures in interpillow hyaloclastites from the Hooggenoeg Formation of the Barberton greenstone belt, South Africa (*left* hand column) and interpillow hyaloclastites from the Euro Basalt of the Pilbara Supergroup, Western Australia (*right* hand column). (**A**) The black zone across the middle part of the picture is composed of titanite which infills the tubes and these are rooted upon a healed boundary between the originally glassy fragments. The fine grained green mineral is chlorite, and the white, stubby mineral grains below the titanite zone are epidote crystals. The boxed area is enlarged in (**B**) which shows the segmented nature of the tubules and the overgrowth of metamorphic chlorite. (**C**) Image of a meta-volcanic interpillow hyaloclastite in which the original glass shards are completely replaced by chlorite, quartz, and epidote and the interstitial spaces are filled with quartz and calcite. There is very little evidence of deformation and the original "jigsaw-fit" breccia textures are still preserved. The dark, spherical spots within the fragments (particularly the lower fragment) are variolitic textures (originally pyroxene needles crystallized around a plagioclase nucleii). (**D**) From the Pilbara shows black zones of titanite along the healed boundary between originally glassy fragments and on which the tubular structures are rooted. The fine grained green mineral is chlorite, and the white to light brownish mineral is calcite. The boxed area is enlarged in (**E**) which shows the segmented nature of the intertwined tubules. (**F**) Is a back scatter electron image showing the size and location of laser pits in the "root zone" of titanite tubes used for U/Pb radiometric dating. The titanite is light grey and the chlorite and quartz form the darker areas

(Furnes et al. 2004; Banerjee et al. 2006, 2007; Staudigel et al. 2006). The tubular textures (Fig. 26A,B,D–F) are by far the most common, and are observed to extend away from healed fractures and/or grain boundaries along which seawater may once have flowed. Some of these tubular structures exhibit segmentation into sub-spherical bodies (Fig. 26B,E). Putative granular textures (from the Barberton greenstone belt) have also been observed (Banerjee et al. 2006, Fig. 6), may have originated along fractures in the originally glassy fragments, or grain margins of shards in interpillow hyaloclastites (Fig. 26C). The widths of the tubular structures vary between 1–9 μm, and their lengths up to 200 μm (Furnes et al. 2007a). The tubes are filled predominantly with titanite (Fig. 27), but quartz and chlorite is also commonly observed.

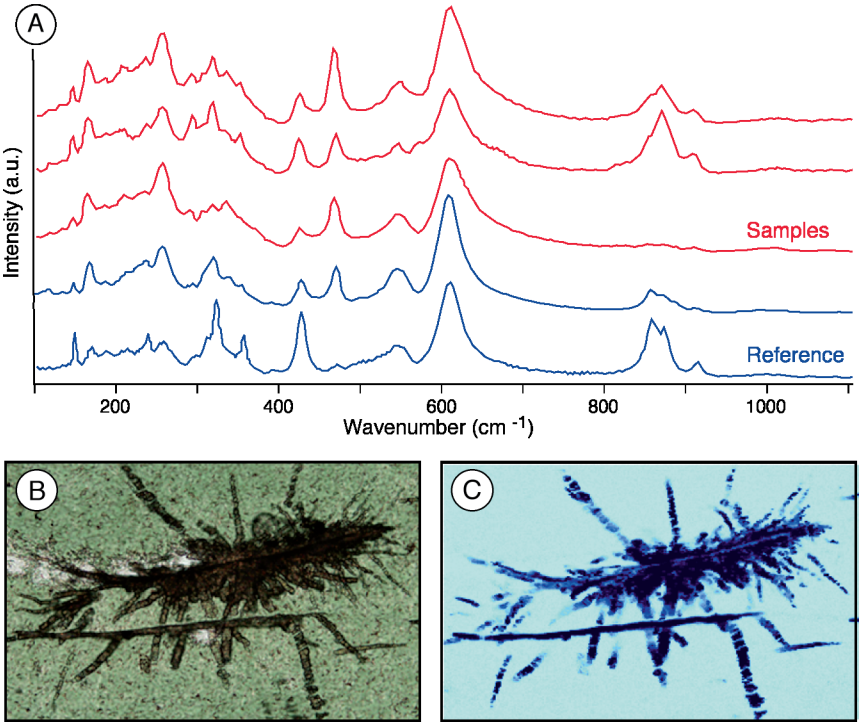

Fig. 27 (**A**) Raman spectra plotted as wavenumber (cm^{-1}) against intensity (in arbitrary units) of a mineral phase shown in red that infills bioalteration textures in meta-volcanic glass and is comparable to the reference spectra obtained from the mineral titanite ($CaTiSiO_4$ shown in *blue*); (**B**) petrographic image of these bioalteration textures in meta-volcanic glass now composed of chlorite from the ~3.4 Ga Barberton greenstone belt of South Africa (cf. Fig. 25); (**C**) a Raman intensity map of the same area showing the titanite infilled cluster of radiating tubes which are septate due to thin divisions created by chlorite overgrowths from the meta-volcanic matrix. (This Raman map was collected by L. Nasdala using a laser excitation of 632.8 nm (8 mW) and 1.5 μm steps, across an area 310 by 190 steps.)

4.4 What Controls the Development of Bioalteration Textures?

Above we have demonstrated that bioalteration textures are found in basaltic glass from *in-situ* oceanic crust, ophiolites and greenstone belts (Figs. 23–26), ranging in age from ~0 Ma to 3500 Ma. To date we do not know what controls the variation in size and morphology of the microbial alteration textures. It is conceivable that comparable microbial consortia in volcanic glass may produce differently shaped bioalteration textures under varying environmental conditions. For illustration, consider microbial colonies grown on agar plates the morphologies of which are controlled by the physics of nutrient diffusion, such that dendritically-branched colonies form when nutrient concentrations are low, as opposed to compact, concentrically zoned colonies when nutrient concentrations are high (e.g., Matsushita et al. 2004). Analogously, microorganisms in volcanic glass may be capable of producing tubular or granular bioalteration morphologies under varying nutrient or substrate conditions. We highlight, therefore, the absence of a one-to-one relationship between the morphologies of bioalteration textures and the dominant microorganism in the constructing microbial consortia.

5 Geochemical Signatures

Supporting evidence for a microbial origin of the textures described herein is provided by X-ray mapping of several elements, particularly carbon. A large number of glassy or originally glassy samples of pillow margins and hyaloclastites from *in-situ* oceanic crust, ophiolites and greenstone belts have been studied. In many cases where SEM imaging found bio-alteration textures, these were associated with elevated concentrations of carbon and possibly also nitrogen and sometimes phosphorus. These X-ray maps were collected using an electron microprobe on iridium-coated thin sections that were prepared using Al-grinding powders to prevent carbon contamination during thin section grinding and polishing. Carbon was routinely measured on two spectrometers and full details of the analytical methods developed are given in Banerjee et al. (2006).

The observed enrichments in carbon are generally highly restricted to the margins of the microbial alteration textures and diminish sharply away from these areas. Elevated levels of carbon have been found in samples of varying age and metamorphic grade and the intensity of the carbon signal gives a qualitative indication of the amount of carbon present. N/C ratios of marine bacteria have been reported to range from 0.07 to 0.35 (Fagerbakke et al. 1996) and these are comparable to samples containing bioalteration textures from Site 896A at the Costa Rica Rift most of which showed N/C values between 0.08 and 0.25 (Torsvik et al. 1998). Due to the mobility of carbon and nitrogen however, both at surface and subsurface conditions, it is quite probable that carbon and particularly nitrogen are lost in differing proportions from microbial alteration textures during burial and later metamorphism. For this reason, no further attempt to quantitatively determine N/C ratios has been undertaken.

Our interpretation is that both carbon and nitrogen are concentrated from seawater by microbial activity within the oceanic crust. We hypothesize that as microbes etch volcanic glass, multiply and die their organic remains are left within the alteration textures produced. These are then incorporated along the margins of the textures during mineralization by clays and iron-oxyhydroxides in the recent oceanic crust and or by titanite in greenstone belts samples. At the nanometer scale the distribution of carbon bearing phases is more complex as revealed by a recent study that used focussed ion beam milling to obtain a wafer from across a tubular bioalteration structure (Benzerara et al. 2007). STXM (scanning transmission X-ray microscopy) and EELS (energy electron loss spectroscopy) found that some of the C is contained in a carbonate phase and some in an organic carbon phase that possibly contains a carbonyl group, with further high resolution sampling required to fully characterize the nm distribution. Concerning phosphorus, which is also sometimes concentrated at the margins of bioalteration structures it is uncertain if microorganisms are able to extract P from the glass. Phosphorus is present in volcanic glass and deep seawater in only very low concentrations and it seems likely that the elevated concentrations associated with microbial alteration textures are due to sequestration by living cells (Torsvik et al. 1998).

Element maps of calcium, magnesium, iron, aluminium, sodium, potassium, silicon, sulphur, chlorine, and titanium were also routinely measured and can be highly informative depending on the phases which mineralize the bioalteration textures (clays, iron oxy-hydroxides, quartz) and the host rock (silicate glass or a metamorphic assemblage that may include chlorite, quartz and carbonate). It is noteworthy that maps of Ca, Mg and Fe do not show enrichments that correlate with carbon highs and this eliminates inorganic carbonates as the source of the carbon linings on the bioalteration textures. Likewise, maps of Cl were used to exclude epoxy as the source of carbon. Maps showing a common enrichment of sodium, potassium and magnesium along fracture planes from which bioalteration radiates, can also be a useful tracer of fluid circulation.

5.1 Modern Oceanic Crust

Figure 28 shows a SEM image and a series of element maps of a region of granular alteration on both sides of a fracture in volcanic glassy material from the central Atlantic Ocean. The zones of granular alteration show slight enrichment in carbon, nitrogen and phosphorus. Carbon also shows bright spots in the outermost parts of the granular textures. Calcium and magnesium are, on the other hand, strongly depleted within the alteration zone. It is important to note that the carbon enrichments do not correlate with any enrichment in Ca, eliminating calcium carbonate as a carbon bearing phase, and hence the carbon is regarded as organic. This feature has repeatedly been shown in a number of papers (e.g., Furnes et al. 2001b; Furnes and Muehlenbachs 2003; Staudigel and Furnes 2004; Staudigel et al. 2004). In particular the enrichments in carbon, nitrogen and phosphorus are very supportive of a

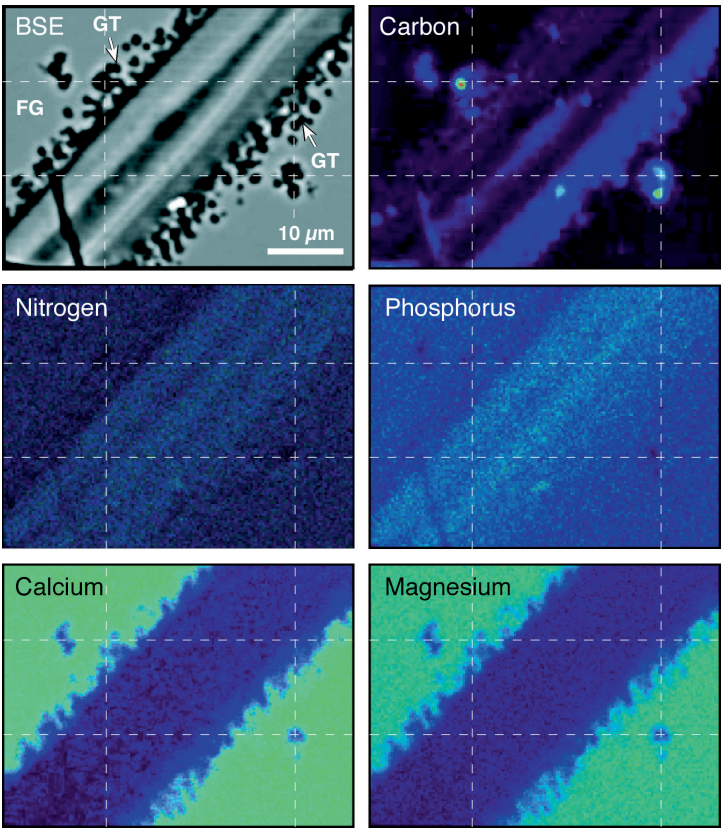

Fig. 28 Back scatter electron image of granular bioalteration on either side of a fracture in volcanic glass from *in-situ* oceanic crust with accompanying X-ray maps showing the distribution of carbon, nitrogen, phosphorus, calcium, and magnesium. Relative concentration scale (from lowest to highest): *black-blue-green-yellow-red*. Sample from Hole 46-396B-5R-2, 36-46 cm from the Atlantic Ocean. FG = fresh glass; GT = granular texture. Vertical and horizontal lines have been drawn on the X-ray maps to aid comparison

microbial involvement in the granular alteration but it does not prove that these cavities are actually made by these microbes. A large number of altered glass rims from the in-situ oceanic crust have been X-ray mapped, and in nearly all, particularly in samples from the younger part of the crust, elevated concentrations of carbon occur.

5.2 Ophiolites

Among the X-ray mapped samples from ophiolites, those from the Troodos ophiolite have provided some of the best results. Figure 29 shows a SEM image along with carbon, nitrogen, phosphorus, calcium and magnesium maps of altered glass

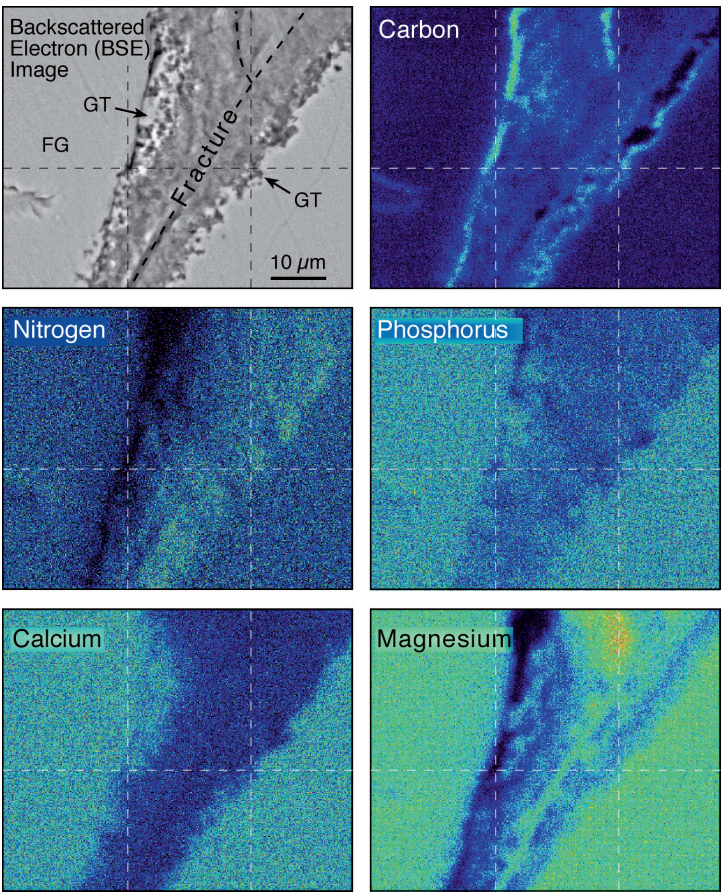

Fig. 29 Back scatter electron image of granular bioalteration fronts along a NE-SW trending fracture (Y shaped, bifurcates in the *top right* of the image) in volcanic glass from the ~90 Ma Troodos ophiolite with accompanying X-ray maps of C, N, P, Ca and Mg distribution. C and N are both enriched along the margins (N only along the right margin; an instrumental artifact due to the position of the spectrometer) of the granular alteration band, although they do not exactly correlate, whereas P shows no enrichment in this example relative to the glass. Calcium is depleted in the granular bioalteration band confirming the absence of carbonate. Magnesium is also in general depleted along the fresh glass/alteration interface, but is concentrated at the centre of the fracture, showing the presence of different authigneic materials within the alteration zone. Relative concentration scale (from lowest to highest): *black-blue-green-yellow-red*. Sample CYP-99-14A is from the Akaki valley. FG = fresh glass; GT = granular texture. Vertical and horizontal lines have been drawn on the X-ray maps to aid comparison

developed adjacent to a fracture. Enrichment in carbon, and to some extent, nitrogen can be seen clearly in these images. Phosphorus, however, is depleted, and this is opposite to what we observe in much younger sample from the *in-situ* oceanic crust (Fig. 28). Calcium and magnesium are also depleted, thereby excluding carbonate as the source of the carbon.

5.3 Greenstone Belts

Along the margins of the tubular structures in hyaloclastites from both the Barberton and Pilbara Archean greenstones, X-ray mapping reveals in some cases elevated concentrations of carbon and, to a lesser extent, nitrogen and phosphorus (Fig. 30).

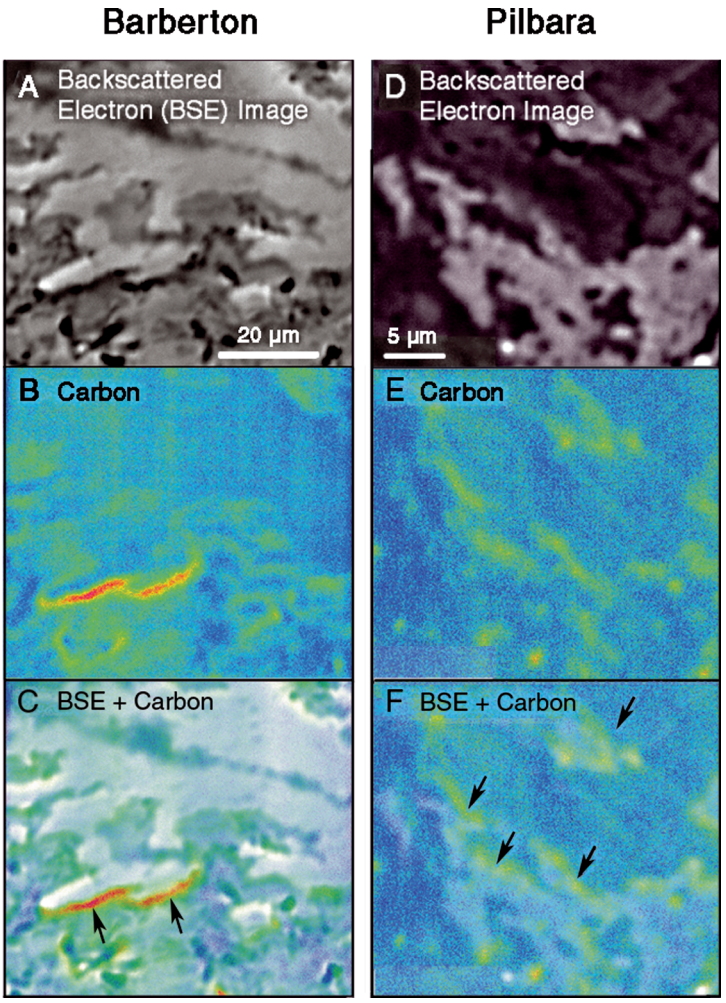

Fig. 30 Back scatter electron (BSE) image of titanite infilled tubular bioalteration textures from the ~3.5 Ga volcanics of the Barberton greenstone belt (*left* hand column) and ~3.4 Ga pillow lavas from the Pilbara Supergroup (*right* hand column) accompanying X-ray maps show the enrichments in carbon (measured using two detectors at different orientations) along the margins of the tubes; highlighted by arrows on the combined BSE and carbon maps in the lower part of the figure. Relative concentration scale (from lowest to highest): *black-blue-green-yellow-red*. Sample 29-BG-03 from the Barberton and 74-PG-04 from the Pilbara. Additional X-ray maps of further elements along with optical images of the studied areas are given in Furnes et al. (2004) and Banerjee et al. (2006) for the Barberton examples and Banerjee et al. (2007) for the Pilbara example

These enrichments are highly restricted to the immediate area of the titanite tubes while quickly diminish away from these areas. Calcium, iron, and magnesium maps (not shown here), from the same region, show opposite trends compared to carbon, again confirming that carbon is not bound in carbonate (see GSA Data Repository Fig. DR1, Banerjee et al. 2007).

6 Carbon Isotope Signatures

A large number of samples of glassy and crystalline samples of pillow lavas from *in-situ* oceanic crust and core-rim pairs from ophiolites and greenstone belts have been analysed for $\delta^{13}C$ measured on disseminated carbonate and the results have been compiled in Fig. 31. We refer the reader back to Section 2.2.4 and Fig. 2 for an explanation of how this data is interpreted. This data is obtained by measurements of the CO_2 liberated by phosphoric acid dissolution of whole rock powders dissolved in 100% phosphoric acid details of the analytical method used are given in Furnes et al. (2001a) and all results are quoted relative to the PDB standard.

The compiled $\delta^{13}C$ (‰) versus wt.% carbonate results from in-situ oceanic crust and ophiolites/greenstone belts, are shown in Fig. 31A,B respectively. In both cases there is a marked shift in the $\delta^{13}C_{carb}$ values of the glassy pillow rim samples towards more negative values than for the crystalline pillow core samples. If we take the $\delta^{13}C_{carb}$ value of -7‰ as the lower limit for magmatic values, the percentages of crystalline (pillow core) and glassy (pillow rim) samples from the *in-situ* oceanic crust that exhibit $\delta^{13}C_{carb}$ values lower than -7‰, are $\sim$ 14% and 52%, respectively. We take this as support for microbial activity within the glassy pillow rim samples for which there is supporting textural evidence; whereas, the crystalline pillow core samples which lack bioalteration textures predominantly show $\delta^{13}C_{carb}$ values between mantle CO_2 (-7‰) and marine carbonate ($0 +/ - 1$‰) values.

The pillow lavas of the ophiolites and greenstone belts (Fig. 31B) show values broadly comparable with those seen for *in-situ* oceanic crust; i.e. the percentages of crystalline and glassy samples that define $\delta^{13}C_{carb}$ values lower than -7‰, are $\sim$ 15% and 35%, respectively. Fig. 32 shows all our $\delta^{13}C_{carb}$ of pillow lavas from ophiolites and greenstones, plotted against weight percent carbonate and we have further sub-divided these data into Archean, Proterozoic and Phanerozoic samples (Fig. 36) in order to compare the similarities and differences between the three plots. In fact, for the pillow lavas from all these sequences we see that the originally glassy margins generally display lower $\delta^{13}C_{carb}$ values than the crystalline interiors. In some samples, however, the glassy margins display the highest $\delta^{13}C_{carb}$ values ($> +1$), a phenomenon particularly demonstrated by the Archean samples (Fig. 32A). In general, the $\delta^{13}C_{carb}$ values of pillow margins show a considerably wider range than the crystalline interiors that are generally bracketed between 0 and -7‰ (Fig. 32).

In order to explore the extent to which the characteristic $\delta^{13}C_{carb}$ values of rims and interior of pillow lavas retain their original values during progressive metamorphism, we have split the samples from ophiolites and greenstone belts

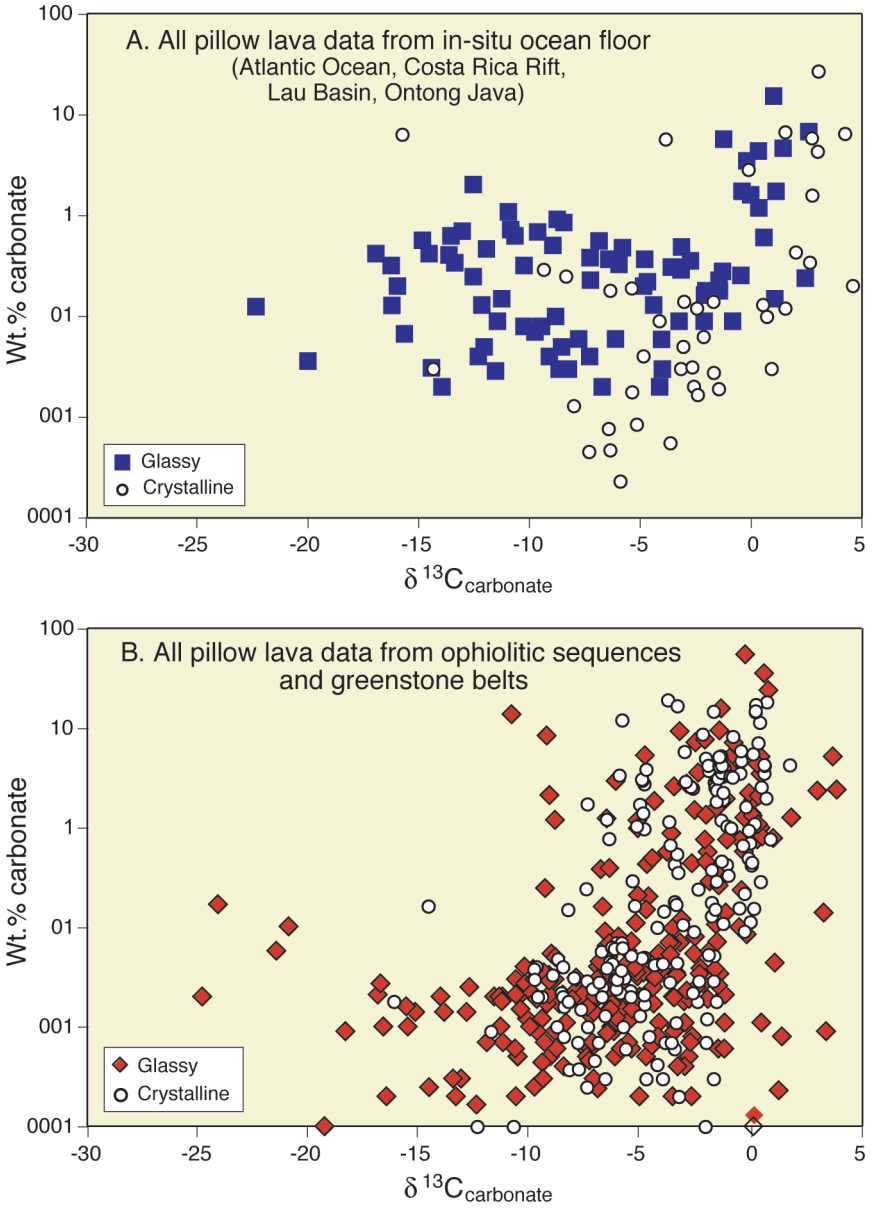

Fig. 31 Plots of $\delta^{13}C_{carbonate}$ versus weight percent carbonate from: (**A**) all measured pillow lavas from *in-situ* oceanic crust; (**B**) all measured ophiolites and greenstone belts. Data from glassy pillow rims are shown by filled symbols and these are more negatively fractionated relative to the samples from the crystalline pillow interiors shown by hollow symbols (cf. Fig. 2)

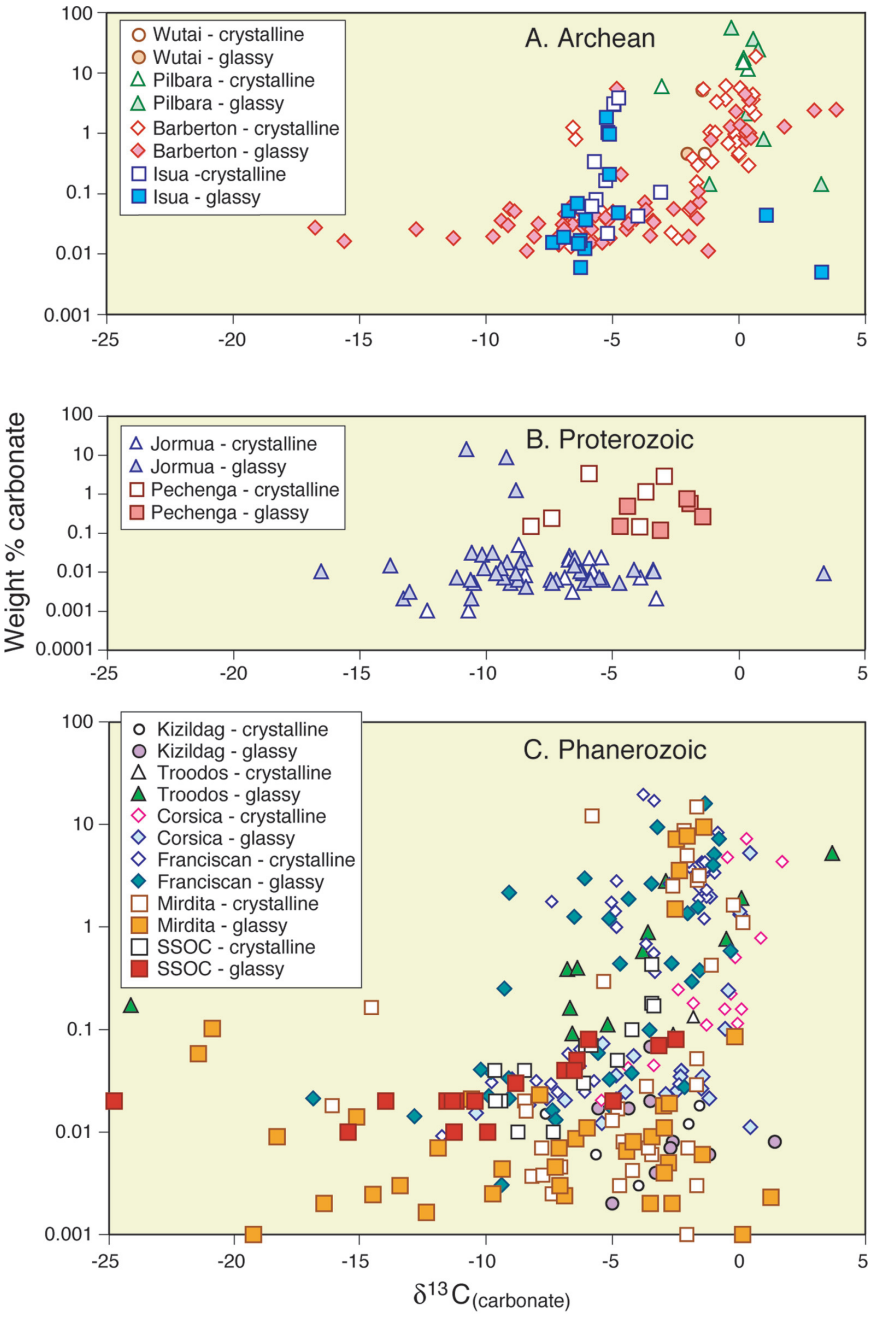

Fig. 32 Plots of $\delta^{13}C_{carbanoate}$ versus weight percent carbonate of crystalline interiors and glassy rims of pillows from Archean, Proterozoic and Phanerozoic ophiolites and greenstone belts

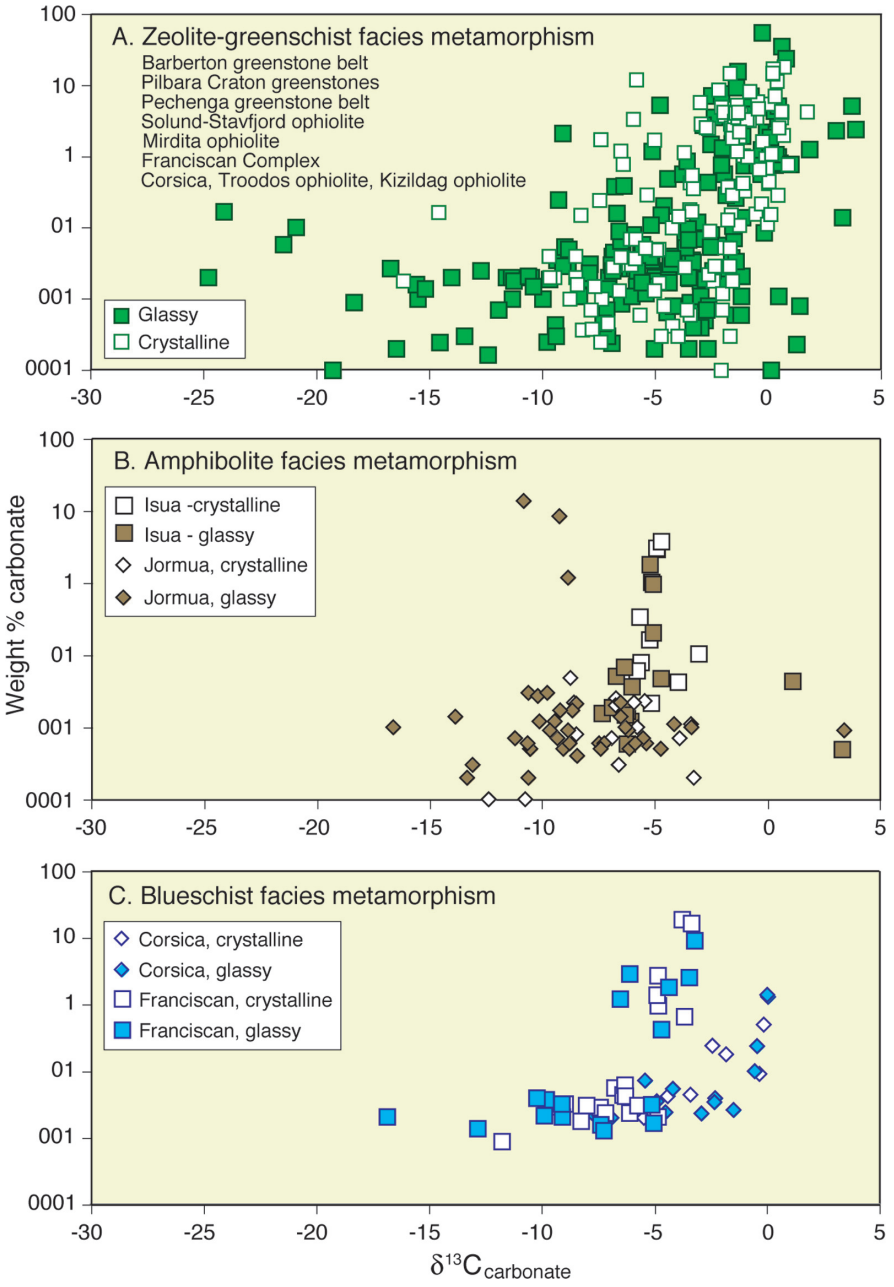

Fig. 33 Plots of $\delta^{13}C_{carbanoate}$ versus weight percent carbonate sub-divided by metamorphic grade: (**A**) zeolite to greenschist facies metamorphism; (**B**) amphibolite facies metamorphism; (**C**) blueschist facies metamorphism. Data from glassy pillow rims are shown by filled symbols and these are more negatively fractionated than the samples from the crystalline pillow interiors shown by hollow symbols (cf. Fig. 2)

according to their metamorphic grade, i.e. zeolite-greenschist-, amphibolite- and blueschist-facies metamorphism (Fig. 33). The majority of the samples have been collected from zeolite-greenschist metamorphic pillows, and the glassy samples show a considerably wider range in the $\delta^{13}C_{carb}$ values than their crystalline counterparts (Fig. 33A). This also applies to the samples that have suffered amphibolite facies metamorphism (Fig. 33B). Even some of the blueschist samples from the Franciscan glassy samples show very low $\delta^{13}C_{carb}$ values, whereas the majority of the crystalline samples are bracketed between 0 and $-7‰$ (Fig. 33C). It thus appears that the $\delta^{13}C_{carb}$ values from metamorphosed pillow margins largely retain their pre-metamorphic values, and that they are comparable with those from non-metamorphic *in-situ* oceanic crust, in spite of even high-grade metamorphism. We emphasize, however, that the glassy blueschist samples from Corsica do not show the low $\delta^{13}C_{carb}$ values. More data is needed to substantiate whether blueschist facies rocks, or even higher metamorphic grade rocks, can still preserve the original carbon isotope signatures. It is interesting in this context to mention that carbon isotope values ($\delta^{13}C$) of some diamonds from majoritic garnet-bearing host eclogites are attributed to an organic source material within subducting oceanic crust (Tappert et al. 2005). These findings support our suggestion that the Franciscan blueschist pillow rims exhibit isotopic values consistent with microbial alteration (Fig. 33C).

7 Significance of Microbial Alteration as a Biomarker

The biogenic textures described above, the associated element distributions (in particular carbon enrichments) and $\delta^{13}C_{carb}$ values documented from meta-volcanic glass back to the Mesoarchean have far reaching implications for the nature and extent of microbial processes. In this section, we discuss some of these aspects in light of our present knowledge.

7.1 Mapping the Oceanic Biosphere

Granular and tubular bioalteration textures are easily observed by ordinary light microscopy upon samples of *in situ* oceanic crust where fresh glass is still present. This is because the dark, commonly mineral-filled structures appear in strong contrast to the light yellowish-brown, isotropic glass (Figs. 23, 24). This makes it possible to identify and quantitatively estimate the extent of bioalteration as a function of depth by reinvestigating DSDP and ODP cores. The only study of this kind to date is that of Furnes and Staudigel (1999), which documented the relative proportions of granular and tubular bioalteration types in basaltic glass as a function of depth (to ~500 m) and temperature in the oceanic crust. In this study, the percentage bioalteration was estimated visually from geological thin sections. The data have been compiled from oceanic crustal sections collected at Sites 417 and 418 of the 110 Ma Western Atlantic, and at Sites 504B and 896A of the 5.9 Ma Costa Rica Rift. This compilation

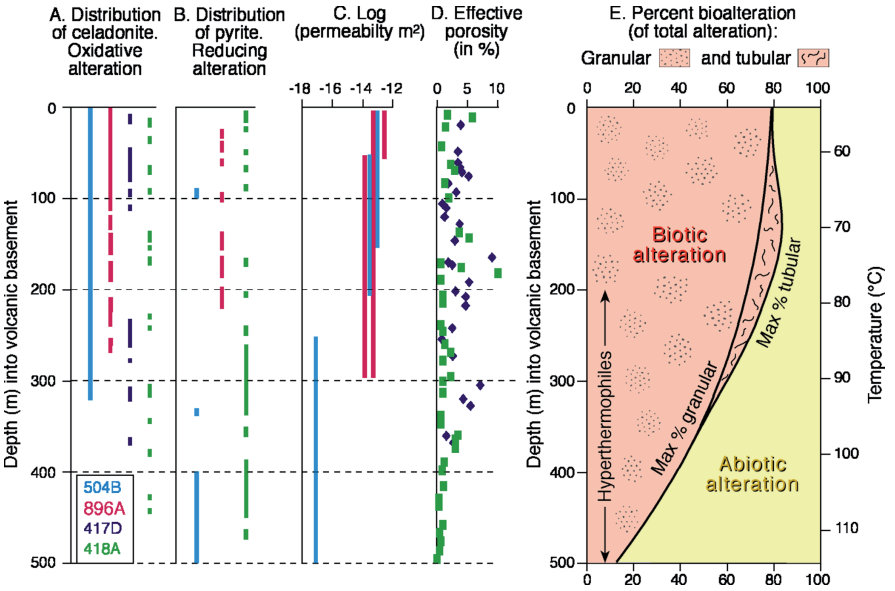

Fig. 34 Down-hole data to show the controls on the distribution of bioalteration textures with depth in the oceanic crust. The data are mainly from holes 396B, 407, 409, 410A, 417D, 418A in the Atlantic Ocean, holes 504B and 896A from the Costa Rica Rift in the Pacific Ocean, and hole 834B in the Lau Basin (for further information, see Fig. 5). (**A**) shows the occurrence of celadonite which is an indicator of oxidative alteration; (**B**) shows the occurrence of pyrite which is an indicator of reducing conditions; (**C**) shows permeability down-hole; (**D**) shows effective porosity determined by comparing air-dried and water-saturated sample weights; (**E**) shows estimates of the relative percentages of granular alteration textures (*pink* dots); tubular alteration (*pink* lines); and abiotic alteration (*yellow*) calculated from thin section observations and redrawn from Furnes et al. (2001b) and Staudigel et al. (2006)

illustrated in Fig. 34 shows that the granular type is by far the most abundant and can be found at all depths into the volcanic basement where the presence of fresh glass allows bioalteration to be traced down to ~550 m. At the surface, as well as below ~350 m into the volcanic basement, the tubular textures are absent or very rare. In the upper ~350 m of the crust the granular alteration type is dominant, being most abundant in the upper 200 m at temperatures below ~ 80°C, and decreasing steadily in abundance to become subordinate at temperatures of ~ 115°C near the currently known, upper temperature limits of hyperthermophilic life. The tubular alteration textures, meanwhile, constitute only a minor fraction, at most ~ 20% of the total alteration and show a clear maximum at ~120–130 m depth corresponding to temperatures of ~ 70°C. (These percentage bioalteration estimates are likely to be an underestimate however, because ambiguous textures were regarded as abiotic in these estimates and glass hydration processes may also have obscured some textures.)

The abundance of bioalteration with depth at Sites 504B and 417/418 increases with permeability and also the presence of mineral phases such as celadonite which

is indicative of relatively oxygenated waters (e.g., Furnes and Staudigel 1999; Furnes et al. 2001b). It is noteworthy that both the 5.9 Ma Costa Rica Rift and the 110 Ma Western Atlantic oceanic sections show similar maxima in the amount of bioalteration as a percentage of the total alteration, despite their very different ages (see Fig. 11 of Furnes et al. 2001b). This suggests that a substantial portion of the bioalteration happens very early and that the net bioalteration pattern is established within ~6 Ma. (It should be appreciated that most drill holes in the oceanic crust have recoveries that can be as low as 20% or less). In broad terms this is consistent with the theoretical estimates of microbial biomass production over time from oxidative alteration and hydrolysis within the upper oceanic crust as it migrates away from an oceanic spreading center (cf., Bach and Edwards 2003). However, as long as fresh glass is present and seawater circulation persists, the bioalteration processes are likely to continue. There exists a wealth of drill core samples of pillow lavas from the *in situ* oceanic crust that are yet to be systematically investigated in this manner for evidence of bioalteration.

7.2 The Oceanic Crust as a Bioreactor

Microbial seafloor alteration has a profound effect on chemical exchange between the oceans and the oceanic crust across the full range of seafloor environments, including: high temperature mid-oceanic ridge hydrothermal systems, low temperature off-axis settings and oceanic hot spots (e.g., Staudigel et al. 1998; Staudigel and Furnes 2004). Microbial communities in the oceanic crust may be mobilized and expelled into the overlying water column during diking events that involve massive expulsion of low temperature hydrothermal effluents into the water column (e.g., Delaney et al. 1998). These bring the microbial biomass into the oceans where they may provide a food source for higher trophic levels. In the converse direction, the subduction of bioaltered oceanic crust deep into the Earth's mantle provides a relatively little-explored geochemical connection between the Earth's biosphere and mantle. The existence of this pathway is supported by the finding of very deep asthenospheric micro-diamonds that have low $\delta^{13}C$ signatures suggestive of a biogenic origin (e.g., Tappert et al. 2005). Taken together these processes comprise an oceanic crustal "bioreactor", changes in the extent and activity of which have profound implications for the evolution of seawater chemistry, and for the composition of the oceanic crust and mantle through geological time. At present relatively little is known about the connections between bioaltered oceanic crust and the mantle; we therefore, here focus instead on the better understood interactions between the oceanic crustal bioreactor and seawater chemistry.

Experimental investigations (e.g., Staudigel et al. 1998) have revealed profound differences between biotic and abiotic seafloor alteration processes. Glass alteration experiments involving surface seawater microbial populations have shown that microbial activity enhances chemical exchange in water-rock reactions, especially for Sr, and results in higher rates of authigenic mineral production along with increased uptake of Ca relative to sterile controls (Staudigel et al. 1998, 2004). Abiotic

alteration, in contrast, results in pronounced uptake of Mg and effective removal of Si (Staudigel et al. 2004). Biotic experiments with a natural seawater microbial inoculum at temperatures up to 100°C have also shown significant mobility of K, Rb, Cs, Li, B, U, Th, Pb, and strongly temperature dependent U-Pb fractionation (Staudigel et al. 1998). Although further experiments are needed to explore the biotic and abiotic controls of these processes, to the first order these findings confirm that microbes have a pronounced effect on element fluxes and mobility during glass alteration in the oceanic crust. Moreover, these differences in chemical redistribution patterns between biotic and abiotic water-rock interactions confirm that they represent two different modes of seafloor alteration. This implies that the chemical fluxes and consequently the seawater composition in the pre-biotic world may have been radically different from the modern world in which seafloor bioalteration is prevalent. Fluid inclusion analyses of Archean rocks may help to track these changes in seawater chemistry (cf. Foriel et al. 2004)

The total biomass found within the modern oceanic crust and its productivity remain unconstrained. Bach and Edwards (2003) estimated that submarine basalts can provide enough energy to support a primary productivity of about 10^{12}g/a cellular C, which represents an upper limit for chemosynthetic carbon fixation in the oceanic crust, although it is unknown as to what extent the deep biosphere utilizes this energy source. In addition the influx of organic carbon entering the oceanic crust via hydrothermal recharge may provide a further energy source for heterotrophic microbes. A complimentary approach is to estimate the maximum numbers of cells required to produce the density of tubular and granular bioalteration textures observed in the oceanic crust. While this approximates the numbers of cells to within one or two orders of magnitude necessary to create the textures found in a given thin section, these data are difficult to extrapolate into a global inventory of the oceanic crustal biomass because their metabolic rates are unknown. It is also difficult to extrapolate the abundance of fresh glass to an oceanic crustal scale given that oceanic drilling rarely recovers more than 30% core. Thus, at present we can only speculate about the biomass and the primary productivity of the deep ocean crustal bioreactor. Nonetheless, the importance of this microbial community is indisputable when considering the geochemical fluxes between seawater, the ocean crust, and the Earth's mantle.

7.3 Tectonic Control of Bioalteration in Modern and Ancient Oceanic Crust

Bioalteration of glass has been found in many submarine volcanic settings that preserve fresh, or minimally altered, glass from fast- to slow-spreading centres, also oceanic plateaus, ophiolites and greenstone belts of all ages (Figs. 4 and 36). These examples provide markedly different seafloor spreading rates and environments which offer different boundary conditions for bioalteration processes, in particular with respect to the depth of water circulation, density of fracturing and the

lithology of the upper part of the oceanic crust (e.g., Dilek et al. 1998; Fig. 4). Where as intermediate- to fast-spreading ridges (i.e., $\sim$ 6–12 cm/yr) exhibit thick extrusive sections that lack major tectonic disruption (e.g., Sinton and Detrick 1992; Fouquet et al. 1996), slow-spreading ridges (i.e., $<$ 2.5 cm/yr) show deep-seated normal faulting and may expose upper mantle rocks at the seafloor enabling deep circulation of hydrothermal solutions into the lower crust and peridotites (Karson 1998). In such settings the deeper fluid circulation may carry microbes to greater depths where they may utilise H_2 and or CH_4 produced by the serpentinization of ultramafics (e.g., Berndt et al. 1996; Kelley 1996). For example, the production of H_2 and CH_4 as a result of serpentinization of ultramafic rocks is presently occurring in the Zambales ophiolite (Abrajano et al. 1990) and the Lost City ultramafic field (Kelley et al. 2005). These contrasting tectonic styles and alteration regimes found at slow- to fast-spreading centres are shown schematically in Fig. 35A,B, and it seems reasonable to hypothesise that the higher H_2 production found at slow-spreading ridges may favour methanogenic bacteria compared to fast-spreading ridges. These differences may be recorded in the carbon isotopes of disseminated carbonates found in pillow basalts at such different sites.

In order to explore the potential for such differences, Furnes et al. (2006) compared the $\delta^{13}C_{carb}$ variations measured upon bioaltered pillow margins from different oceanic basins. They found substantial overlap in data between basins but distinct ranges in $\delta^{13}C_{carb}$ (Fig. 35). The $\delta^{13}C$ of finely disseminated carbonates from bioaltered, glassy basaltic pillow rims from slow- and intermediate-spreading oceanic crust of the central Atlantic Ocean (CAO) ranges from $-17‰$ to $+3‰$ (PDB), whereas those from the faster-spreading Costa Rica Rift (CRR) define a much narrower range and cluster at lighter values between $-17‰$ and $-7‰$ (Fig. 35C; Furnes et al. 2006). A similar $\delta^{13}C_{carb}$ pattern has been observed in some ophiolites; for example, the Jurassic Mirdita ophiolite in Albania shows a structural architecture similar to that of the slow-spreading CAO crust and a similar range in $\delta^{13}C_{carb}$ values (Fig. 35D). In contrast, the Late Ordovician Solund-Stavfjord Ophiolite Complex (SSOC) in western Norway exhibits structural and geochemical evidence indicative of an intermediate-spreading rate environment and displays $\delta^{13}C_{carb}$ signatures similar to those of the modern CRR oceanic crust (Fig. 35D). While much remains to be done to document systematic differences in $\delta^{13}C_{carb}$ between different ocean basins, the hypothesis that methanogenic bacteria may be a more important component of the bioalteration community at slow-spreading centres appears to be supported by the current data. Ophiolites, in particular, offer much potential for further testing this hypothesis because they provide an opportunity to study ancient fluid transport and alteration regimes in three-dimensional field exposure.

7.4 Bioalteration and the History of Early Life

Microbes that colonize volcanic glass may be among the earliest life forms on Earth. Textural evidence of bioalteration in submarine, originally glassy pillow lava rims

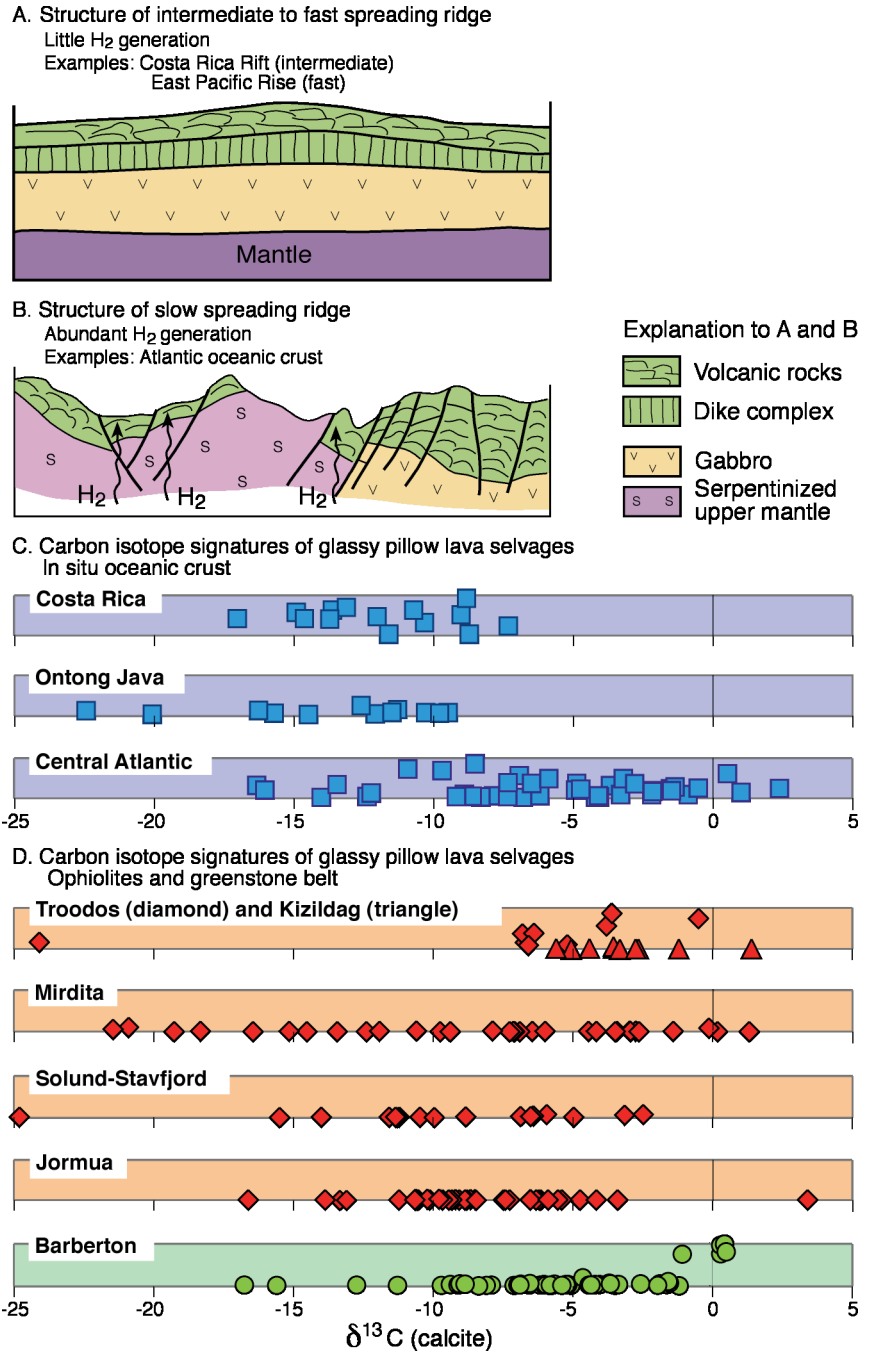
A. Structure of intermediate to fast spreading ridge
Little H2 generation
Examples: Costa Rica Rift (intermediate)
East Pacific Rise (fast)
Mantle
B. Structure of slow spreading ridge
Abundant H2 generation
Examples: Atlantic oceanic crust
H2
H2
H2
Explanation to A and B
Volcanic rocks
Dike complex
Gabbro
Serpentinized upper mantle
C. Carbon isotope signatures of glassy pillow lava selvages
In situ oceanic crust
Costa Rica
Ontong Java
Central Atlantic
-25
-20
-15
-10
-5
0
5
D. Carbon isotope signatures of glassy pillow lava selvages
Ophiolites and greenstone belt
Troodos (diamond) and Kizildag (triangle)
Mirdita
Solund-Stavfjord
Jormua
Barberton
-25
-20
-15
-10
-5
0
5
δ13C (calcite)

and hyaloclastites from the 3.3–3.5 Ga Barberton Greenstone Belt of South Africa (BGB) and the Pilbara Supergroup of western Australia (PWA) are reviewed above (Section 4.3, Fig. 26; see also Furnes et al. 2004; Banerjee et al. 2006, 2007). These titanite-filled bioalteration textures also have geochemical signatures (BGB and PWA, Fig. 30) and isotopic data (Fig. 31, BGB) that are suggestive of a biogenic origin. Furthermore, the syngenicity of these structures has been confirmed by direct U-Pb radiometric dating of the PWA examples in addition to the observation that the BGB bioalteration textures are cross-cut by early metamorphic mineral phases (Furnes et al. 2004). This radiometric dating was conducted using a new multicollector-ICP-MS technique for measuring $^{206}Pb/^{238}U$ ratios within titanite from the "root zones" at the centre of tubular clusters (Banerjee et al. 2007; and methodology in Simonetti et al. 2006). A minimum age of 2921 $\pm$ 110 Ma was obtained which is $\sim$ 400 Ma younger than the accepted $\sim$3350 Ma eruptive age of the Euro Basalt pillows, given by a U-Pb zircon age from an interbedded tuff (Nelson 2005). This titanite date corresponds to the age of regional metamorphism related to the last phase of deformation and widespread granite intrusion (the North Pilbara Orogeny) that affected our sample site in the western part of the East Pilbara Terrane at $\sim$2930 Ma (Van Kranendonk et al. 2002, 2007). Since chlorite formation, which occurred around $\sim$2930 Ma, or earlier ($\sim$3.24 Ga; Wijbrans and McDougall 1987), overprints the titanite tubules we therefore interpret this age to represent a minimum estimate for titanite formation. This implies a $<$ 400 Ma post eruptive period during which the bioalteration textures in the Euro Basalt were mineralized; however, it does not exclude the possibility that the textures formed soon after eruption and were mineralized somewhat later. Presently we do not know whether biological processes contribute to the formation of titanite, or in other words, whether it is a biomineral. We draw attention to the fact that titanium can be passively accumulated during microbial etching of glass (e.g. Banerjee and Muehlenbachs 2003), and that Ti-rich nodules have been found in association with microbial alteration of Pleistocene Hawaiian basaltic glass (Walton and Schiffman 2003).

Fig. 35 Schematic diagram summarizing the inferred relationship between tectonism and the development of $\delta^{13}C_{carbonate}$ signatures measured on volcanic glasses from slow and fast spreading ridges: (**A**) shows the typical "layer cake" structure of an intermediate to fast spreading ridge; (**B**) shows the generalized structure of a slow spreading ridge with exposure of serpentinized upper mantle rocks and widespread H_2 generation. In the lower part of the figure, $\delta^{13}C_{carbonate}$ versus weight percent carbonate (range 0–1% on the vertical axis) is plotted for: (**C**) volcanic glasses from in-situ oceanic crust and (**D**) ophiolites and greenstone belts. This reveals that samples from intermediate to fast spreading ridges (e.g. Costa Rica and SSOC) have a narrower range of $\delta^{13}C_{carbonate}$ values typically between $-17‰$ to $-7‰$ which is consistent with the bacterial oxidation of organic matter. Whereas samples from slow spreading ridges (e.g. the Central Atlantic and Mirdita Ophiolite) have a wider range of $\delta^{13}C_{carbonate}$ values which include positive values up to $+4‰$ that are suggestive of the lithotrophic utilization of CO_2 by methanogenic bacteria that may utilize the H_2 generated at slow spreading centers (see also Furnes et al. 2006)

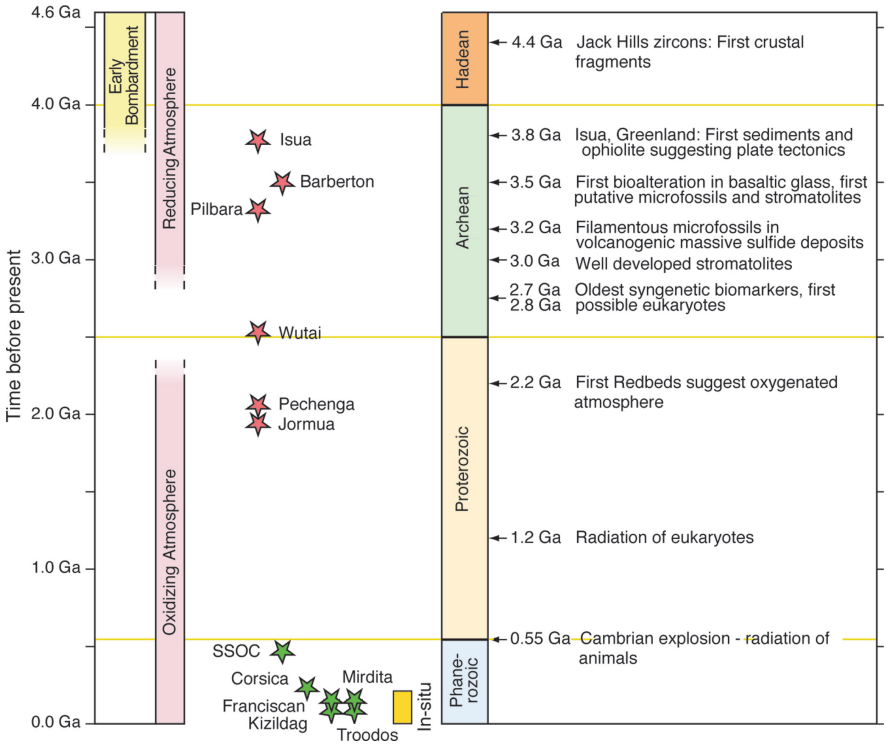

Fig. 36 Geological timeline showing the investigated Precambrian ophiolites and greenstone belts (*red* stars), Phanerozoic ophiolites (*green* stars), and *in-situ* oceanic crust (*yellow* bar), seen in conjunction with a schematic evolution of life (broadly following the review of Nisbet and Sleep 2001). Data from Isua are from Rosing (1999) and Furnes et al. (2007b), and data from Jack Hills are from Wilde et al. (2001)

These findings of Archean bioalteration textures are placed on a geological timeline in Fig. 36 that summarizes the major events in the evolution of the Earth's biosphere. This emphasizes the longevity of bioalteration processes through geological time, stretching from modern *in-situ* oceanic crust, through the Phanerozoic and Proterozoic as sporadically recorded in ophiolites, to the some of the earliest pillow lavas on Earth as preserved in greenstone belts. The Archean mineralized bioalteration traces from Australia and South Africa predate the oldest, previously known euendolithic microfossils described from ~1.7 Ga silicified stromatolites in China (Zhang and Goloubic 1987). Furthermore, this timeline shows that our bioalteration textures fall in the interval at ~3.4–3.8 Ga, when the earliest purported microfossils (e.g., Schopf and Packer 1987; Ueno et al. 2001) and stromatolites (e.g., Walter et al. 1980; Hofmann et al. 1999) have been found and thus meta-volcanic glasses provide a new target lithology that may help to decipher the origins of life in some of these earliest ~3.5 Ga pillow lavas on Earth. Given that volcanic lavas constitute a

volumetrically more significant component of the early Archean greenstone belts than the more traditionally sought chert horizons, they provide abundant opportunities for seeking fossilized evidence of life within the ancient crust (see also Section 7.5).

Considering this possibility, an endolithic mode of life may have been an attractive strategy in the early Archean, conferring many advantages on an early biosphere. Firstly, the oceanic crust may have provided abundant electron donors, principally Fe and Mn, found in basaltic rocks along with electron acceptors for chemolithoautotrophic organisms. Secondly, circulating fluids in the early oceanic crust may have provided carbon for heterotrophic organisms derived either from biotic carbon possibly recycled from the overlying water column, or abiotic carbon derived from alteration of the abundant ultramafic rocks. Lastly, crustal habitats would have provided protection from the elevated UV irradiation, abundant meteoritic and cometary impacts that affected the early Earth.

These submarine volcanic lavas from the Pilbara and Barberton are not however, the world's oldest. The earliest, ~3.8 Ga evidence of purported life on Earth is solely geochemical and based on isotopically light carbon in graphite contained within amphibolite to granulite grade metamorphic rocks in the Isua and Akilia supracrustal complexes of southwest Greenland (Schidlowski 1988, 2001; Mojzsis et al. 1996; Rosing 1999; McKeegan et al. 2007). This evidence is strongly debated (see Moorbath 2005 and references therein) and new light on this discussion may be shed by the investigation of the pillow basalts for bioalteration textures. Work to date has, however, failed to find reliable bioalteration textures in these rocks.

The discovery of bioalteration textures in the Archean begs the question: what role did submarine volcanoes play during the origin of life itself? Previous evidence to support a "hydrothermal cradle for life" comes from purported microfossils and stromatolites in ~3.45 Ga black hydrothermal cherts (e.g., Ueno et al. 2001; Van Kranendonk 2006) and filamentous microfossils in ~3.2 Ga volcanogenic massive sulfide deposits (Rasmussen 2000). Much remains to be done to map and constrain the nature of viable habitats in early volcanic seafloor settings and to explore whether volcanoes were the primary environment where life originated, or a secondary environment where life found shelter and/or co-developed with other settings (see Section 7.5 below).

The possibility of subaqueous basaltic glass alteration on early Mars has also been suggested and might involve both abiotic and biotic processes (e.g., Banerjee et al. 2004). The recent discovery in the Nakhla meteorite of carbonaceous vein filling material with tubular and bleb shaped microstructures that are similar to terrestrial bioalteration textures have renewed interest in these hypotheses (McKay et al. 2006; Gibson et al. 2006). In addition, microtubular weathering channels in olivines and pyroxenes from this same class of meteorite have been recently described by Fisk et al. (2006). Testing of the biogenicity and syngenicity of these meteoritic structures relies heavily on terrestrial comparisons and will undoubtedly help to strengthen the criteria used to establish the veracity of ancient bioalteration textures.

7.5 Tracing Back and Mapping the Pattern of Early Bioalteration

The bioalteration of volcanic glass is among the oldest fossilized evidence for life on Earth, and its textural expressions appear to have remained remarkably conservative through geological time. The question of whether we can see the same pattern of bioalteration in pillow lavas of the ancient oceanic crust as in the young, *in situ* oceanic crust is particularly intriguing. To answer this question we can as yet only provide some provisional data based upon bioalteration textures found in the Hooggenoeg Formation of the Barberton greenstone belt and the Euro Basalt of the Pilbara Craton. We firstly assume that these biotextures must have developed when the ambient temperatures were below ~ 113°C to permit the existence of life (Stetter et al. 1990). It is unlikely that bioalteration could have occurred continuously throughout the relatively thick Archean volcanic sequences, some of which

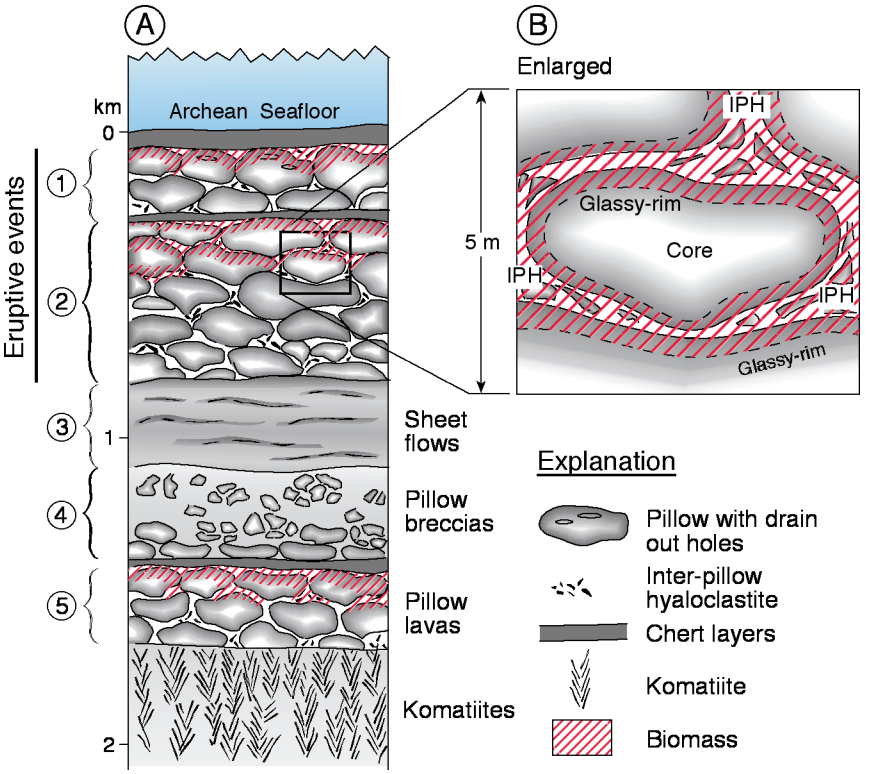

Fig. 37 Model of bioalteration in the Archean seafloor: (**A**) schematic column of a pillow lava pile with interbedded sheet flow produced in 5 eruptive events with interbedded komatiites and seafloor cherts, the biomass shown by red hashes is patchy and concentrated towards the tops of pillow lava eruptive packages; (**B**) enlarged view of a single pillow showing the concentration of endolithic biomass in the glassy pillow rims and inter-pillow hyaloclastites. This model is based upon observation made in the measured Archean greenstone belt sections illustrated in Fig. 17

were probably erupted relatively quickly and buried at temperatures that were too high for life to exist. It is therefore not surprising that examples of bioalteration textures found to date are limited to apparently narrow horizons of these thick submarine lava sequences. For example, the only bioalteration textures found to date in the interpillow hyaloclastite from the Euro Basalt are from the lower part of the 5–8-km-thick basalt succession (Fig. 17). The basal flows of the Euro Basalt are dated at 3350 +/ − 2 Ma, whereas a thin felsic volcaniclastic unit in the upper part of the formation has yielded an age of <3346 Ma (see Fig. 2 in Van Kranendonk 2006), suggesting that most of this very thick volcanic succession was erupted within a few million years, probably exceeding temperature viable for life during much of this time. Similarly, from the 2–3-km-thick succession of submarine basalts (pillow lavas and massive sheet flows) of the Hooggenoeg Formation in the Barberton greenstone belt, bioalteration textures have been found only within restricted pockets of interpillow hyaloclastites in the upper part of the sequence (Fig. 17). Based upon these data, we have constructed a working model for the distribution of biomass in the ancient oceanic crust as shown in Fig. 37 that differs from the more continuous distribution pattern documented from the *in-situ* oceanic crust (Fig. 34).

A further point to consider in this context is the predominance of tubular alteration textures in Archean lavas that contrasts with the alteration textures in *in-situ* oceanic crust, where granular textures are by far the most predominant. Indeed, only rare examples of possible granular textures have been identified along fractures in originally glassy fragments of hyaloclastite from the Archean Hoeggenoeg Formation (see Fig. 6 of Banerjee et al. 2006). The predominance of the tubular over granular alteration textures in Archean lavas may be explained by the masking of the finer, granular textures by titanite mineralization and re-crystallization of the host rock. Conversely, the (early) precipitation of titanite to infill many of the larger tubular textures may have enhanced their preservation by limiting the destructive effects of ongoing re-crystallization of the host rock. In this way, the pattern of Archean oceanic crustal bioalteration might have been modified by taphonomic processes i.e. changes during diagenesis and metamorphism, which may have significantly modified the original distribution pattern of bioalteration.

8 Summary

In this chapter, we have summarized results obtained over the last 15 years which argue that submarine volcanic rocks are and have been for most of Earths history an important habitat for microbial life. To illustrate this conclusion we present data from *in-situ* oceanic crust (0–110 Ma), ophiolites (∼90–1995 Ma) and greenstone belts (∼2000–3800 Ma). During the microbial colonization and simultaneous dissolution of volcanic glass referred to here as *bioalteration*, distinct textural, elemental and isotopic signatures are produced. Two principal types of textures, *granular* and *tubular* are formed. The granular type are individual and coalesced aggregates of spherical bodies usually less than 1 μm in diameter, whereas the tubular type are

long, up to ~200 μm tubes commonly 1–5 μm in diameter. These two textural types are invariably rooted in fractures in the glass and are distinct from the regularly banded alteration rinds produced by abiotic alteration (palagonitization). The bioalteration textures are formed by microbial dissolution or etching that produces pits or holes in the glass which are subsequently infilled by secondary minerals, initially clay minerals and zeolites that are transformed to chlorite, calcite, quartz and titanite during metamorphism. Locally elevated concentration of biologically significant elements, especially carbon, nitrogen, phosphorus and sulphur, are commonly observed within these bioalteration textures and offer significant support for their biogenicity. Further, there is a systematic difference in the $\delta^{13}C$ values of disseminated carbonate between glassy pillow rims and crystalline pillow interiors. The latter are bracketed between primary mantle CO_2 values and those expected from marine carbonates whereas pillow rims and hyaloclastites display a significantly greater range in $\delta^{13}C_{carbonate}$ values that is consistent with microbial activity. Even in the sequences that have experienced amphibolite and blueschist metamorphism this shift in isotope values persists, indicating that this bioalteration signal can survive high grade metamorphism.

The significance of these biosignatures for modern and ancient oceanic crustal processes is summarized below:

- **Mapping the oceanic biosphere**. Conspicuous bioalteration textures visible in thin section have made it possible to quantitatively estimate the extent of bioalteration as a function of depth in the sub-seafloor. This suggests that bioalteration predominates in the upper ~350 m of the glassy volcanic pile of the *in-situ* oceanic crust.
- **The oceanic crust as a bioreactor**. Although little is known about "glass-eating" microbial communities their ecologies and metabolisms, it is known that bioalteration increases the available glass surface area thereby enhancing reaction rates. It is thus likely that microbial activity results in increased exchange of chemical components between seawater and the crust.
- **Tectonic control of bioalteration in modern and ancient oceanic crust**. The carbon isotope signatures ($\delta^{13}C$) of finely disseminated carbonates in bioaltered pillow rims from slow- and fast-spreading oceanic crust differ. This is thought to be related to the liberation of H_2 during serpenitization which is much greater at slow-spreading ridges where it may support the lithotrophic utilization of CO_2 by methanogenic Archaea. This difference in $\delta^{13}C_{carb}$ values appears also to be found in ophiolites of slow versus fast spreading affinities.
- **Bioalteration and history of early life**. Bioalteration textures found in metavolcanic glasses provide a new target for deciphering the origins of life in some of the oldest, well-preserved rocks (~3.5 Ga) on Earth. Titanite mineralized textures in meta-pillow lava rims are comparable to those found in the modern oceanic crust and have a relatively high preservation potential. These structures can be considered amongst the earliest ichnofossils in the fossil record.
- **Tracing back and mapping the pattern of early bioalteration**. In the thick volcanic piles of the Archean greenstone belts that we have studied (Barberton

and Pilbara) the distribution of tubular bioalteration textures is apparently patchy and has been modified by subsequent metamorphism. This contrasts with the *in-situ* oceanic crust in which biotextures can be found continuously throughout.

Acknowledgments We acknowledge the help of many colleagues with the work reviewed herein describing the microbial bioerosion of volcanic glass, including: I.H. Thorseth, T. Torsvik, O. Tumyr, and A. Simonetti. Financial support for this research was provided by the Norwegian Research Council; the National Sciences and Engineering Research Council of Canada; the US National Science Foundation; the Agouron Institute and the National Research Foundation of South Africa. We thank F. Daniel of Nkomazi Wilderness for hospitality and the Mpumalanga Parks Board for access during field work in the Barberton Mountain Land of South Africa. This research used samples and data provided by the Ocean Drilling Program (ODP). ODP was sponsored by the NSF and participating countries under management of Joint Oceanographic Institutions (JOI), Inc. Participation for NB on the ODP Leg 192 was provided by Canada ODP. The Geological Survey of Western Australia, A. Hickman and C. Stoakes are also thanked for assistance with fieldwork in the Pilbara. Torgeir Andersen introduced us to the blueschist pillow lavas in Corsica, and R.C. Erickson assisted us on the classical Ward Creek blueschist locality in California. V. Melezhik and E. Hanski introduced us to the Pechenga greenstone belt (Russia), G. Zhao and P. Robinson to the Wutai area in the North China Craton, and M. Rosing to the Isua supracrustal belt (Greenland). We thank all these persons for their help. We also thank L. Nasdala for permission to publish Raman spectroscopy data shown in Fig. 27. This work has greatly benefited from the constructive review by Wolfgang Bach, Nils Holm and Dave Wacey. J. Ellingsen kindly helped with the illustrations. This paper is published with the permission of the Executive Director of the Geological Survey of Western Australia. This is AEON contribution number 46.

References

Abrajano TA, Sturchio NC, Kennedy BM, Muehlenbachs K, Bohlke JK (1990) Geochemistry of reduced gas related to serpentinization of Zambales ophiolite, Philippines. Appl Geochem 5:625–630

Alt JC, Mata P (2000) On the role of microbes in the alteration of submarine basaltic glass: a TEM study. Earth Planet Sci Lett 181:301–313

Alt JC, Kinoshita H, Stokking LB, et al (1993) Proc. ODP, Init. Repts, 148. (U. S. Government Printing Office), Washington

Alt JC, Laverne C, Vanko DA, Tartarotti P, Teagle DAH, Bach W, Zuleger E, Erzinger J, Honnorez J, Pezard PA, Becker K, Salisbury MH, Wilkens RH (1996) Hydrothermal alteration of a section of upper oceanic crust in the eastern equatorial Pacific: a synthesis of results from site 504 (DSDP Legs 69, 70, and 83, and ODP Legs 111, 137, 140 and 148). In: Alt JC, Kinoshita H, Stokking LB, Michael JP (eds) Proc. ODP, Sci. Results 148, College Station, TX, (Ocean Drilling Program), pp 417–434

Amend JP, Teske A (2005) Expanding frontiers in deep subsurface microbiology. Palaeogeo Palaeoclim Palaeoecol 219:131–55

Armstrong RA, Compston W, de Wit MJ, Williams IS (1990) The stratigraphy of the 3.5–3.2 Ga Barberton Greenstone Belt revisited: a single zircon ion microprobe study. Earth Planet Sci Lett 101:90–106

Bach W, Edwards KJ (2003) Iron and sulphide oxidation within the basaltic ocean crust: implications for chemolithoautotrophic microbial biomass production. Geochim Cosmochim Acta 67:3871–3887

Balashov A (1996) Paleoproterozoic geochronology of the Pechenga-Varzuga structure, Kola Peninsula. Petrology 4:1–22

Banerjee NR, Muehlenbachs K (2003) Tuff Life: bioalteration in volcaniclastic rocks from the Ontong Java Plateau. Gechem Geophys Geosyst 4(4). doi:1029/2002GC000470

Banerjee NR, Furnes H, Muehlenbachs K, Staudigel H, de Wit M (2004) The potential for early life hosted in basaltic glass on Mars. Second Conference on Early Mars: Geologic, hydrologic, and climatic evolution and the implications for life. Jackson Hole, Wyoming, USA

Banerjee NR, Furnes H, Muehlenbachs K, Staudigel H, de Wit MJ (2006) Preservation of microbial biosignatures in 3.5 Ga pillow lavas from the Barberton Greenstone Belt, South Africa. Earth Planet Sci Lett 241:707–722

Banerjee NR, Simonetti A, Furnes H, Staudigel H, Muehlenbachs K, Heaman L, Van Kranendonk MJ (2007) Direct dating of Archean microbial ichnofossils. Geology 35:487–490

Bebien J, Shallo M, Mania K, Gega D (1998) The Shebenik Massif (Albania): a link between MOR- and SSZ-type ophiolites? Ofiliti 23(1):7–15

Benzerara K, Menguy N, Banerjee NR, Tyliszczak T, Brown GE Jr, Guyit F (2007) Alteration of submarine basaltic glass from the Ontong Java Plateau: a STXM and TEM study. Earth Planet Sci Lett 260:187–200

Berndt ME, Allen DE, Seyfried DE Jr (1996) Reduction of CO_2 during serpentinitization of olivine at 300°C and 500 bar. Geology 24:351–354

Boyet M, Blichert-Toft J, Rosing M, Storey M, Telouk P, Albarede F (2003) ^{142}Nd evidence for early Earth differentiation. Earth Planet Sci Lett 214:427–442

Brandl G, de Wit MJ (1997) The Kaapvaal Craton, South Africa. In: de Wit MJ, Ashwal L (eds) Greenstone Belts. Oxford Univ Press, UK, pp 581–607

Cloos M (1990) Nicasio pillow basalts: a fragment of sea-mount accreted during Franciscan subduction, northern California. A.A.P.G., Pacific Section Guidebook No 66:9–16

Coleman RG (2000) Prospecting for ophiolites along the California continental margin. In: Dilek Y, Moores EM, Elthon D, Nicolas A (eds) Ophiolites and Oceanic Crust: New Insights from Field Studies and the Ocean Drilling Program. Geol Soc Am Spec Pap 351:351–364

Coleman RG, Lee DE (1963) Glaucophane-bearing metamorphic rock types of the Cazadeno area, California. J Petrol 4:260–301

Dal Piaz GV, Zirpoli G (1979) Occurrence of eclogite relics in the ophiolitic nappe from Marine d'Albo, Northern Corsica. N Jb Miner Mh 3:118–122

Daniel J-M, Jovilet L, Goffe B, Poinssot C (1996) Crustal-scale strain partitioning: footwall deformation below the Alpine Oligo-Miocene detachment of Corsica. J Struct Geol 18:41–59

Delaney JR, Kelley DS, Lilley MD, Butterfield DA, Baross JA, Wilcock WSD, Embley RW, Summit M (1998) The quantum event of oceanic crustal accretion: impacts of diking at mid-ocean ridges. Science 281:222–230

de Ronde CEJ, de Wit MJ (1994) Tectonic history of the Barberton greenstone belt, South Africa: 490 million years of Archean crustal evolution. Tectonics 13:983–1005

de Wit MJ (2004) Archean greenstone belts do contain fragments of ophiolites. In: Kusky TM (ed) Precambrian Ophiolites and Related Rock. Developments in Precambrian Geology 13 Elsevier, Amsterdam, Holland

de Wit MJ, Hart RA, Hart RJ (1987). The Jamestown Ophiolite Complex, Barberton mountain belt: a section through 3.5 Ga oceanic crust. J Afr Earth Sci 6:681–730

Detrick R, Honnorez J, Bryan WB, Juteau T, et al. (1988) Proc. ODP, Init. Repts, 106/109. (U. S. Government Printing Office), Washington

Dilek Y, Thy P (1998) Structure, petrology, and seafloor spreading tectonics of the Kizildag ophiolite, Turkey. In: Mills RA, Harrison K (eds) Modern ocean floor processes and the geologic record. Geol Soc London Spec Publ 148:43–69

Dilek Y, Moores EM, Furnes H (1998) Structure of modern oceanic crust and ophiolites and implications for faulting and magmatism at oceanic spreading centers. In: Buck R, Karson J, Delaney P, Lagabrielle Y (eds) Faulting and Magmatism at Mid-Ocean Ridges. Geophysical Monograph, American Geophysical Union, Washington, DC 106:216–266

Dilek Y, Furnes H, Shallo M (2007) Suprasubduction zone ophiolite formation along the periphery of Mesozoic Gondwana. Gondwana Res 11:453–475

Dmitriev L, Heirtzler J, et al (1978) Init. Repts. DSDP, 46. (U. S. Government Printing Office), Washington

Edwards KJ, Rogers DR, Wirsen CO, McCollom TM (2003) Isolation and Characterization of Novel Psychrophilic, Neutrophilic, Fe-oxidising, Chemolithoautotrophic α- and γ-Proteobacteria from the Deep Sea. Appl Environ Microbiol 69:2906–2913

Edwards, KJ; Bach W; McCollom TM (2005). Geomicrobiology in oceanography: microbe-mineral interactions at and below the seafloor. Trends in Microbiol 13:449–456

Evarts RC, Schiffman P (1983) Submarine hydrothermal metamorphism of the Del Puerto ophiolite, California. Am J Sci 283:289–340

Fisk MR, Giovannoni SJ, Thorseth IH (1998) The extent of microbial life in the volcanic crust of the ocean basins. Science 281:978–979

Fisk MR, Staudigel H, Smith DC, Haveman SA (1999) Evidence of microbial activity in the oldest ocean crust: EOS 80:F84–85

Fisk MR, Thorseth IH, Urbach E, Giovannoni SJ (2000) Investigation of microorganisms and DNA from surface thermal water and rock from the east flank of the Juan de Fuca Ridge. In: Fisher A, Davis EE, Escutia C (eds) Proc. ODP, Sci. Results 168. College Station, TX (Ocean Drilling Program), 167–174

Fisk MR, Storrie-Lombardi MC, Douglas S, Popa R, McDonald G, Di Meo-Savoie C (2003) Evidence of biological activity in Hawaiian subsurface basalts. Geochem Geophys Geosyst 4(4). doi:10.1029/2003GC000387

Fisk MR, Popa R, Mason OU, Storrie-Lombardie MC, Vicenzi EP (2006) Iron-magnesium silicate bioweathering on Earth (and Mars?). Astrobiology 6(1):48–68

Foriel J, Philippot P, Rey P, Somogyi A, Banks D, Menez B (2004) Biological control of Bl/Br and low sulphate concentration in a 3.5-Gyr-old seawater from North Pole, Western Australia. Earth Planet Sci Lett 228:451–463

Fouquet Y, Knott R, Cambon P, Fallick A, Rickard D, Desbruyeres D (1996) Formation of large sulfide mineral deposits along fast spreading ridges. Example from off-axial deposits at 12°43'N on the East Pacific Rise. Earth Planet Sci Lett 144:147–162

Fournier M, Jovilet L, Goffe B, Dubois R (1991) Alpine Corsica metamotphic core complex. Tectonics 10:1173–1186

Furnes H, Thorseth IH, Tumyr O, Torsvik T, Fisk MR (1996) Microbial activity in the alteration of glass from pillow lavas from Hole 896A. In: Alt JC, Kinoshita H, Stokking LB, Michael PJ (eds) Proceedings of the Ocean Drilling Program, Ocean Drilling Program, College Station, TX Scientific Results 148:191–206

Furnes H, Staudigel H (1999) Biological mediation in ocean crust alteration: how deep is the deep biosphere? Earth Planet Sci Lett 166:97–103

Furnes H, Muehlenbachs K, Tumyr O, Torsvik T, Thorseth IH (1999) Depth of active bio-alteration in the ocean crust: costa Rica Rift (Hole 504B). Terra Nova 11:228–233

Furnes H, Muehlenbachs K, Torsvik T, Thorseth IH, Tumyr O (2001a) Microbial fractionation of carbon isotopes in altered basaltic glass from the Atlantic Ocean, Lau Basin and Costa Rica Rift. Chem Geol 173:313–330

Furnes H, Staudigel H, Thorseth IH, Torsvik T, Muehlenbachs K, Tumyr O (2001b) Bioalteration of basaltic glass in the oceanic crust. Geochem Geophys Geosyst 2(8). doi:10.1029/2000GC000150

Furnes H, Muehlenbachs K, Tumyr O, Torsvik T, Xenophontos C (2001c) Biogenic alteration of volcanic glass from the Troodos ophiolite, Cyprus. J Geol Soc London 158:75–84

Furnes H, Hellevang B, Dilek Y (2001d) Cyclic volcanic stratigraphy in a Late Ordovician marginal basin, west Norwegian Caledonides. Bull Volcanol 63:164–178

Furnes H, Muehlenbachs K, Torsvik T, Tumyr O, Lang S (2002a) Bio-signatures in metabasaltic glass of a Caledonian ophiolite West Norway. Geol Mag 139:601–608

Furnes H., Thorseth IH, Torsvik T, Muehlenbachs K, Staudigel H, Tumyr O (2002b) Identifying bio-interaction with basaltic glass in oceanic crust and implications for estimating the depth of the oceanic biosphere: a review. In: Smellie JL, Chapman MG (eds) Volcano-Ice Interaction on Earth and Mars. Geol Soc London, Spec Publ 202, 407–421

Furnes H, Muehlenbachs K (2003) Bioalteration recorded in ophiolitic pillow lavas. In: Dilek Y, Robinson PT (eds) Ophiolites in Earth's History, vol 218. Geological Society of London Special Publications, pp 415–426

Furnes H, Banerjee NR, Muehlenbachs K, Staudigel H, de Wit MJ (2004) Early life recorded in Archean pillow lavas. Science 304:578–581

Furnes H, Banerjee NR, Muehlenbachs K, Kontinen A (2005) Preservation of biosignatures in metaglassy volcanic rocks from the Jormua ophiolite complex, Finland. Precamb Res 136: 125–137

Furnes H, Dilek Y, Muehlenbachs K, Banerjee NR (2006) Tectonic control of bioalteration in modern and ancient oceanic crust as evidenced by C-isotopes. The Island Arc 15:143–155

Furnes H, Banerjee NR, Staudigel H, Muehlenbachs K, de Wit M, McLoughlin N, Van Kranendonk M (2007a) Bioalteration textures in recent to mesoarchean pillow lavas: a petrographic signature of subsurface life in oceanic igneous rocks. Precamb Res 158:156–176

Furnes H, de Wit M, Staudigel H, Rosing M, Muehlenbachs K (2007b) A vestige of Earth's oldest ophiolite. Science 315:1704–1707

Gibson EK, Clemett SJ, Thomas-Keprta KL, McKay DS, Wentworth SJ, Robert F, Verchovsky AB, Wright IP, Pillinger CT, Rice T, Van Leer B (2006) Observation and analysis of in situ carbonaceous matter in Nakhla: part II (2006). The 37th Lunar and Planetary Science Conference, Houston 2006, abstract 2039

Giovannoni SJ, Fisk MR, Mullins TD, Furnes H (1996) Genetic evidence for endolithic microbial life colonizing basalic glass/seawater interfaces. In: Alt J, Kinoshita H, Stokking LB, Michael PJ (eds) Proceedings of the Ocean Drilling Program, Scientific Results, Ocean Drill. Program, College Station, Texas 148:207–214

Hanski EJ, Huhma H, Smolkin VF, Vaasjoki M (1990) The age of the ferropicritic volcanics and comagmatic intrusions at pechenga, Kola Peninsula, USSR. Geol Soc Finl Bull 62:123–133

Hoefs J (1997) Stable Isotope Geochemistry, Springer, pp 201

Hofmann HJ, Grey K, Hickman AH, Thorpe RI (1999) Origin of 3.45 Ga Coniform Stromatolites in the Warrawoona Group, Western Australia. Bull Geol Soc Am 111:1256–1262

Ingersoll RV (2000) Models for the origin and emplacement of Jurassic ophiolites of northern California. In: Dilek Y, Moores EM, Elthon D, Nicolas A (eds) Ophiolites and Oceanic Crust: new insights from field Studies and the Ocean Drilling Program. Geol Soc Am Spec Pap 351:395–402

Karson JA (1998) Internal structure of oceanic lithosphere: a perspective from tectonic windows. In: Buck R, Karson J, Delaney P, Lagabrielle Y (eds) Faulting and Magmatism at Mid-Ocean Ridges. Geophysical Monograph, 106:177–218. American Geophysical Union, Washington, DC

Kelley DS (1996) Methane-rich fluids in the oceanic crust. J Geophys Res 101:2943–2962

Kelley DS, Karson JA, Früh-Green GL, Yoerger DR, Shank TM, Butterfield DA, Hayes JM, Schenk MO, Olson EJ, Proskurowski G, Jakuba M, Bradley A, Larson B, Ludvig K, Glickson D, Buckman K, Bradley AS, Brazelton WL, Roe K, Elend MJ, Delacour A, Bernasconi SM, Lilley MD, Baross JA, Summons RE, Sylva S (2005) A serpentine-hosted ecosystem: The Lost City hydrothermal field. Science 307:1428–1434

Kelts K, McKenzie JA. (1982) Diagenetic dolomite formation in Quarternary anoxic diatomaceous muds of Deep Sea Drilling Project Leg 64, Gulf of California. Init. Reps. DSDP, 64. (U. S. Government Printing Office), Washington, pp 553–569

Komiya T, Maruyama S, Masusa T, Nohda S, Hayashi M, Okamoto K (1999) Plate tectonics at 3.8-3.7 Ga: Field evidence from the Isua accretionary complex, southern West Greenland. J Geol 107:515–554

Kontinen A (1987) An early Proterozoic ophiolite – The Jormua mafic-ultramafic complex, northeastern Finland. Precamb Res 35:313–341

Kröner A, Zhao GC, Wilde SA, Zhai MG, Passchier CW, Sun M, Guo JH, O'Brian PJ, Walte N (2001) A Late Archaean to Palaeoproterozoic Lower to Upper Crustal Section in the Hengshan-Wutaishan Area of North China. Guidebook for Penrose Conference Field Trip, September 2002. Chinese Academy of Sciences, Beijing, pp 63

Krumbein WE, Urzi CECA, Gehrman C (1991) Biocorrosion and biodeterioration of antique and medieval glass. Geomicrob J 9:139–160
Lemoine M, Tricard P, Boillot G (1987) Ultramafic and gabbroic ocean floor of the Ligurian Tethys (Alps, Corsica, Appennines): In search of a genetic model. Geology 15:622–625
Lovley DR, Chapelle FH (1995) Deep subsurface microbial processes. Rev Geophys 33:365–381
Lysnes K, Thorseth IH, Steinsbu BO, Øvreås L, Torsvik T, Pedersen RB (2004) Microbial community diversity in seafloor basalts from the Arctic spreading ridges. FEMS Microbiol Ecol 50:213–230
Luydendyk BP, Cann JR. et al (1978) Init. Repts. DSDP, 49, Washington (U. S. Government Printing Office)
Malpas J, Moores EM, Panayiotou A, Xenophontos C (1990) Ophiolites: Oceanic Crustal Analogues. Proceeding of the Symposium "Troodos 1987". The Geological Survey Department, Ministry of Agriculture and Natural Resources, Nicosia, Cyprus, pp 733
Maruyama S, Liou JG (1988) Petrology of Franciscan metabasites along jadeite-glaucophane type facies series, Cazadero, California. J Petrol 29:1–37
Matsushita M, Hiramatsu F, Kobayashi N, Ozawa T, Yamazaki Y, Matsuyama T (2004) Colony formation in bacteria: experiments and modelling. Biofilms 1:305–317. doi:10.1017/S1479050505001626
McKay DS, Clemett SJ, Thomas-Keprta KL, Wentworth SJ, Gibson EK, Robert F, Verchovsky AB, Pillinger CT, Rice T, Van Leer B (2006) Observation and analysis of in situ carbonaceous matter in Nakhla: part I. The 37th Lunar and Planetary Science Conference, Houston 2006, abstract 2251
McKeegan KD, Kudryavtsev AB, Schopf JW (2007) Raman and ion microscopic imagery of graphitic inclusions in apatite from older than 3830 Ma Akilia supracrustal rocks, west Greenland. Geology 35(7):591–594
McLoughlin N, Brasier MD, Wacey D, Green OR, Perry RS (2007) On biogenicity criteria for endolithic microborings on early earth and beyond. Astrobiology 7:10–26
McLoughlin N, Furnes H, Banerjee NR, Staudigel H, Muehlenbachs K, de Wit M, Van Kranendonk M (2008) Micro-Bioerosion in Volcanic Glass: extending the Ichnofossil Record to Archean basaltic crust. In: Wisshak M, Tapanila L (eds) Springer Verlag
Melezhik VA, Sturt BA (1994) General geology and evolutionary history of the early Proterozoic Polmak-Pasvik-Pechenga-Imandra/Varzuga-Ust'Ponoy Greenstone Belt in the north-eastern Baltic Shield. Earth Sci Rev 36:205–241
Melezhik VA, Huhma H, Fallick AE, Whitehouse MJ (2007) Temporal constraints on the Paleoproterozoic Lomagundi-Jatuli carbon isotope event. Geology 35(7):655–658
Mellor E (1922) Les lichen vitricole et la déterioration dex vitraux d'église: Thèse de dochert thesis, Sorbonne, Paris
Mojzsis SJ, Arrhenius G, McKeegan KD, Harrison TM, Nutman AP, Friend CRL (1996) Evidence of life on Earth before 3800 million years ago. Nature 384:55–59
Moorbath S (2005) Dating earliest life. Nature 434:155
Myers JS (2001) Protoliths of the 3.8-3.7 Ga Isua greenstone belt, West Greenland. Precamb Res 105:129–141
Nelson DR (2005) GSWA geochronology dataset, In: Compilation of geochronology data, June 2005 update. Western Australia Geological Survey, GSWA 178042
Nicolas A, Boudier F, Meshi A (1999) Slow spreading accretion and mantle denudation in the Mirdita ophiolite (Albania). J Geophys Res 104:15155–1517
Nisbet EG, Sleep NH (2001) The habitat and nature of early life. Nature 409:1083–1090
Nutman AP (1986) The early Archaean to Proterozoic history of the Isukasia area, southern West Greenland. Grønlands Geol Unders Bull 154:80
Ohnenstetter D, Ohnenstetter M, Rocci G (1976) Etude des metamorphismes successife des cumulates ophiolitiques de Corse. Bull Soc Geol France XVIII:115–134
Palmer HC, Tazaki K, Fyfe WS, Zhou Z (1988) Precambrian glass. Geology 16:221–224
Panayiotou A (ed) (1980) Ophiolites. Proceedings of the International ophiolite Symposium, Cyprus 1979. Cyprus Geological Survey Department, pp 781

Parson I, Hawkins J, Allan J, et al. (1992) Proc. ODP, Init. Repts, 135. (U. S. Government Printing Office), Washington

Paul A, Zaman MS (1978) The relative influences of Al_2O_3 and Fe_2O_3 on the chemical durability of silicate glasses at different pH values. J Mat Sci 13:1499–1502

Peacock MA (1926) The petrology of Iceland. Part I, The basic tuffs. Trans Roy Soc Edinburgh 55:51–76

Pedersen K (1997). Microbial life in deep granitic rocks. FEMS Microbiol Rev 20:399–414

Pedersen K, Ekendahl S, Tullborg E-L, Furnes H, Thorseth IH, Tumyr O (1997) Evidence of ancient life at 207 m depth in a granitic aquifer. Geology 25:827–830

Peltonen P, Kontinen A, Huhma H (1996) Petrology and geochemistry of metabasalts from the 1.95 Ga Jormua ophiolite, Northeastern Finland. J Petrol 37:1359–1383

Rasmussen B (2000) Filamentous microfossils in a 3,250-million-year-old volcanogenic massive sulphide deposit. Nature 405:676–679

Robinson PT, Flower MFJ, Swanson DA, Staudigel H (1979) Lithology and eruptive stratigraphy of Cretaceous oceanic crust, western Atlantic Ocean. In: Donelly T, Francheteau J, Bryan W, Robinson P, Flower M, Salisbury M. et al (eds) Init. Repts. DSDP, LI, LII, LIII. (U. S. Government Printing Office), Washington

Rosing MT (1999) ^{13}C-depleted carbon microparticles in >3700-Ma sea-floor sedimentary rocks from West Greenland. Science 283:674–676

Rosing MT, Rose NM, Bridgwater D, Thomsen HS (1996) Earliest part of Earth's stratigraphic record: a reappraisal of the >3.7 Ga Isua (Greenland) supracrustal sequence. Geology 24:43–46

Ross KA, Fisher RV (1986) Biogenic grooving on glass shards. Geology 14:571–573

Santelli CM, Bach W, Edwards KJ (2006). Microorganisms and the weathering of basalt at the seafloor. Geochim Cosmochim Acta 70 (issue 18) A556 (Goldschmidt Conference Abstracts) doi:10.1016/j.gea.2006.06.1027

Schidlowski M (1988) A 3800-million-year isotopic record of life from carbon in sedimentary rocks. Nature 333:313–318

Schidlowski M (2001) Carbon isotopes as biogeochemical recorders of life over 3.8 Ga of Earth history: evolution of a concept. Precamb Res 106:117–134

Schiffman P, Williams AE, Evarts RC (1984) Oxygen isotope evidence for submarine hydrothermal alteration of the Del Puerto ophiolite, California. Earth Planet Sci Lett 70:207–220

Schiffman P, Evarts RCE, Williams AE, Pickthorn WJ (1991) Hydrothermal metamorphism in oceanic crust from the Coast Ranges ophiolite of California:fluid-rock interaction in a rifted island arc. In: Peters TJ., Nicolas A, Coleman RG (eds) Ophiolite Genesis and Evolution of the Oceanic Lithosphere. Kluwer Academic Publishers, Dordrecht, pp 399–425

Schippers A, Neretin LN, Kallmeyer J, Fendelman TG, Cragg BA, Parkes RJ, Jørgensen BB (2005) Prokaryotic cells of the deep sub-seafloor biosphere identified as living bacteria. Nature 433:861–64

Schmincke H-U, Bednarz U (1990) Pillow, sheet flow and breccia flow volcanoes and volcanotectonic hydrothermal cycles in the Extrusive Series of the northeastern Troodos ophiolite (Cyprus). In: Malpas J, Moores EM, Panayiotou A, Xenophontos C (eds) Ophiolites Oceanic Crustal Analogues, Proceedings of the Symposium "Troodos 1987". The Geological Survey Department, Ministry of Agriculture and Natural Resources, Nicosia, Cyprus, pp 185–206

Schopf JW, Packer BM (1987) Early Archean (3.3 Billion to 3.5 Billion-Year-Old) Microfossils from Warrawoona Group, Australia. Science 237:70–73

Schumann G, Manz W, Reitner J, Lustrino M (2004) Ancient Fungal Life in North Pacific Eocene Ocenaic Crust. Geomicrobiol J 21:241–246

Shallo M (1995) Volcanics and sheeted dykes of the Albanian SSZ ophiolite. Buletini i Shkencave Gjeologjike 91:99–118

Shervais JW, Hanan BB (1989) Jurassic volcanic glass from the Stonyford volcanic complex, Franciscan assemblage, northern California Coast Ranges. Geology 17:510–514

Simonetti A, Heaman LM, Chacko T, Banerjee NR (2006) In situ petrographic thin section U–Pb dating of zircon, monazite, and titanite using laser ablation–MC–ICP-MS. Internat J Mass Spectrometry 253:87–97

Sinton JM, Detrick RS (1992) Mid-ocean ridge magma chambers. J Geophys Res 97:197–216
Smolkin VF, Bayanova TB, Fedotov Zh A (2003) Ore-bearing mafic-ultramafic rocks of the Pechenga-Allarechka area, Kola region: isotopic dating. In: Proceedings of the II Russian Conference on Isotope Geochemistry, St. Petersburg, pp 467–470 (in Russian)
Staudigel H, Chastain RA, Yayanos A, Bourcier R (1995) Biologically mediated dissolution of glass. Chem Geol 126:119–135
Staudigel H, Yayanos A, Chastain R, Davies G, Verdurmen EATh, Schiffman P, Bourcier R, De Baar H (1998) Biologically mediated dissolution of volcanic glass in seawater. Earth Planet Sci Lett 164:233–244
Staudigel H, Furnes H (2004) Microbial mediation of oceanic crust alteration. In: Davis E, Elderfield H (eds) Hydrology of the Oceanic Lithosphere. Cambride University Press, pp 608–626
Staudigel H, Furnes H, Kelley K, Plank T, Muehlenbachs K, Tebo B, Yayanos A (2004) The Oceanic Crust as a Bioreactor. In: AGU Monograph 144. Deep Subsurface Biosphere at Mid-Ocean Ridges pp 325–341
Staudigel H, Furnes H, Banerjee NR, Dilek Y, Muehlenbachs K (2006) Microbes and Volcanos: A tale from the Oceans, Ophiolites and Greenstone Belts. GSA Today 16(10). doi:10.1130/GSAT01610A.1
Stetter KO, Fiala G, Huber G, Segerer A (1990) Hypothermophilic microorganisms. FEMS Microbiol Rev 75:117–124
Storrie-Lombardi MC, Fisk MR (2004) Elemental abundance distributions in suboceanic basalt glass: Evidence of biogenic alteration. Geochem Geophys Geosyst 5(10). doi:10.1029/2004GC000755
Stroncik N, Schmincke H-U (2001) Evolution of palagonite: Crystallization, chemical changes, and element budget. Geochem Geophys Geosyst 2(7). doi:10.1029/2000GC000102
Swanson SE, Schiffman P (1979) Textural evolution and metamorphism of pillow basalts from the Franciscan Complex, western Marin County, California. Contrib Mineral Petrol 69: 291–299
Tappert R, Stachel T, Harris JW, Muehlenbachs K, Ludwig T, Brey GP (2005) Subducting oceanic crust: The source of deep diamonds. Geology 33:565–568
Templeton AS, Staudigel H, Tebo BM (2005) Diverse Mn(II)-Oxidizing bacteria isolated from submarine Basalts at Loihi Seamount. J Geomicrobiol 22:127–139
Thorseth IH, Furnes H, Tumyr O (1991) A textural and chemical study of Icelandic palagonite of varied composition and its bearing on the mechanism of the glass-palagonite transformation. Geochim Cosmochim Acta 55:731–749
Thorseth IH, Furnes H, Heldal M (1992) The importance of microbiological activity in the alteration of natural basaltic glass. Geochim Cosmochim Acta 56:845–850
Thorseth IH, Torsvik T, Furnes H, Muehlenbachs K (1995a) Microbes play an important role in the alteration of oceanic crust. Chem Geol 126:137–146
Thorseth IH, Furnes H, Tumyr O (1995b) Textural and chemical effects of bacterial activity on basaltic glass: an experimental approach. Chem Geol 119:139–160
Thorseth IH, Torsvik T, Torsvik V, Daae FL, Pedersen RB, Keldysh-98 Scientific party (2001) Diversity of life in ocean floor basalts. Earth Planet Sci Lett 194:31–37
Thorseth IH, Pedersen RB, Christie DM (2003) Microbial alteration of 0–30-Ma seafloor and sub-seafloor basaltic glasses from the Australian Antarctic Discordance. Earth Planet Sci Lett 215:237–247
Torsvik T, Furnes H, Muehlenbachs K, Thorseth IH, Tumyr O (1998) Evidence for microbial activity at the glass-alteration interface in oceanic basalts. Earth Planet Sci Lett 162:165–176
Ueno Y, Maruyama S, Isozaki Y, Yurimoto H (2001) Early Archean (ca. 3.5 Ga) microfossils and ^{13}C-depleted carbonaceous matter in the North Pole area, Western Australia: Field occurrence and geochemistry, In: Nakashima S, Maruyama S, Brack A, Windley BF (eds) Geochemistry and the origin of life. Universal Academy Press Inc, Tokyo, pp 203–236

Van Kranendonk MJ (2006) Volcanic degassing, hydrothermal circulation and the flourishing of early life on Earth: A review of the evidence from c. 3490-3240 Ma rocks of the Pilbara Supergroup, Pilbara Craton, Western Australia. Earth-Sci Rev 74:197–240

Van Kranendonk MJ, Pirajno F (2004) Geochemistry of metabasalts and hydrothermal alteration zones associated with c. 3.45 Ga chert and barite deposits: implications for the geological setting of the Warrawoona Group, Pilbara craton, Australia. Geochemistry: Exploration Environment Analysis 4:253–278

Van Kranendonk MJ, Hickman AH, Smithies RH, Nelson DN, Pike G (2002) Geology and tectonic evolution of the Archaean North Pilbara terrain, Pilbara Craton, Western Australia. Econ Geol 97(4):695–732

Van Kranendonk MJ, Collins WJ, Hickman A, Pawley MJ (2004) Critical tests of vertical vs. horizontal tectonic models for the Archean East Pilbara Granite-Greenstone Terrane, Pilbara Craton, Western Australia. Precamb Res 131:173–211

Van Kranendonk MJ, Hickman AH, Smithies RH, Champion DC (2007) Review: secular tectonic evolution of Archaean continental crust: interplay between horizontal and vertical processes in the formation of Pilbara Craton, Australia. Terra Nova 19:1–39

Wakabayashi J (1992) Nappes, tectonics of oblique plate convergence, and metamorphic evolution related to 140 million years of continuous subduction, Franciscan Complex, California. J Geol 100:19–40

Wakabayashi J (1999) The Franciscan Complex, San Francisco Bay Area: A record of subduction complex processes. In: Wagner DL, Graham SA (eds) Geologic Field Trips in Northern California. California Division of Mines Special Publication 119:1–21

Walter MR, Buick R, Dunlop JSR (1980) Stromatolites, 3,400–3,500 Myr old from the North Pole area, Western Australia. Nature 284:443–445

Walton AW, Schiffman P (2003) Alteration of hyaloclastites in the HSDP 2 Phase 1 Drill Core 1. Description and paragenesis. Geochem Geophys Geosyst 4(5). Doi: 10.1029/2002GC000368

Walton AW, Schiffman P, Macperson GL (2005) Alteration of hyaloclastites in the HSDP 2 Phase 1 Drill Core: 2. Mass balance of the conversion of sideromelane to palagonite and chabazite. Geochem Geophys Geosyst 6(9). doi: 10.1029/2004GC000903

Wijbrans JR, McDougall I (1987) On the metamorphic history of an Archaean granitoid greenstone terrane, East Pilbara, Western Australia, using the $^{40}Ar/^{39}Ar$ age spectrum technique. Earth Planet Sci Lett 84:226–242

Wilde SA, Valley JW, Peck WH, Graham CM (2001) Evidence from detrital zircons for the existence of continental crust and oceans on the Earth 4.4 Gya ago. Nature 409:175–178

Zavarzina DG, Sokolova TG, Tourova TP, Chernyh NA, Kostrikina NA, and Bonch-Osmolovskaya EA (2007) Thermincola ferriacetica sp nov, a new anaerobic, thermophilic, faculatively chemolithoautotrophic bacterium capable of dissimilatory Fe(III) reduction. Extremophiles 11:1–7

Zhai MG, Yan YH, Lu WJ, Zhou JB (1985) Geochemistry and evolution of the Qingyuan Archean granite-greenstone terrain, N. China. Precamb Res 27:37–62

Zhao G, Wilde SA, Cawood PA, Sun M (2001) Archean blocks and their boundaries in the North China Craton: lithological, geochemical, structural and *P-T* path constraints and tectonic evolution. Precamb Res 107:45–73

Zhang Z, Goloubic S (1987) Endolithic microfossils (cyanophyta) from early Proterozoic Stromatolites, Hebei China. Acta Micropaleontol Sin 4:1–12

Zhou GC, Wilde SA, Cawood PA, Lu LZ (1998) Thermal evolution of the Archean basement rocks from the eastern part of the North China Craton and its bearing on tectonic setting. Int Geol Rev 40:706–721

http://www.springer.com/978-1-4020-8305-1

Links Between Geological Processes, Microbial Activities & Evolution of Life
Microbes and Geology
Dilek, Y.; Furnes, H.; Muehlenbachs, K. (Eds.)
2008, XVI, 348 p., Hardcover
ISBN: 978-1-4020-8305-1